Influence of Sensorimotor Noise on the Planning and

Control of Reaching in 3-Dimensional Space

by

Gregory Allen Apker

A Dissertation Presented in Partial Fulfillment
of the Requirements for the Degree
Doctorate of Philosophy

Approved February 2012 by the
Graduate Supervisory Committee:

Christopher Buneo, Chair
Stephen Helms Tillery
Marco Santello
Veronica Santos
Jennie Si

ARIZONA STATE UNIVERSITY

May 2012

ABSTRACT

The ability to plan, execute, and control goal oriented reaching and
grasping movements is among the most essential functions of the brain. Yet, these
movements are inherently variable; a result of the noise pervading the neural
signals underlying sensorimotor processing. The specific influences and
interactions of these noise processes remain unclear. Thus several studies have
been performed to elucidate the role and influence of sensorimotor noise on
movement variability.

The first study focuses on sensory integration and movement planning
across the reaching workspace. An experiment was designed to examine the
relative contributions of vision and proprioception to movement planning by
measuring the rotation of the initial movement direction induced by a perturbation
of the visual feedback prior to movement onset. The results suggest that
contribution of vision was relatively consistent across the evaluated workspace
depths; however, the influence of vision differed between the vertical and later
axes indicate that additional factors beyond vision and proprioception influence
movement planning of 3-dimensional movements.

If the first study investigated the role of noise in sensorimotor integration,
the second and third studies investigate relative influence of sensorimotor noise
on reaching performance. Specifically, they evaluate how the characteristics of
neural processing that underlie movement planning and execution manifest in
movement variability during natural reaching. Subjects performed reaching
movements with and without visual feedback throughout the movement and the

ii

patterns of endpoint variability were compared across movement directions. The results of these studies suggest a primary role of visual feedback noise in shaping patterns of variability and in determining the relative influence of planning and execution related noise sources.

The final work considers a computational approach to characterizing how sensorimotor processes interact to shape movement variability. A model of multi-modal feedback control was developed to simulate the interaction of planning and execution noise on reaching variability. The model predictions suggest that anisotropic properties of feedback noise significantly affect the relative influence of planning and execution noise on patterns of reaching variability.

ACKNOWLEDGEMENTS

I was fortunate enough to be offered a Science Foundation of Arizona Graduate Research Fellowship in the programs inaugural year. It is certainly not an overstatement that the Science Foundation of Arizona played a major role in bringing me to ASU and setting the wheels in motion to bring me to this point.

While at Vanderbilt University, I had the good fortune to work with Dr. Mark Does in the Biomedical Engineering Department and Dr. Mark Wallace in the Neuroscience Department. Each of these professors had a distinct and positive effect on my academic identity and certainly deserve acknowledgement here.

My gratitude toward my adviser, Dr. Christopher Buneo, cannot be stated strongly enough. His enduring patience and respect were pivotal to my development as a scientist and intellectual. I will leave it by simply stating that his role in my graduate career transcended "adviser" to be a council, a colleague and a friend. I would also like to thank the members of my committee for their time and consideration of my work and my ideas. Their feedback has been invaluable in this process.

I owe so much to my parents. Their untold sacrifice and unparalleled commitment to raise me is the genesis of any achievement of mine. Their support has been unyielding, taken many forms, and remains my single greatest motivator compelling me to go beyond what is expected towards the remarkable.

Lastly, but only because it's easiest to find there, I want to give special mention to Jamie, whose charm and character has touched every aspect of my life Thank you for the joy you have brought me, and the adventures yet to come.

TABLE OF CONTENTS

LIST OF FIGURES:

CHAPTER 1

INTRODUCTION

Limb movements are inherently variable; a characteristic that is largely attributed to 'noise' in neural signals arising during sensorimotor processing (Desmurget & Grafton, 2000). The origins of sensorimotor noise arise from stochastic behavior in network mechanisms and cellular processes involved in signal transduction (Faisal et al., 2008). Depending upon the stage at which noise arises, its effect on movement differs. Specifically, noise arising during sensation and planning of motor commands is expected to have a different effect on movement than noise associated with the execution of those commands. As a result, elements of sensorimotor noise are typically classified as contributing to either 'planning noise' or 'execution-noise'. In addition, both visual and proprioceptive feedback are limited in the precision in which they can encode estimates of limb and target position, a characteristic called 'uncertainty' (van Beers et al., 1999). This uncertainty also results in variability in planning and movement errors (Shi and Buneo, 2009), and thus it is convenient to consider it a component of planning noise.

Recent evidence suggests the brain employs specific strategies to integrate neural signals that compensate for the effects of this noise and improve reaching performance. For instance, it has been argued that visual and proprioceptive feedback are integrated to minimize uncertainty in limb position in the horizontal plane (Angelaki et al., 2009; Bays & Wolpert, 2007). Similarly, others have suggested that behavioral variability results from the optimal or 'near optimal'

1

integration of movement planning and execution related noise (Faisal and Wolpert, 2009). However, many previous studies have confined movement to the horizontal plane or implemented other constraints on movement to simplify their tasks. Such constraints limit the complexity of sensorimotor control and thus may not generalize to more natural, unconstrained movements (Desmurget et al., 1997; Scheidt et al., 2005). As a result, it is not clear to what degree noise in sensorimotor control manifests during normal, unconstrained reaching movements to targets throughout the 3-dimensional (3D) workspace. To address these issues, several studies have been performed to elucidate the role and influence of sensorimotor noise on the planning and control of movements in 3D.

The first study focuses on sensory integration and movement planning outside of the horizontal plane. To date, much of our knowledge of this process comes from studies of a limited region of the workspace. These studies have argued that integration of sensory feedback in the horizontal plane can be approximated as the sum of somatic and visual position cues weighted by the relative reliability of each modality (Wolpert, 2007). However, there is evidence to suggest that integration outside of the horizontal plane may be more complex, as additional factors (such as the effects of gravity) are involved. In addition, findings in the horizontal plane also suggest that the weighting of vision and proprioception may vary in depth. To date, these predictions have not yet been directly assessed for unconstrained 3D movements. To probe these questions, an experiment was designed to probe the integration of visual feedback during movement planning to vertical targets at multiple depths.

The second and third studies investigated the characteristics of neural processing that underlie movement planning and execution that can result in movement variability. The variability we observe in behavior is inevitably affected by both of these sources of noise (Thaler and Todd, 2009); however they are often studied independently. Understanding how noise from the different stages of sensorimotor control interacts to shape reaching performance is pivotal to our ability to draw inferences about neural mechanisms of sensorimotor control from behavior. As a first step, a reaching task was designed to accentuate both sensory and non-sensory sources of reaching variability. Movements were analyzed to assess the respective contributions of planning and execution to movement variability as well as how they interact during movement to shape observed behavior. Patterns of endpoint variability were quantified and compared between task conditions to assess the relative contribution of the underlying noise sources to movement variability.

The final work detailed here considers a computational approach to characterizing how noisy sensorimotor processes contribute and interact to shape patterns of movement variability. Similar algorithms have provided important insight into the underlying neural mechanisms responsible for feedback control. However, these models have often made simplifying assumptions which ultimately limit their explanatory and predictive capacity. For instance, previous studies have largely considered only a single sensory modality, or have used unrealistic feedback parameters despite evidence which suggests that the specific spatial properties of multiple sensory modalities influence the control of reaching

3

(McIntyre et al., 1997, van Beers et al., 2002b). Thus these aspects of feedback control must be considered when attempting to emulate sensorimotor control of reaching. As an initial step towards this end, a multi-modal feedback control model of sensorimotor integration and movement variability was developed to provide a more complete characterization of the interaction of planning and execution noise on human reaching performance.

CHAPTER 2

BACKGROUND

The ability to plan, execute, and control goal oriented reaching movements is an essential function of the brain. This process requires seamless integration across disparate sensory modalities and dynamic motor processes to localize the hand and generate motor commands. Yet, the neural processes which underlie sensorimotor control are inherently uncertain and stochastic in nature. This manifests as noise in these signals, affecting the ability to reliably plan and execute desired movements. At the behavioral level the effects of this noise in sensorimotor processes is variability in reaching. To improve reaching performance, there is a growing body of evidence which suggests the brain filters these signals to reduce the effects of this noise. In fact, this function of the nervous system extends beyond the context of reaching to include postural (Kuo, 1995), perceptual (Ernst and Banks), and decision making (Kording and Wolpert, 2006). Thus the mechanism of improving the signal-to-noise ratio of neural signals may be a critical function of the brain. Given the connection between reaching variability and sensorimotor signal noise, characterizing how noise in sensorimotor control manifests in behavior may provide insight into how the brain performs one of its most fundamental functions.

Sources of Movement Variability

With respect to reaching, variability refers to differences in limb and hand position between movements to the same position. This variability is attributed to random fluctuations in the signals encoding reaching parameters (i.e. hand or

5

target position). These fluctuations are tantamount to noise in the neural signal. Illustrated in Figure 2.1, neural signals are inevitably subject to noise stemming from multiple aspects of sensorimotor processes ranging from stochastic behavior in cellular processes and network mechanisms of signal transduction (Faisal et al., 2008). Noise in sensorimotor control is commonly separated into two distinct groups: noise associated with the planning of movement (including sensation of reaching parameters such as limb and target position), collectively called "planning noise", and those arising from processes associated with the execution of that plan, referred to together as "execution noise". It is important to note that these two processes do not affect movement in a purely serial manner. Sensory feedback of the limb and target are continuously compared throughout movement, and used to update the motor the plan throughout the movement. Thus, planning noise may also be thought of as variability arising during the process of planning and updating the motor plan. Execution noise is then also dependent upon both the initial planning as well as updating processes as these will affect the nature of the motor commands.

Noise from both groups has been shown to significantly affect patterns of reaching variability (Carrozzo et al., 1999; Churchland et al., 2006a; Churchland et al., 2006b; McIntyre et al., 1998; Gordon et al., 1994; Harris & Wolpert, 1996; van Beers et al., 2004). For instance, the processes which underlie signal transduction through motor neurons and across the neuromuscular junction, as well as the subsequent muscle activity level are stochastic in nature. This property will result in trial-to-trial variability in the strength of contraction between

6

movements from an identical motor plan, and are referred to collectively as 'execution noise'.

In addition to variability due to execution related noise, variability in movement can also arise from trial-to-trial fluctuations in the motor plan for the same initial hand and target positions, a.k.a. 'planning noise'. For instance, noise in sensory estimates arising from the thermodynamic or quantum mechanical properties of receptor and neuron activation/signal transduction results in variability in the encoded position of the limb and target. In addition, planning noise has been shown to be largely the result of uncertainty in the sensory feedback encoding reach parameters. Uncertainty here refers to the inability to disambiguate between true limb positions with a region of space. The larger the region of space in which the feedback modality cannot precisely encode limb position, the greater the uncertainty. Thus, the same hand position may be perceived differently between two trials, resulting in variability in the motor plan. The stochastic properties of sensory receptors and afferent signal transduction further contributes to sensory uncertainty , and thus sensory uncertainty constitutes an important component of planning noise (Osborne et al., 2005).

Both planning and execution noise are present during every movement resulting in behavioral variability proportional to the amount of noise in these processes. It is has been suggested that the brain has developed mechanisms of integration and control which mitigate the effects of planning and execution noise to optimize performance (van Beers et al., 2002b; Harris and Wolpert, 1998). In the sections to follow, we will review the nature of planning and execution noise

and how each is believed to effect movement variability, as well as the mechanisms believed to underlie sensorimotor control that minimize behavioral variability.

Movement Planning and Uncertainty

As previously stated, planning noise constitutes the noise which arises during the processes associated with determining the motor command, including estimation of the limb and target position. As stated previously, this process does not stop at movement onset, but also constitutes the feedback control processing of the motor commands throughout the movement. Thus, the neural processes which constitute planning phase range from afferent sensory signals, the cortical processes which culminate in activation of central motor neurons (such as those in the motor cortex), as well as the activity of interneurons in the spinal column which either further process the signal of primary motor neurons or are involved in reflex control from sensory signals in the muscles. A recent study of activity in the dorsal premotor cortex found that a significant amount of total variability in movement velocity is traceable to variability in the motor plan (Churchland et al., 2006a; Churchland et al., 2006b). Given that sensory feedback is an important source of behavioral variability, it is possible that much of this planning noise is associated with the sensory feedback used to develop internal estimates of limb and target position (Shi & Buneo, 2009).
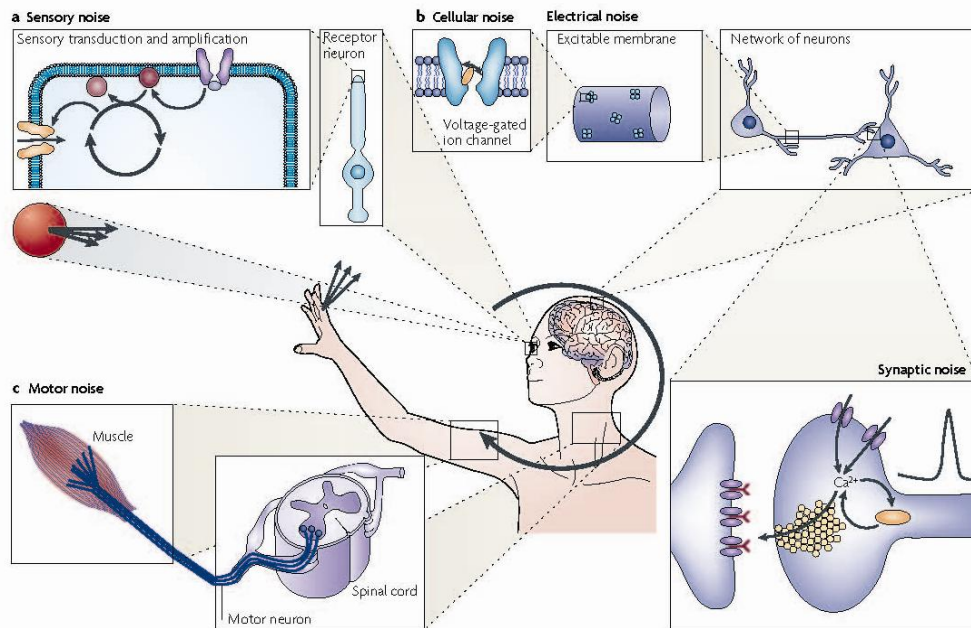
Figure 2.1. Sources of noise in sensation and motor control. Faisal et al. (2008),

Nat Rev Neurosci.

Within the brain, internal estimates of limb and target position can be found throughout the parietal-frontal network (Caminiti et al., 1996, Battaglia-Mayer et al., 2003). For instance, limb position modulation has been observed in several regions of parietal lobe, particularly in parietal areas 5 and 7a, as well as the medial intra-parietal area (MIP) (Graziano et al., 2000; Buneo & Andersen, 2006, Battaglia-Mayer et al., 2007). Activity in both area 5 and MIP has been shown to encode the relative position of the hand and target (i.e. the movement vector), as well as the position and velocity of the hand in a fixed eye or body-centered reference frame (Ashe & Georgopoulus, 1994; Lacquaniti et al., 1995; Eskandar & Assad, 1999; Buneo et al., 2002; Averbeck et al., 2005). Similarly, target related estimates can also be found throughout the parietal lobe (Buneo and Andersen, 2006). Such encoding properties represent several integral prerequisites associated with the planning of reaching movements and support a strong role of the parietal lobe in movement planning.

In addition, movement planning related activity has also been observed in both dorsal and ventral premotor areas of the frontal lobe (PMd and PMv, respectively). Through its connectivity with the parietal lobe, neurons in PMd and PMv receive both somatosensory and visual feedback (Caminiti et al., 1996) and have been shown to encode information related to the static position and configuration of the arm (Pesaran et al., 2006; Scott et al., 1997). For instance, activity PMd has been shown to encode information regarding of movement direction and amplitude (Messier &Kalaska, 2000; Pesaran et al., 2006, Cisek &

Kalaska, 2005), further implicating this area in the planning and coordination of reaching movements.

The ability to reliably generate movement plans is dependent on the functionality of all of these cortical areas. However, impairment to any of these areas (e.g. stroke, disease, etc) can result in sensorimotor deficits, often, manifesting in greater movement variability (Contreras-Vidal & Buch, 2002; Hermsdorfer & Goldenberg, 2002; Longstaff & Heath, 2006; Thies et al., 2009). Understanding how planning-related noise normally arises and is managed in these areas is critical for interpreting the exaggerated variability that often follows nervous system damage. Because sensory feedback are vital to internal state estimation and movement planning, it seems reasonable to assume that the characteristics of sensory noise have an equally influential role in shaping planning noise. In fact, in a recent study of variability in oculomotor control, Osborne et al. (2005) reported that the majority of variability in motor output could be attributed to variability in proprioceptive feedback. Thus, understanding the nature of sensory noise is of paramount importance to understanding the influence of planning noise on movement variability.

Sensory encoding of reaching parameters. Accurate estimation of hand position requires the integration of visual and somatic cues. Interestingly, inherent differences in the arrangement of the sensory receptors results in limb position information encoded in modality-specific reference-frames. For instance, visual estimates of position appear to be encoded with respect to the cyclopean eye, commonly referred to as an eye-centered reference frame (McGuire & Sabes,

2009; McIntyre et al., 1997, 1998). Vision provides a very reliable estimate of the

spatial relationship between objects in the environment making visual feedback

particularly salient for movement planning. This is consistent with

neurophysiological evidence that suggests the internal estimates of limb and target

position are encoded in an eye-centered reference frame in multiple parietal

regions associated with movement planning such as MIP, LIP and area 7 (Buneo

et al., 2002; Buneo and Andersen, 2006), as well as in PMd (Batista et al., 2007).

The role of proprioceptive feedback in reaching cannot be understated as it

provides postural and kinetic feedback integral to movement planning and state

estimation (Sober and Sabes, 2003; Sainburg et al., 1993; Vindras et al., 1998;

Desmurget & Grafton, 2000). Like vision, the arrangement of proprioceptors in

the arm results in proprioceptive estimates of limb orientation to be primarily

encoded with respect to the body (Scott & Loeb, 1994; McGuire and Sabes, 2009;

McIntyre et al., 1998). Information about limb orientation is pivotal for planning

and coordinating the appropriate sequence of motor commands which has led

some to suggest a prominent role in the specification of motor commands during

movement planning (Sober and Sabes, 2003). Proprioceptively derived estimates

of hand position can also be found in the parietal lobe. This is particularly evident

in area 5, which sits immediately anterior of MIP, an ideal position to affect

movement planning related activity in these areas (Buneo and Andersen, 2006). In

fact, activity in area 5 and MIP has even been shown to encode reaching

parameters in multiple reference frames, indicative of the influence of non-

visually derived estimates of limb in this area (Buneo et al., 2002).

Sensory uncertainty. As previously mentioned, inherent to any sensory signal is a measure of uncertainty affecting the reliability of encoded information about limb position. The spatial characteristics of uncertainty in limb position estimation are believed to arise largely from the nature/arrangement of the sensory receptors specific to each modality (Proske, 2005; Scott & Loeb, 1994; Wolpert, 2007). Thus, there are differences in the spatial patterns of uncertainty associated with each modality; a factor which appears to affect the specific role of each modality during movement planning and control (Kording & Wolpert, 2004; Scheidt et al., 2005; Sober & Sabes, 2003; van Beers et al., 2002; van den Dobbelsteen et al., 2001; Viguier et al., 2001). These patterns for estimation of arm position via vision and proprioception are illustrated in Figure 2.2. Localization via somatic cues is believed to be more precise (less uncertain) for hand positions closer to the body, and become more variable at more distant positions (van Beers et al., 1998). Vision, too, becomes less precise around the limits of the reaching workspace (Viguier et al., 2001). Additionally, sensory uncertainty appears to be direction dependent. That is, proprioception is believed to be more precise in estimating position in depth than along the azimuth, while vision has been shown to be more precise in azimuth than in depth (van Beers et al., 1998; van Beers et al., 1999).

The mechanism by which visual and proprioceptive information are integrated has been extensively studied. Despite this focus, their specific roles and contributions to sensorimotor control remain a matter of some debate (Bagesteiro et al., 2006; Berkinblit et al., 1995; Lateiner & Sainburg, 2003; McGuire & Sabes,

13

2009; Sainburg et al., 2003; Sarlegna & Sainburg, 2007; Sober & Sabes, 2003; van Beers et al., 1999). In most situations visual estimates have been shown to dominate perception; however, information from both senses is known to contribute to planning limb movements (Buneo et al., 2002; Rossetti et al., 1995; Soechting & Flanders, 1989; van den Dobbelsteen et al., 2001; Sober and Sabes, 2003). One prominent theory of sensory integration posits that sensory feedback signals are weighted on basis of their relative encoding reliability (the inverse of variability and uncertainty). In fact, a growing number of behavioral and neurophysiological studies have provided evidence in support of this perspective of cue integration (Angelaki et al., 2009; Deneve et al., 2001; Ernst & Banks, 2002; Wolpert et al., 1995, Wolpert, 2007).
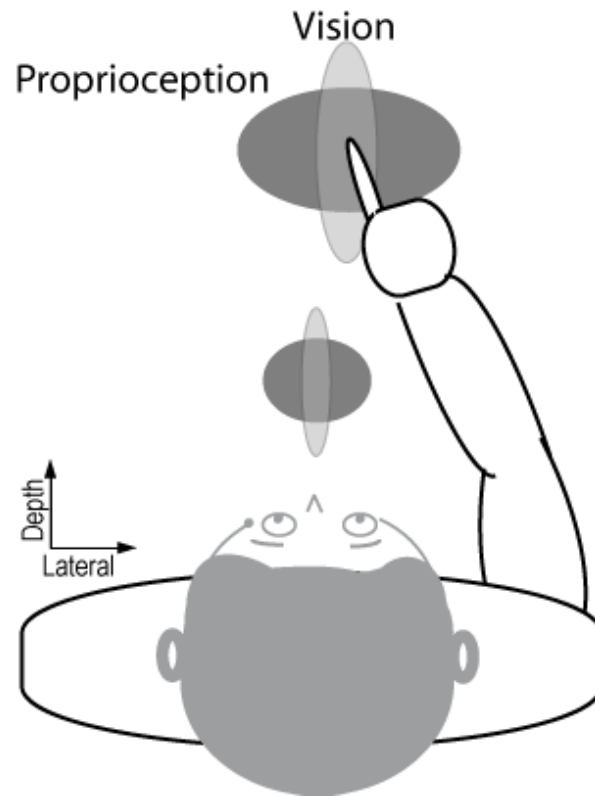
Figure 2.2. Spatial anisotropy in feedback uncertainty during position estimation.

In general, visual feedback provides a more reliable estimate of the limb position

along the lateral axis than in depth. Proprioception generally is more precise in

depth compared to laterally. Both senses become less reliable further from the

body. Adapted from van Beers et al. (2002b) *Exp Brain Res*.

Sensory integration. As previously described, modality specific receptor organization results in different reference frames used to encode limb position. These differences in encoding have been used to investigate the integration of sensory feedback in limb position estimation (Vindras & Viviani, 1998). For instance, when vision of the hand is given, reach endpoint errors appear to be most consistent with viewer/eye-centered coordinates; however, when visual feedback is withheld, endpoint errors appear to be in non-eye-centered reference frame and in some cases best accounted for in a body-centered frame (Carrozzo et al., 1999; McIntyre et al., 1997). These behavioral findings have a strong neurophysiological basis as many cortical areas associated with movement planning and sensorimotor control have also been shown to encode estimates of limb position in both eye-centered and limb-centered coordinate frames (Buneo et al 2002, Batista et al. 2007; Pesaran et al., 2006).Thus, many reaching related areas of the cortex receive multiple feedback inputs and are thus likely directly involved in the integration of visual and proprioceptive estimates of limb position.

The prevalence of viewer/eye-centered patterns of endpoint error have been used to infer the dominance of visual feedback in the estimation of limb position (Carrozzo et al., 1999; McIntyre et al., 1997, 1998), a finding which has been echoed at the neural level in the encoding of limb position in parietal area 5/MIP and in PMd (Buneo et al., 2002; Battaglia-Mayer et al., 2003; Battaglia-Mayer et al., 2007; Batista et al., 2007). However, these investigations did not attempt to posit a mechanism of integration, largely focusing on the spatial characteristics underlying behavioral variability; subsequent studies have

16

suggested it may be related to the properties of sensory uncertainty specific to each modality (Kording & Wolpert, 2004; Scheidt et al., 2005; Sober & Sabes, 2003; van Beers et al., 1999; van Beers et al., 2002b; van den Dobbelsteen et al., 2001, Viguier et al., 2001).

To minimize the influence of unreliable feedback, it is believed that the brain employs a scheme of integration which takes into account the previously described modality-specific characteristics of sensory noise. Specifically, recent work on multisensory integration suggests that sensory feedback is weighted by its relative reliability (Ernst & Banks, 2002; Kording & Wolpert, 2004; van Beers et al., 2002; Gu et al., 2008). In essence, this theory posits that when multiple signals are combined the integrated estimate is "optimal" with respect to minimal variability in localization of the limb (Wolpert, 2007); a prediction which is consistent with studies of human perception (Bays & Wolpert, 2007; van Beers et al., 1999; van Beers et al., 2002b).

At the neural level, population and single cell activity in multimodal areas have been shown to be consistent with this theory of sensory integration (for a review, see Angelaki et al., 2009). A prime example of this was provided by a recent study by Gu et al., (2008), wherein multimodal neurons in the dorsal medial superior temporal area exhibited 'sub-additive' combination of unimodal inputs encoding the same preferred direction, a behavior consistent with predictions of the weighted sum integration of unimodal inputs (Ma et al., 2006)

With respect to reaching, this theory allows us to predict how vision and proprioception will be integrated given the anisotropic nature of their respective

reliabilities. Specifically, visual feedback would be expected to dominate along both the horizontal and vertical axes (van Beers et al., 1998; van Beers et al., 2002b). Conversely, proprioceptive estimates of the hand in depth may be weighted more strongly relative to vision (van Beers et al., 1998). Indeed, some of these patterns have been confirmed in behavioral studies of limb position estimation (van Beers et al., 1999; van Beers et al., 2002b); while others (i.e. those pertaining to integration outside of the horizontal plane) have yet to be fully explored.

In addition to being conceptually straightforward, this theory of sensory integration also provides a mathematical framework to model sensory integration. This framework will be addressed more thoroughly later in this chapter; however it should be noted here that many of the predictions of this theory have been substantiated by empirical evidence (Kording & Wolpert, 2004; van Beers et al., 2002b). Thus, this mechanism may represent a potential strategy employed by the brain to mitigate the effects of sensory noise.

Sensory integration in 3D space. Despite being extensively studied in the horizontal plane, relatively little work has been performed to investigate whether mechanisms of sensory integration observed in 2D would generalize to 3D space. However, evidence from integration in the horizontal plane has yielded testable hypotheses of how this process may be occurring. For instance, due to the anisotropic nature of visual and proprioceptive reliabilities, visual feedback would be expected dominate along both the horizontal and vertical axes (Carrozzo et al., 1999; McIntyre et al., 1998; van Beers et al., 2002; Viguier et al., 2001), as well

as exhibit depth dependent changes in contribution (van Beers et al., 1998;). In addition, there is evidence which suggests the precision of both visual and somatic feedback decreases with distance from the body (van Beers et al., 1998; van Beers et al., 1999; Viguier et al., 2001). Given that the senses are believed to be weighted on the basis of their relative reliability, one would expect the integration of the two senses to vary with workspace depth. This prediction has yet to be directly evaluated. It remains unknown whether the weighting of the senses changes appreciably across the workspace. Investigating this potential workspace dependence will provide a more comprehensive understanding of workspace dependent sensory integration. This issue also has the potential to significantly affect interpretation of results, past and present, of experiments involving movements in depth.

The vertical plane is ideally suited to investigate these predictions as integration can be examined without the potential confound of moving in depth; however, integration in the vertical has also yet to be adequately evaluated. Recent evidence suggests sensory integration and movement planning may be significantly more complex for unconstrained movements outside of the horizontal plane (Desmurget et al., 1997; Le Seac'h & McIntyre, 2007; Scheidt et al., 2005). For instance, somatosensation provides important postural and kinetic feedback throughout the reach (Desmurget & Grafton, 2000; Sainburg et al., 1993; Vindras et al., 1998). This information may be particularly important for movements in the vertical plane, as orientation of the limb joints plays a significant role in the anticipation of the effects of gravity (Gentili et al., 2007; Le

Seac'h & McIntyre, 2007). Such findings underscore the need to more fully explore sensory integration in 3D during estimation of limb position. Examining these potential workspace dependencies is an important step toward a more comprehensive understanding of the processes and mechanisms which underlie this integration.

Sensory uncertainty and planning noise. As previously described, planning noise arises from the peripheral and central neural processes required to specify motor commands (Faisal et al., 2008; van Beers et al., 2004). An important constituent of planning noise for reaching movements is the uncertainty associated with sensory feedback (Osborne et al., 2005). Earlier in this chapter, we described vision as being considerably more precise along the azimuth direction than the depth direction (van Beers et al., 1998). In essence, the brain is better able to disambiguate radial position from visual signals than position in depth. The same is true with respect to the encoding uncertainty of somatic feedback of limb position; however it provides a more clear sense of position in depth than in azimuth. The inability to precisely distinguish between results in trial-to-trial fluctuations in the central signals associated with sensory estimates of limb position is thus tantamount to noise in the neural signals.

During movement planning, estimates of both the hand and target position are compared to derive the required motor commands. While typically sensed unimodally (i.e. via vision) estimates of target position are also subject to uncertainty in its estimation. Similar to encoding of limb position/orientation, this uncertainty manifests as noise in the neural signals encoding target position.

Therefore, planning noise results from the combination of uncertainty in limb position/orientation with the uncertainty associated with encoded target position.

At the neural level, uncertainty in estimation of the limb and target and the subsequent planning noise would be expected to be most apparent in those areas identified as being involved in movement. Traditionally, position estimates are considered to be encoded in specific activity levels of a cell or neural population that correlate to a given position of the limb. Within this structure, planning noise may manifests as variability in the cell or population activity between trials despite identical limb and/or target positions (Churchland et al., 2006a; Deneve et al., 2001). This has lead to a probabilistic theory of stimulus encoding wherein the encoding of a given limb position can be represented by a distribution of activity levels (Ma et al., 2006, Ma & Pouget, 2008). Thus, the range of activity levels that may result from a particular limb position may be a neural correlate of uncertainty in the estimation as it limits the ability of the brain to distinguish one position from another (Ma & Pouget, 2008). As neural estimates of limb and target position are combined, this variability in the encoding of each parameter will result in variability in the encoded movement plan between trials, which subsequently will affect behavior. This was the conclusion of the recent work by Churchland and colleagues who, in an elegant analysis of peri-movement activity in premotor cortex, were able to attribute a substantial portion of behavioral variability to variability in neural (motor preparation) activity in premotor cortex (Churchland et al., 2006a; Churchland et al., 2006b).

The influence of planning noise on movement variability. Planning noise results in trial-to-trial variability in the motor plan. Thus, even in the absence of variability in motor performance, planning noise will result in reaching errors. If the same movement is performed repeatedly, the result will be a distribution of endpoint errors which describe the spatial nature of planning variability. Given that the nature of planning noise is largely dependent on the feedback uncertainty, one would expect evidence of planning noise to manifest in movement errors similar in shape to those of sensory uncertainty described for visual and proprioceptive feedback. For instance, variability due to visually-related planning noise would be expect to be largely oriented along the depth axis; whereas planning noise associated with proprioceptive noise would be expected to yield endpoint errors distributed more strongly along azimuth. Each of these predictions have been observed in the patterns of endpoint variability following reaching movements suggesting a prominent role of planning related noise in shaping of reaching variability (Shi and Buneo, 2009; McIntyre et al., 1997, 1998; Carrozzo et al. 1999).

Motor Commands and Execution Variability

After the motor command is specified, cortical motor neurons are activated. The motor signals are carried down the corticospinal tract via the pyramidal tract out of the brain and down the spinal cord along the lateral or anterior corticospinal tracts. These axons connect with lower motor neurons (by direct synapse or often via interneurons) onto alpha motor neurons, whose axons carry the motor command out of the spinal cord along the anterior root toward

22

their respective muscle fibers. The alpha motor neuron and the muscle fibers it innervates constitute a motor unit. The number of motor units recruited depends on the size of force of the contraction specified during planning.

The motor command signal carried by the neurons is transmitted to the muscles via neuromuscular junction, a special synapse which connects nervous and muscle tissue. Within the muscle fibers, the impulse travels through T-tubules where it is disseminated to the muscle cells. The electrical signal is transduced into muscle contraction by actin-myosin binding within the sarcomeres of the muscle cells, which produces the limb movements. Each individual action potential produces a twitch response in the muscle fiber. As the firing rate of the motor neuron increases, the twitch responses "fuse" to produce a single prolonged contraction.

Execution noise. As previously described, execution noise is the result of variability arising during the transformation of the specified movement plan into the contraction of the muscles to generate movement (van Beers et al., 2004). Thus, whereas planning related neural processes culminate in the activation of neurons which project directly to muscles, the processes which constitutes the execution phase are the neural processes associated with carrying that signal to the target muscle tissue and the transduction of the electrical signal into muscle contraction and force production. Variability in force production can arise from several factors. For one, the same cellular and network processes that affect afferent sensory signals also affect efferent motor command signals. Thus, there is noise already present following the activation of the cortical motor neurons and

continues to arise throughout transduction. Similarly, because timing of action potentials is pivotal to force production, variability in the temporal structure of the motor command can result in variability of muscle force. Lastly, even if the motor signals were perfectly timed, variability in the muscle force can arise from the stochastic processes associated with the contraction of the sarcomeres within muscle tissue, which will also produce movement variability (Faisal et al., 2008). Therefore, these motor commands are inevitably corrupted by noise, which would result in movement variability even for identical motor plans.

In contrast to the processes associated with planning noise, the neural processes associated with execution noise do not have the opportunity to be mitigated by central processing. On the contrary, noise in the motor command is amplified as it descends through the divergence of motor neuron onto multiple muscle fibers, across the neuromuscular junction and across all the sarcomeres (Faisal et al., 2008;). Thus, the processes underlying execution noise can have a profound and detrimental effect on reaching performance. In fact, it has been shown that the characteristics of execution noise play an important role in the strategies employed during motor control (Harris & Wolpert, 1998, Wolpert et al., 1995; Todorov and Jordan, 2002) and the mechanisms of motor adaptation (van Beers, 2009), emphasizing the influence of execution noise on how the brain coordinates reaching movements.

The influence of execution noise on behavioral variability depends largely on the characteristics of the motor command and the resulting movement. In 2004, van Beers and colleagues attempted to quantify these effects in a task

24

designed to minimize the influence of planning related noise. The authors found that the amount of endpoint variability was largely signal dependent in nature, varying with the size of the motor commands along the direction of movement, particularly the terminal movement vector (van Beers et al., 2004). Thus, the influence of execution noise on reaching variability would be expected to manifest as endpoint variable errors elongated along the movement vector and scaling with the speed of the movement.

State Estimation and Sensorimotor Control

The ability to reliably and accurately encode limb position is critical to sensorimotor control and successful reaching. When the hand is at rest, sensory feedback provides adequate information for the estimation of limb and target position to plan motor commands. Results from behavioral studies have shown that limb state estimation is derived from a combination visual and proprioceptive cues. Thus, at the neural level cells involved in encoding estimates of limb state would have to be multimodal in nature, receiving both intrinsic visual and proprioceptive inputs. Within the parieto-frontal network there are a few areas whose neurons are likely to play a role in encoding estimates of limb position. Of note, parietal area 5 of the superior parietal lobe and both PMv and PMd, are particularly well situated to encode limb state as the activity of many cells in these areas are sensitive to vision, proprioception, or both (Buneo et al., 2002; Buneo & Andersen, 2006; Battaglia-Mayer et al., 2007; Battista et al., 2007).

Interestingly, in addition to receiving intrinsic sensory signals, a few of these areas also receive input from motor areas, providing area 5 and PMd/v with

efferent motor signals (MacDonald & Paus, 2003; Caminiti et al., 1996; Battaglia-Mayer et al. 2007). One explanation for this is that during movement, there is a significant lag between the sensory estimates of limb position and the real-time position of the hand. To overcome this, many have proposed that the brain must use the descending motor commands to generate a forward estimate of the hand (Desmurget & Grafton, 2000; Jordan & Rumelhart, 1992; Wolpert et al., 1995). The efferent motor signals could provide precisely this sort of dynamic information needed to generate real-time estimates of the limb. Indeed, PMd neurons have been shown to encode dynamic information of limb state, such as movement direction and velocity (Moran & Schwartz, 1999). Similarly, activity in the posterior parietal cortex recorded during movement provided strong evidence for a role of these neurons in forward estimation of the limb for online control (Mulliken et al 2008).

While the copy of efferent motor commands provides a means to estimate the real-time position of the limb, it is important to note the reliability of the estimate they provide is limited because of the influence of execution noise (in so far as these motor commands ultimately represent the actual movement generated). Thus, the process of state-estimation during movement must not only account for uncertainty in the sensory feedback, but also the noise associated with execution. As a result, sensorimotor control entails the constant interaction of planning and execution noise processes.

Interaction of planning and execution noise. It follows from the above discussion that during normal movement the brain must not only compensate for

the uncertainty associated with sensory feedback, but also noise arising at every stage of sensorimotor processing (Buneo et al., 1995; Faisal et al., 2008; Shi & Buneo, 2009; van Beers et al., 2004: Vindras et al., 1998). However, many studies of sensorimotor integration have used behavioral constraints, such as movements in 2D space or requiring slow movement (Desmurget et al., 1997; van Beers et al,. 2004), to artificially reduce the influence of noise at one level from interfering with those under study. This is due in part to the fact that studying movements with minimal constraints can be problematic, and in many cases the behavioral consequences of each process can be considerably overlapping. For instance, patterns of variability following movements with a significant component in the depth direction have often been found to be significantly elongated along the depth axis (Carrozzo et al., 1999, McIntyre et al., 1997, 1998; van Beers et al., 2004). These results could be interpreted as resulting from noise in execution (van Beers et al., 2004), noise in visual estimation of the target and/or hand (van Beers et al., 1998; Viguier et al., 2001) or noise occurring during other stages of planning (Carrozzo et al., 1999; McIntyre et al., 1997, 1998). In addition, a recent study of movements to targets in the horizontal plane argued that endpoint variability was best explained as the interaction of central and peripheral noise sources (Thaler & Todd, 2009).

While instrumental in characterizing their individual properties, task constraints which alter the normal processes of reaching limit our ability to assess the respective influences of planning and execution noise on normal movement variability. Moreover, it is uncertain to what degree these two sources of noise

combine and/or interact during a movement to shape variability. A recent suggestion was that they combine in a 'near-optimal' manner (Faisal & Wolpert, 2009); however this only examined total variability during a 2D reaching task. Thus little is known about how their interaction in the spatial domain differs during unconstrained reaching. This is a critical weakness in our understanding of one of the essential functions of the brain. The effects of this interaction are relevant to our understanding of such diverse sensorimotor functions as position estimation (van Beers et al., 1998; van Beers et al., 1999; van Beers et al., 2002), cue integration (Kording & Wolpert, 2004), as well as motor adaptation (van Beers et al., 2009) and planning (Harris & Wolpert, 1998). However, still more work needs to be done to further characterize the individual and combined influences of sensory and motor processes on the control of natural, unconstrained reaching movements.

Sensorimotor control of 3D movements. Reaching variability has been the focus of many sensorimotor investigations; however, much of this research has focused on movements limited largely to the horizontal plane. The level of difficulty/complexity involved in 3D coordination is far greater than that for 2D control (Desmurget et al., 1997; Blohm et al., 2009). Thus, constrained or planar reaches may not be able to fully represent the mechanisms used by the brain to plan and coordinate natural movement (Scheidt et al., 2005). As a result, it is unclear how well observations made of 2D movements generalize to similar movements made in 3D. With respect to reaching performance and variability, it is difficult to predict to what extent the added complexity will affect the

contributions of planning and execution noise on movement variability. For instance, one might expect that the increased complexity of forming a 3D motor plan may result in a greater influence of planning noise in behavioral variability. Conversely, because the specified movement plan may be more complex, involving significantly more muscle and joint action, elevated levels of execution related noise may pervade 3D endpoint distributions. As a result without direct evaluation, it is difficult to draw any conclusions *apriori* about this aspect of feedback control of 3D movements.

Computational Sensorimotor Integration

Computational models of sensory integration and movement production have provided numerous insights into both the behavioral observations as well as the neural underpinnings of sensorimotor control. In fact, numerous models have been developed to approximate the many aspects of sensorimotor control (van Beers et al., 1999; van Beers et al., 2004; Sober and Sabes, 2003; Saunders & Knill, 2004; Guigon et al., 2008). Of particular relevance are those approaches which attempt to model the perceptual and behavior consequences that arise from noise properties of sensory and motor processes.

Sensory integration. Sensory feedback integration is a complex process which appears to be highly context dependent, varying with a number of experimental constraints (Sober & Sabes, 2003; Scheidt et al., 2005). In the pursuit of better understanding of cue integration, many have turned towards various computational frameworks, producing a myriad of mathematical models (van Beers et al., 1998; van Beers et al., 2002b; Sober and Sabes, 2003). These

models run the gamut from simple to complex, each capturing particular elements of sensory integration.

As alluded to earlier in this chapter, there is growing evidence to suggest that sensory feedback integration is dictated in large part on the basis of the properties of uncertainty inherent to each modality. Specifically, the contribution of a given input is weighted by its reliability (the inverse of uncertainty) relative to the other available sources of feedback (for a review, see Wolpert & Kording, 2006). With respect to reaching, the integration of the visual and proprioceptive estimate of the arm would follow from:

$$X_{combined} = \frac{1/\sigma_V^2}{1/\sigma_P^2 + 1/\sigma_V^2}X_V + \frac{1/\sigma_P^2}{1/\sigma_P^2 + 1/\sigma_V^2}X_P \qquad (1)$$

Where X_V and X_P are the visual and proprioceptive estimates of limb position and σ_V^2 and σ_P^2 are the variances of those estimates, respectively. Further, under this framework the uncertainty associated with the combined estimate can also be calculated:

$$\sigma^2_{combined} = \frac{\sigma_V^2 \sigma_P^2}{\sigma_P^2 + \sigma_V^2} \qquad (2)$$

The resulting uncertainty of the integrated estimate also has the distinction of being the minimum value possible given the uncertainty of the inputs. Thus this strategy of integration is optimal in that it minimizes variance. This scheme of integration has been applied to many aspects of human perception and even sensorimotor control and evidence for optimal or near optimal integration of sensory feedback has found support from both behavioral (Ernst & Banks, 2002; Kording & Wolpert, 2004; Wolpert, 2007) and neurophysiological studies

30

(Deneve et al., 2001; Angelaki et al., 2009; Ma & Pouget, 2008; Morgan et al., 2008). This mechanism of integration has an important impact on movement variability: minimizing the uncertainty in the feedback estimate of the limb also reduces the levels of feedback noise, thereby reducing behavioral variability, believed to be a primary goal of the central nervous system (Harris & Wolpert, 1998; Kording & Wolpert, 2004). In fact, as discussed below, the principles of minimum variance optimality have found recent popularity as a strategy underlying the whole of sensorimotor control of reaching.

Optimal feedback control of reaching. In addition to recent evidence suggesting the brain combines sensory information in a statistically-optimal manner (i.e. minimal variance), similar principles have been observed throughout the stages of sensorimotor processing. During movement, sensory information of the limb significantly lags behind the real-time position of the hand, limiting the efficacy of feedback control (Rumelhart & Jordan, 1992;Wolpert et al., 1995; Harris & Wolpert, 1998; Desmurget & Grafton, 2000). To account for this, it has been suggested that brain employs a similar strategy to integrate lagging sensory feedback with a predictive estimate derived from efferent motor commands to yield an optimal, real-time estimate during movement (for a review, see Wolpert, 2007). This has resulted in the suggestion that the underlying neural processes act as an optimal feedback control filter (Mulliken et al., 2008; Todorov & Jordan, 2002; Wolpert et al., 1995). Similar to that of optimal sensory integration, this computational framework has been effectively used as a model of the neural processing underlying sensorimotor control to mimic/predict observations made at

31

both the behavioral and neurophysiogical levels (Deneve et al., 2007; Guigon et al., 2008; Saunders & Knill, 2004; Todorov & Jordan, 2002).

An example of such a feedback controller for reaching is illustrated in Figure 2.3. Here, the motor commands for reaching movements are generated in response to comparison of the internal estimates of the hand and target position. Throughout the movement, the internal estimate of the hand is constantly updated from the combination of sensory feedback estimate, the previous internal estimate, and the predicted estimate derived from the consequences of the motor output. Similar to sensory feedback, both the internal estimate and predictive estimate are tainted with uncertainty and signal noise. The feedback control model accounts for this by filtering the influence of incoming sensory estimate, in this case via the Kalman gain, on the basis of its reliability relative to that of the internal estimate of the hand. As a result, the combined estimate of hand position is also the minimum variance estimate, thereby reducing variability in motor planning. In this way, the integration of these estimates is analogous to the optimal sensory integration described above.

With respect to the control of reaching, Todorov & Jordan (2002) demonstrated that such optimal feedback control models can reliably reproduce normal human behavior during non-visually guided reaching movements (Todorov & Jordan, 2002). However, this was done assuming isotropic noise properties of proprioceptive feedback; instead the authors choose to focus on the effect of the changes in the relative levels of noise between sensory and motor processes. Saunders & Knill (2004) employed a similar approach to modeling

sensory-motor integration using some established properties of variability in visual estimation in the feedback control model. However, in this example, the authors did not incorporate a proprioceptive feedback signal, nor did they account for the anisotropic nature of visual feedback uncertainty. In Guigon et al. (2008), the authors included predictions of both visually guided and non-visually guided movements (Guigon et al., 2008). However, this was done assuming that the availability of vision would eliminate feedback noise altogether.

Both visual and proprioceptive feedback provide important of information and contribute to the perception of hand position and improved reaching performance (Rossetti et al., 1995; Desmurget & Grafton, 2000; Sainburg et al., 1993;Vindras et al. 1998; Carrozzo et al., 1999; McIntyre et al., 1997; Battaglia-Mayer et al., 2003; Sober & Sabes, 2003). Thus neither feedback modality can be ignored when designing a model of sensory feedback control. To gain a more complete picture of how noise in the neural processing underlying sensorimotor control affects behavioral variability an important step is to incorporate both visual and proprioceptive input into a feedback control model of reaching.

It is important to note that any feedback control model, which represents the internal processes underlying sensorimotor control, does not necessarily represent the activity of a single area or population of neurons. Rather, it only broadly represents the behavior of the entire network of cortical areas involved in sensorimotor control. Indeed, neurophysiological studies have found evidence for a number of the constituent processes and principles underlying this model (i.e. efference copy, minimum variance estimation, etc...), many of which are

described above. Therefore, the ability to reproduce reaching behavior by these principles will provide important insight into interactions and integration of the cortical areas associated sensorimotor control.
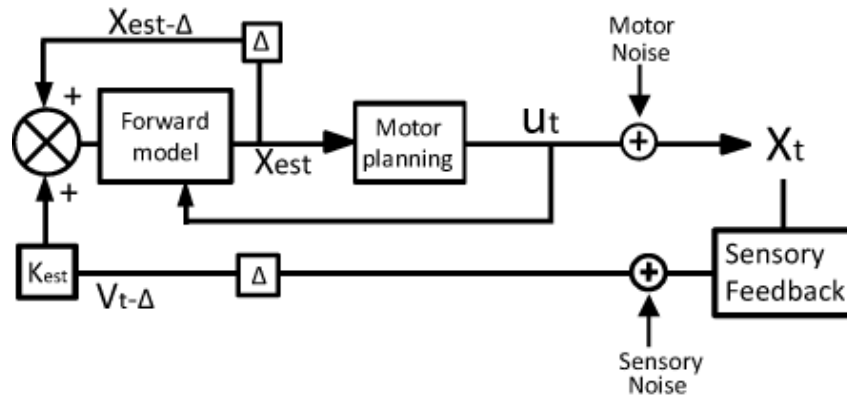
Figure 2.3. Block diagram for the feedback control of reaching. Xt represents the

state of the system (limb and target) and Xest represents the internal estimate of

the system developed by the brain from noisy sensory feedback. The estimate is

used to generate subsequent motor commands which are also corrupted by noise.

CHAPTER 3

CONTRIBUTIONS OF VISION AND PROPRIOCEPTION TO ARM MOVEMENT PLANNING IN THE VERTICAL PLANE

Introduction

The role of sensory information in the planning and execution of limb movements remains an outstanding question in motor neuroscience. One approach to studying the relative contributions of different sensory modalities in movement planning involves dissociating somatosensory (proprioceptive and/or tactile) and visual limb position cues prior to movement onset and quantifying the resulting effects on the early phases of movement. Studies employing this approach have demonstrated that misaligned sensory feedback at the starting position affects movement directions and amplitudes in a manner consistent with the motor system taking both vision and proprioception into account when planning movements (Rossetti et al.,1995; Sober & Sabes, 2003). In an elegant study combining behavioral analysis and computation modeling, Sober and Sabes (2003) showed that vision and proprioception contribute differentially to different aspects of movement planning, with vision playing a larger role in specifying the movement vector and proprioception being more important for planning the corresponding joint-based motor command. In addition, Sainburg and colleagues have shown that visual and proprioceptive cues contribute differentially to the planning of movement vector direction vs. distance (Bagesteiro et al., 2006; Lateiner & Sainburg, 2003; Sainburg et al., 2003).

In all of these studies, visual and somatosensory cues were dissociated along axes within the horizontal plane. However, there are several reasons to expect that the roles of these cues might differ for planned movements in the vertical plane. For example, arm kinematics vary for movements performed along different directions in the vertical plane, specifically in their time-to-peak velocity and relative time spent in acceleration vs. deceleration (Gentili et al. 2007; Papaxanthis et al., 2003; Papaxanthis et al., 2005). These findings suggest that, in contrast to horizontal plane movements, the production of vertical plane movements involves an optimization of both inertial *and* gravitational forces (Gentili et al. 2007). Moreover, experiments conducted in microgravity suggest this optimization is part of a movement *planning* strategy designed to anticipate the effects of gravity on the limb (Papaxanthis et al., 2005). According to this scheme, planning of arm movements in the vertical plane would take into account not only visual and somatosensory information about limb position but vestibular information as well, as suggested by several recent studies (Knox & Hodges, 2005; Le Seac'h & McIntyre, 2007; Mars et al., 2003).

The varying gravitational torques exerted on the arm when moving along different directions in the vertical plane would most likely be taken into account during the planning of motor commands. As described above, in the horizontal plane this stage of motor planning appears to rely more on proprioception than on vision. Proprioception likely plays an even more important role in planning motor commands during the production of unconstrained arm movements in the vertical plane. For example, proprioceptive signals appear to be perceived more readily in

terms of limb segment inclinations relative to vertical than as joint angles (Soechting & Ross, 1984; Worringham et al., 1987) supporting the idea that proprioception plays a key role in anticipating arm configuration dependent effects of gravity (Proske, 2005). In addition, proprioception likely plays an important role in distinguishing among the nearly infinite sets of arm postural paths (and therefore motor commands) that are consistent with a given planned movement vector in 3D space, which would be critical for movement planning in the vertical plane.

As an initial step toward understanding the mechanisms of multisensory integration during unconstrained 3D arm movements, we analyzed the effects of misaligned visual and somatosensory cues on reaching movements that were planned and executed along different directions in the vertical plane. We hypothesized that, similar to observations in the horizontal plane, movements would be altered in a manner consistent with the motor system taking into account both vision and proprioception during movement planning, but would be biased more strongly by proprioception, for the reasons described above. Moreover, since sensing the inclination of limb segments via proprioception may be more difficult as these segments become more vertically oriented (Worringham et al., 1987), we hypothesized that the contribution of proprioception to movement planning could vary with movement direction in the vertical plane, becoming stronger for more laterally directed movements.

Material and Methods

      Subjects. Twelve subjects (10 men, 2 women) between the ages of eighteen and thirty-two were recruited to perform the experiments. All procedures were approved by the Arizona State University Institutional Review Board and all subjects read and signed an informed consent form prior to participating. Subjects were briefed on the experimental procedures and what to expect when moving within the virtual environment but were naïve to the purpose of the study.

      Apparatus. The experimental apparatus consisted of a large, standing frame which supported a stereoscopic 3-D monitor (Dimension Technologies Incorporated, Rochester, NY), a metal shield and a chinrest (Fig. 3.1A, B). The monitor projected onto a mirror embedded within the shield. Subjects were seated with their head positioned on the chinrest in such a way that the eyes were aligned with the center of the mirror. The metal shield also served to block the arm from view, ensuring that all visual feedback was provided via the monitor projection.

      Motion tracking. An LED was positioned on the subject's fingertip to monitor the position of the hand throughout the reach. Fingertip/LED position was continuously monitored by a Visualeyez ™ VZ-3000 motion tracker (Phoenix Technologies Inc., Burnaby, British Columbia) at 150 Hz (0.5 mm spatial resolution). Visual feedback of position was relayed to subjects in real time via a virtual reality (VR) environment developed in Vizard® (WorldViz LLC. Santa Barbara, CA) and was displayed on the 3-D monitor as a green sphere of approximately 5 cm diameter in the 'near' workspace, as were the reach targets (see below).
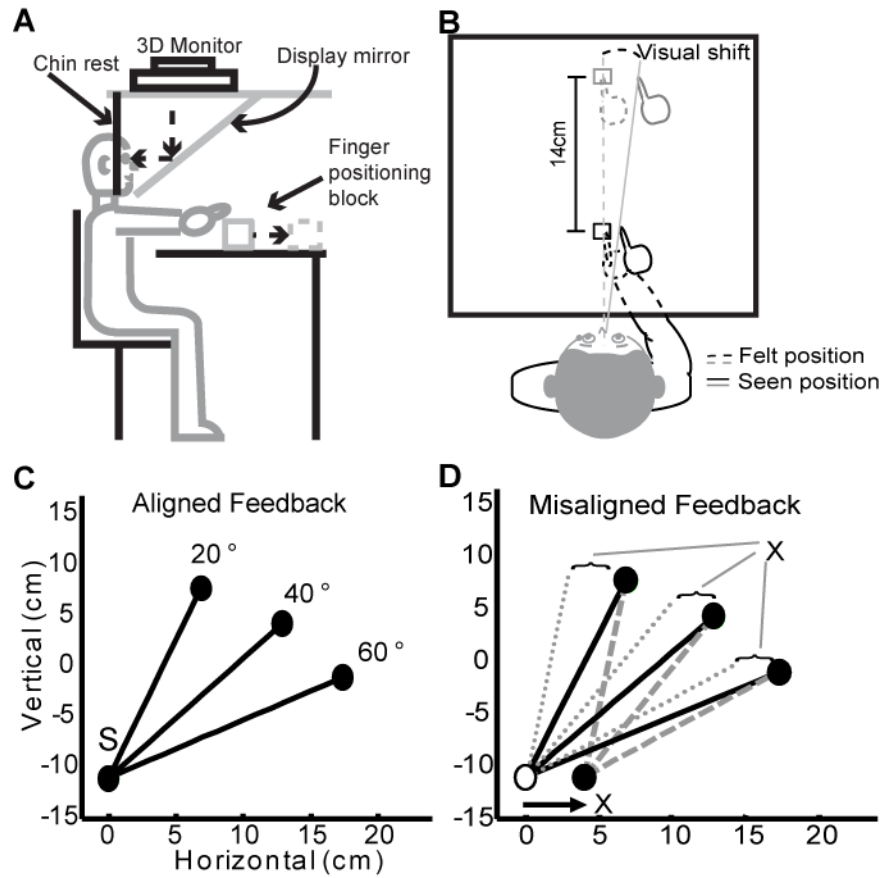
Figure 3.1. Experimental paradigm. **A.** Experimental apparatus. **B**. Visual

information was kept constant across workspace depths by scaling target positions

and visual displacements by a constant visual angle. **C-D**. Target layout in the

veridical (**C**) and shifted (**D**) feedback conditions, viewed from behind the

subject. In **D**, dashed lines connect the fully shifted hand position with the targets.

Dotted lines show the corresponding errors that would arise at the actual starting

position (S).

Experimental design. On a given trial, subjects reached to one of three targets oriented at 20, 40, and 60 degrees from the vertical line passing through the starting position (Fig. 3.1C-D). The starting position was located on a small block placed on the tabletop and centered on the body midline. The vertical (frontal) plane containing the starting and target positions constituted the task workspace. Since previous studies in 2D have suggested that the contributions of vision and proprioception to movement planning could be depth-dependent (van Beers et al., 1998), two workspaces were used; the 'near' workspace was located approximately 22 cm from the body surface, while a 'far' workspace was located 14 cm farther in depth, approximately 36 cm from the body (Fig. 3.1B). The angular relationship between the starting position and targets was identical in both workspaces. The distance between the starting position and each of the targets was constant within each workspace, but this distance was scaled with depth to maintain an approximately constant visual relationship between the starting and target positions. As a result, the distance between the starting position and targets was approximately 18 cm in the near workspace and approximately 23.5 cm in the far workspace.

Experiment 1. Horizontally displaced feedback. In this experiment, we varied the horizontal alignment of visual and proprioceptive cues at the starting position. Two feedback conditions were used: aligned and misaligned. In the aligned condition, visual feedback coincided with the finger's actual position at the starting location, which was kept constant via a tactile cue placed on top of the block illustrated in Fig. 3.1B. In the misaligned condition, visual feedback of

finger position was shifted to the right by 4.23 degrees of visual angle. This resulted in a real shift of 3.823 cm and 5cm in the near and far workspaces respectively. The use of different shifts for the different workspaces was done to maintain an approximately constant visual displacement between the felt and seen positions of the finger at each workspace depth. Though a tactile cue was provided to help localize the starting position, limb position was largely conveyed through proprioception, thus we use this latter term when referring to felt position.

The experiment involved four different blocks, one for each combination of the experimental variables: 1) Aligned-feedback in the near workspace, 2) misaligned-feedback in the near workspace, 3) aligned-feedback in the far workspace, and 4) misaligned-feedback in the far workspace. A blocked design was used because subjects detected the misaligned feedback when aligned and misaligned trials were interleaved; this was not the case when using the blocked design. As in Rossetti et al. (1995), in order to prevent adaptation no error feedback was provided to the subjects, and post-hoc analysis indicated this was indeed the case (see Results). The order of blocks was randomized. Subjects had no prior knowledge of the task conditions in a given block. Within each block, subjects completed thirty trials, ten to each target in random order.

Each trial began with the subject moving his/her unseen finger to the starting position (Fig. 3.1B). The starting position was associated with a small behavioral window (1.5 cm diameter) and once it was acquired visual feedback of the finger was provided. After a 350 ms holding period within the starting window, a target would appear, cueing movement. Upon leaving the start position

42

window, visual feedback of the finger was removed while the target remained illuminated. Thus, subjects experienced a brief but variable time window where the starting position and target position were simultaneously viewed, which aided movement planning, but movements were executed without online visual feedback of the moving hand.

Subjects were instructed to move quickly and accurately to the presented targets. Trials were considered successful if the subject remained within the allowable target window for 350 msec. Knowledge of results was provided via an auditory tone that signaled the trial was a success, but this information could not be used to further adjust endpoint position.

Experiment 2: Vertically displaced feedback. This experiment was identical to Exp.1 in every way except the displacement of visual feedback was in the positive vertical (upward) direction. Subjects executed reaching movements to the same three target positions from the same physical starting position.

Data analysis. Movement data were smoothed offline using a regressive/low-pass filter and instantaneous tangential velocities were calculated by differentiating the position data along the movement path. As in previous studies, we inferred the relative contribution of each sensory modality to the estimated position of the limb (and therefore movement planning) by analyzing the errors in initial movement direction that resulted from misaligned feedback (Sober & Sabes, 2003). Errors in movement direction in the frontal plane were evaluated at ~130 msec after movement onset. This time point was chosen to rule

out any effects of feedback signals, which can influence movement trajectories as early as ~150 msec after movement onset (Prablanc & Martin, 1992).

Due to the experiment design, errors in initial movement direction were expected to vary with target location, becoming progressively smaller for more lateral targets in Exp. 1 (illustrated in Fig. 3.1D) and for more vertical targets in Exp. 2. Thus, to evaluate potential target-dependent effects on the contributions of vision and proprioception to movement planning we calculated the changes in movement directions induced by the misaligned feedback and expressed them as a fraction of the maximum change that could be expected given the misalignment (which differed for each target). This provided a relative contribution index (*RCI*) of visual feedback for movements planned to each target position and workspace depth. The RCI was calculated as:

$$RCI_{d,t} = \left(\bar{\theta}_{aligned,d,t} - \theta_{misaligned,d,t} \right)/\theta_{d,t} \tag{1}$$

Where $\theta_{d,t}$ is the maximum change in movement direction expected for target *t* at workspace depth *d*, $\bar{\theta}_{aligned,d,t}$ is the average initial movement direction in the aligned condition for target *t* at workspace depth *d*, and $\theta_{misaligned,d,t}$ is the corresponding initial movement direction on misaligned trials. Due to the normalization procedure, an *RCI* of 1 indicated full reliance on vision while an *RCI* of 0 meant no reliance on vision.

Velocities, movement times, and induced changes in movement direction in each workspace were analyzed statistically using 2-way ANOVAs with factors target direction and feedback condition. Effects of target direction on *RCI*s in

44

each workspace were analyzed statistically using 1-factor ANOVAs. One-factor

ANOVAs were also used to assess the effect of trial number (and therefore time)

on the *RCIs* associated with each target location. Due to differences in variances

between the two experiments, a non-parametric Mann-Whitney U-test was used to

assess differences in RCIs arising from the direction of perturbation (horizontal

vs. vertical). The significance level for all statistical tests was $\alpha=0.05$.

Results

  Experiment 1: Horizontally displaced visual feedback. In both the

aligned and misaligned feedback conditions, subjects generally produced quick,

direct movements from the perceived starting position to the targets. For example,

in the near workspace average movement times were 463 +/-73 msec in the

aligned condition and 483 +/-83 msec in the misaligned feedback condition. In the

far workspace average movement times were 485 +/-95 msec in the aligned

condition and 466 +/-92 msec in the misaligned feedback condition. Figure 3.2

shows example movement paths for one representative subject in the aligned (2A)

and misaligned (2B) feedback conditions. These figures show that movements on

misaligned trials were generally rotated counter-clockwise compared to those on

aligned feedback trials, consistent with the rotation expected if the subject

incorporated both vision and proprioception into their estimate of initial hand

position (see Fig. 3.1D).

  Figure 3.2C shows the change in initial movement direction induced by

the misaligned feedback for all six subjects, as well as for the population. Data for

each target in the far workspace are shown. In this figure, a rotation of 0º would

indicate that subjects completely ignored the displaced visual feedback, planning and executing their movements based on somatosensory cues alone. In contrast, rotations of 12.17 °, 10.69 °, and 7.43 ° would be expected if subjects relied entirely on the displaced visual cues to produce their movements to the 20 °, 40 °, and 60 ° targets, respectively (as indicated by the bars at the far right). When data from all subjects and targets were combined, a significant main effect of the horizontal visual displacement on movement direction was observed in both the near and far workspaces (2-factor ANOVA, df=1, F=115.06, p<0.05). No effect of workspace or interactions effects were found. For each target, the induced rotations were generally between those expected for full reliance on proprioception and full reliance on vision, consistent with a movement plan that took into account both somatosensory and visual cues. In addition, most subjects demonstrated the pattern of gradually decreasing rotation for more horizontal targets, as expected given the direction of visual displacement. The most notable exception to this trend was Subject 6, who showed shift induced rotations that differed substantially from those of the other subjects. As a result, this subject's data were not included in the analyses of RCI (below).

As described in Material and Methods, we calculated the relative contributions of vision and proprioception separately for each target by normalizing the induced changes in movement direction by the maximum change expected given the horizontal visual displacement. Figure 3.3A shows the relative contribution indices (RCIs) for each target in the near and far workspaces. As expected given the results shown in Fig. 3.2, the RCIs were generally between

that expected for full reliance on vision (RCI=1) and full reliance on

proprioception (RCI=0). In both workspaces the mean RCI demonstrated a

tendency to decrease for more lateral targets. However, when the RCIs were

compared statistically across target locations using a 1-factor ANOVA, no

significant differences were found in either workspace. Combining the data across

all targets in both workspaces, we found that the mean RCI was 0.48 (+/-0.63).

This index was only slightly less than 0.5, suggesting vision and proprioception

contributed relatively equally to movement planning when these cues were

dissociated along the horizontal axis.

The relative contributions of vision and proprioception to movement planning in

this experiment did not appear to result from an adaptive process but instead

appeared to be present from the very first exposure to the displaced visual

feedback. This conclusion is based on the following observations. First, a one-

way ANOVA of the *RCI*s associated with different trials within a block was

performed by combining data across subjects for each trial (Lukos et al., 2010).

This analysis showed no difference in *RCI* across trials for any target location. In

addition, one subject returned and repeated the experiment in the near workspace,

performing twenty reaches to each target in separate blocks. The *RCI* associated

with the first five trials to each target was compared to that of the last 5 trials,

with no significant change noted in these indexes over the different blocks of

trials.
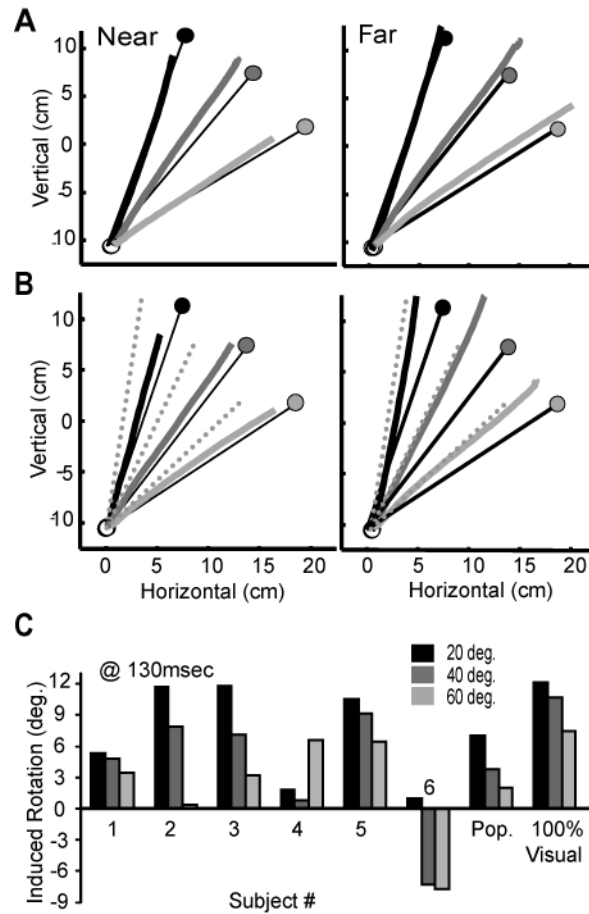
Figure 3.2. Effects of sensory misalignment on movement direction. **A.** Average movement paths from a single subject to targets in both workspaces in the aligned condition. Solid black lines: straight line paths to the target. **B**. Corresponding paths in the misaligned condition. Filled circles: target positions. Dotted lines: paths expected under full visual reliance. **C**. Misalignment induced changes in movement directions to each target in the far workspace for each subject and for the population. Bars to the far right illustrate the changes expected if subjects relied entirely on vision to plan their movements.

48

Experiment 2: Vertically displaced visual feedback. Given

proprioception's likely role in anticipating arm configuration dependent effects of

gravity, we reasoned that the contributions of proprioception and vision to

movement planning might show different properties when these cues were

dissociated along the vertical axis. To examine this possibility, subjects were

asked to perform the same reaching task as in Exp. 1 but under conditions where

the visual displacement was in the positive vertical direction. Here, movements on

misaligned trials were generally rotated *clockwise* relative to aligned trials (as

expected given the displacement direction). Although more variable than in

Exp.1, the degree of rotation and *RCI*s in Exp.2 also generally fell between the

indices expected for full reliance on vision and proprioception (Fig. 3.3B). In

addition, RCIs showed target-dependent trends that were similar to those in Exp.

1, decreasing progressively for more lateral targets. In fact, *RCI*s were

significantly different across targets in the near workspace (1-factor ANOVA,

df=2, F=3.82, p<0.05). Although the far workspace showed a similar trend, *RCI*s

were not significantly different across targets in this workspace. Combining the

data across all targets in both workspaces, we found that the mean *RCI* was 0.27

(+/-1.0). This index was significantly less than that associated with horizontal

visual displacements (Mann-Whitney U-test, df=1, chi^2= 15.21, p<0.05),

suggesting a generally stronger contribution of proprioception in movement

planning when vision and proprioception were dissociated along the vertical axis.
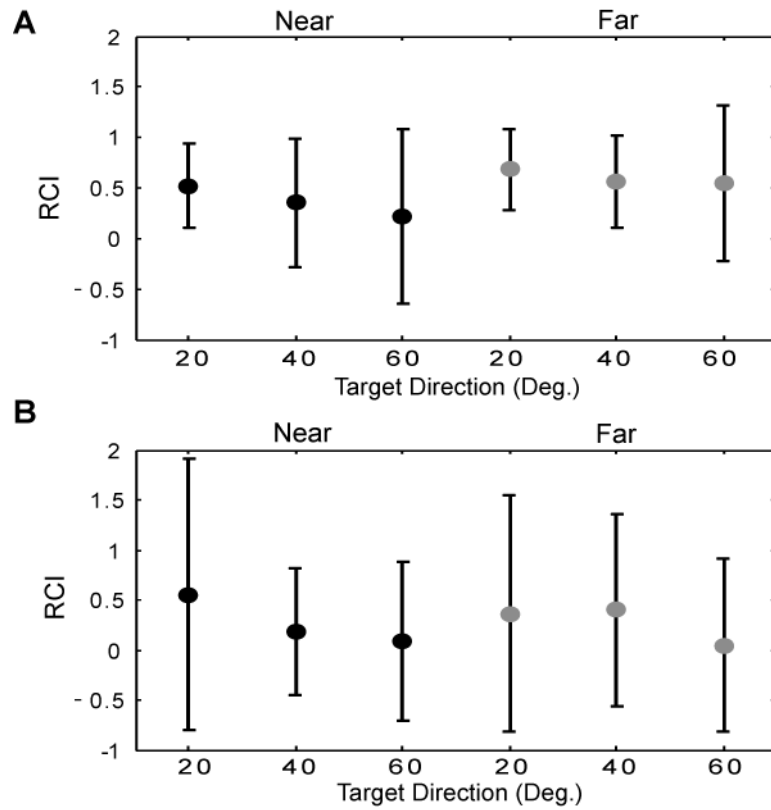
Figure 3.3. Contributions of vision and proprioception to movement planning. **A**.
Relative contributions of vision and proprioception (RCIs) for reaches to each
target in the near (black) and far (gray) workspaces in Exp. 1 (horizontally
displaced feedback). **B**. RCIs in Exp. 2 (vertically displaced feedback). Error bars:
Standard deviations.

Discussion

To our knowledge the present study is the first to investigate misaligned sensory cues at the starting position of unconstrained arm movements performed in the vertical plane. We also believe it is the first to investigate the effects of misaligned visual and somatosensory cues along the vertical axis. The findings suggest that vision and proprioception are both taken into account when planning vertical plane movements. Although we hypothesized that proprioception would contribute more strongly than vision to movement planning in the vertical plane, this appeared to be the case only in Exp. 2, where vision was dissociated along the vertical axis. This suggests that the contributions of vision and proprioception take into account factors other than the differing biomechanical requirements associated with moving along different directions in the vertical plane. For example, cue reliability is believed to be a major factor in determining the weighting of sensory cues in both the perceptual and motor domains (Angelaki et al., 2009). Thus, the differing contributions of vision and proprioception in Exps. 1 & 2 may point to differences in the relative reliabilities of vision and proprioception along the vertical and horizontal axes. This may arise from differences in the noise characteristics of the senses along the vertical and horizontal axes, or from differences in the contributions of other senses (e.g. vestibular) along these axes.

We also found that when visual and somatosensory cues were dissociated along the vertical axis in the near workspace, the relative contributions of vision and proprioception varied significantly with target location. In fact, this trend

51

pointed toward a larger contribution for vision for more vertical targets, as predicted if sensing the inclination of limb segments via proprioception was more difficult for these targets (Worringham et al., 1987). This general trend was also observed in the far workspace, as well as for both workspaces during horizontal displacements of visual feedback, though in these latter cases the observed trends failed to reach statistical significance. Nevertheless the present results provide evidence that the CNS may take into account the planned movement direction with respect to vertical when determining the relative contributions of vision and proprioception to movement planning. This interpretation would be consistent with proprioception's proposed role in anticipating arm configuration dependent effects of gravity.

As discussed in the Introduction, the effects of gravity would be expected to be accounted for during the planning of motor commands, rather than during the planning of movement vectors. These effects might alter the contributions of proprioception and vision to the planning of motor commands in the vertical direction. Stronger and more consistent effects of target location and/or direction of sensory misalignment might be revealed therefore by examining these stages of motor planning in isolation, which would require both behavioral measures and a suitable computational model of movement production in the vertical plane (Sober & Sabes, 2003). This type of model would be considerably more complex than for horizontal plane movements as it would need to account not only for the effect of gravitational forces on arm movements in different directions but also for the kinematically redundant nature of arm motion for unconstrained movements

52

in 3D space. However, this approach represents a logical next step in determining

the contributions of vision and proprioception to arm movement planning in the

vertical plane.

CHAPTER 4

INTERACTING NOISE SOURCES SHAPES PATTERNS OF ARM

MOVEMENT VARIABILITY IN 3D SPACE

Introduction

Limb movements are inherently variable. This variability is the result of

noise arising during the transformation of sensory signals into motor commands

('planning noise') as well as noise generated during the transformation of

commands into movements ('execution noise'; van Beers et al., 2004). Planning

noise includes uncertainty arising during the sensing process (Fig. 4.1) and

several studies have pointed to visual and/or proprioceptively derived uncertainty

as an important source of movement variability (Osborne et al., 2005; Shi &

Buneo 2009; van den Dobbelsteen et al., 2001; Vindras et al., 1998). Noise

generated during other stages of planning, e.g. during coordinate transformations

or during the specification of the required movement vector have also been shown

to contribute significantly to movement variability in humans (Gordon et al.,

1994; McIntyre et al., 1998; 1997; Vindras & Viviani, 1998). While figure 4.1

illustrates the feed-forward effects of planning noise, this process continues to

affect reaching performance throughout the movement as online feedback control

of the hand requires constant modification of the movement plan. In addition, a

recent neurophysiological study in non-human primates has shown that variability

in neural activity prior to movement onset can account for nearly half of the

variability in movement speed (Churchland et al., 2006a), further emphasizing the

strong contribution of planning noise to movement variability. As indicated

above, execution related noise can also profoundly affect movements (Buneo et al., 1995); in fact it has been suggested that in many circumstances patterns of arm movement variability are largely determined by execution-related noise (van Beers et al., 2004).

The interaction of planning and execution noise during natural movements is poorly understood, despite being essential for understanding the exaggerated variability that results from damage to the nervous system. At least two factors have contributed to this lack of understanding. First, in many psychophysical studies, behavioral constraints are built into the experimental procedures which serve to reduce the effect of noise at one stage of movement production from interfering with those under study, thereby obviating analysis of the interaction of noise sources. Second, analysis of endpoint distributions, a chief method for quantifying movement variability, is often confounded by the inherently similar behavioral consequences of planning and execution related noise in certain contexts. For example, in the studies by McIntyre and colleagues (1997, 1998), movements were made from starting positions near the body to targets located further in depth. The resulting endpoint errors were found to be elongated along the depth axis, which could conceivably have resulted from noise in execution (as movements had relatively large depth components), noise in visual estimation of the target or hand (as vision is relatively unreliable along the depth axis; see below) or noise occurring during other stages of planning, as argued by the investigators. It is equally possible that the interaction of two or more of these sources contributed to the observed endpoint variability (Thaler & Todd, 2009).

55

Recently, it has been argued that planning and execution related noise combine in a "near-optimal" manner (Faisal & Wolpert 2009). However, the relative contribution of each noise source to endpoint variability depends on a number of factors, including variations in the relative reliability of sensory information across the reaching workspace. For example, estimation of hand position depends on both visual and somatic cues. The precision of these cues is anisotropic in nature, being more reliable along azimuthal axes than in depth for vision and vice-versa for somesthesis (van Beers et al., 1999; 1998; van Beers et al., 2002b). In addition, the absolute precision of both cues appears to vary with position in the workspace, being less precise further from the body surface. These findings suggest that the contribution of sensor noise, and thus planning noise, to overall movement variability should vary with the position of the hand in the workspace.
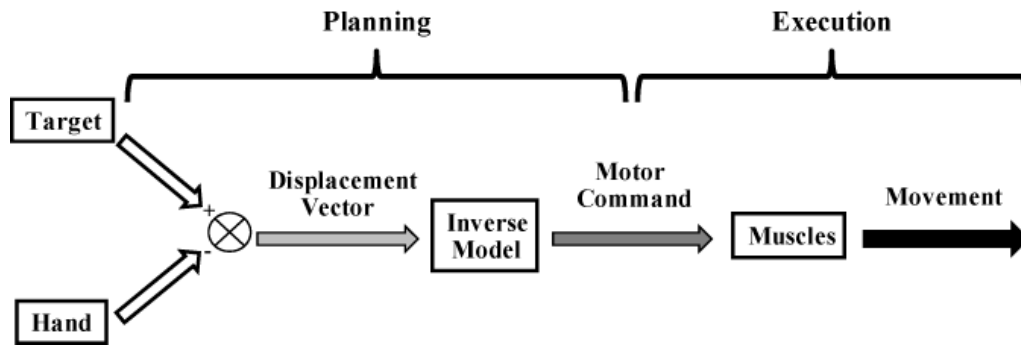
Figure 4.1. Simplified schematic representation of the processes involved in reach

planning and execution. Planning noise arises from noisy sensor estimates of hand

and target position and during the coordinate transformations required to produce

a displacement vector. Additional noise is added at later stages of processing,

including at the levels of the neuromuscular junction and muscles (execution

noise) to produced observed patterns of behavioral variability. It is important to

note that this illustrates the feed-forward process of movement planning;

however, this process is also involved in online feedback control of the limb

during movement. Thus, the affects of sensory and planning noise can be seen

throughout the movement.

Studies of planar arm movements have shown that execution related noise results in patterns of endpoint variability that depend on the required movement direction (van Beers et al., 2004). As a result, endpoint variability will vary not only with the position of the hand in the workspace but also with the path that the hand took to reach that position. Execution noise can be traced in part to noise in the commands to the muscles, the lengths and moment arms of which vary substantially with arm configuration. Thus, patterns of movement variability might even be expected to vary for the same movement vector executed at different positions in the workspace. This is particularly true for unconstrained movements in 3D space, which necessitate more complex sensorimotor transformations than those that are more constrained (Desmurget et al., 1997).

In the present investigation we studied the interaction of planning and execution noise across a large portion of the 3-D workspace of the arm. Seven human subjects performed reaches to targets arranged in three vertical planes separated in depth, and movements were made with and without visual feedback of the hand. In contrast to previous studies, starting positions were contained within the same vertical planes as the targets. As a result, required movement vectors were perpendicular to the depth axis, i.e. the axis along which visual planning noise would be expected to dominate. Planning and execution noise were accentuated by randomizing target positions from trial to trial and by switching the final target position during movement, requiring rapid, online changes in movement planning and execution. We hypothesized that movement variability would be largely dominated by execution noise and that this

dominance would be most apparent under visual conditions, where visual planning noise was relatively low. We found that in the presence of hand vision patterns of endpoint errors were anisotropic, with the principal axis of variability being largely oriented along the depth axis. In contrast, in the non-vision condition endpoint errors were larger and more isotropic. In both conditions, patterns of endpoint errors were only well aligned with the movement vector when movements were directed primarily along the depth axis. The results suggest that visual planning related noise determines the anisotropic nature of reach movement endpoints in 3D space, with execution noise acting to amplify or reduce this anisotropy in a direction dependent manner.

Methods

Subjects. Seven (7) subjects (4 women, 3 men) between the ages of twenty-one and twenty-five were recruited to perform the experiment. Prior to the experiment, subjects were briefed on the experimental procedures and what to expect when moving within the virtual environment but were naïve to the purpose of the study. The experiment complied with and was approved by the Arizona State University Institutional Review Board prior to subject recruitment and data collection and all subjects read and signed an informed consent form prior to participating.

Apparatus. The experimental apparatus consisted of a large, standing frame which supported a stereoscopic 3-D monitor (Dimension Technologies Incorporated, Rochester, NY), a metal shield and a chinrest (Fig. 4.2A). The monitor projected down through an opening in the frame onto a mirror embedded

59

within the metal shield, which also served to block the arm from view. The shield was suspended from the frame at a 45 degree angle with respect to the monitor. Subjects were seated directly in front of the shield with their head positioned on the chinrest in such a way that the eyes were aligned with the center of the mirror.

Motion Tracking. During an experiment, an LED was positioned on the subject's fingertip to monitor the position of the hand throughout the reach. LED position was continuously monitored by a Visualeyez ™ VZ-3000 motion tracker (Phoenix Technologies Inc., Burnaby, British Columbia) at a rate of 150 Hz (0.5 mm spatial resolution). The position data was fed back to the subjects via a virtual reality (VR) environment developed in Vizard® (WorldViz LLC. Santa Barbara, CA) and displayed on the 3-D monitor as a green sphere of approximately 5 cm diameter in the 'near' depth plane (see below). This system provided feedback of the hand within the virtual workspace in near real time. In addition, a large cube was rendered in the virtual environment to provide additional depth cues. Movement data were smoothed offline using a regressive/low-pass filter to reduce sampling noise and instantaneous tangential velocity was calculated by differentiating the position data along the movement path.

Experimental Design. The task was to execute a sequence of two reaches to targets located in each of 3 vertical planes positioned at different distances from the body (i.e. in depth; Fig. 4.2B). The VR environment was calibrated in such a way that the nearest plane of targets was located approximately 20 cm from the body surface, with each successive target plane located 8 cm farther in depth, making the respective depths of the planes 20 cm, 28 cm, and 36 cm. The

targets, as well as the centrally located starting position were rendered as green spheres of approximately 5 cm diameter in the near plane. This target size was chosen such that depth discrimination between target planes in the VR environment was clearly apparent facilitating judgment of target depth. As shown in Fig. 4.2B, targets were arranged on a circle in each vertical plane and were positioned 9 cm from the centrally located starting position. There were four primary targets (T1), located along the x (horizontal) and y (vertical) axes of the display. Each T1 was associated with two potential secondary targets (T2) located immediately clockwise or counterclockwise from a given T1. As a result, each T2 was approached from two different T1s, which allowed a comparison of the endpoint variability at a given T2 when this target was approached from two different directions. Note that starting locations for each vertical target plane were also varied in depth. As a result, required movement sequences were perpendicular to the axis along which visual planning noise would be expected to dominate, i.e. along the depth axis, in contrast to previous investigations of reach endpoints in 3D space (e.g. McIntyre et al., 1997, 1998).
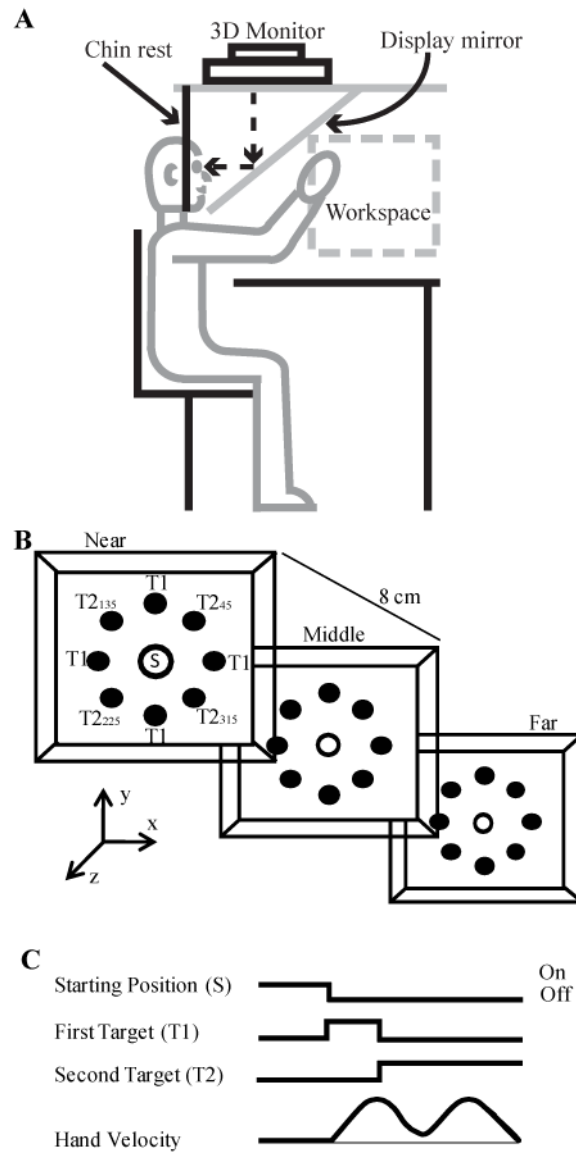
*Figure 4.2.*Experimental design **A.** Experimental apparatus. **B.** Target layout for each experimental depth. T1s represent position of initial targets, T2s the position of secondary targets. Each T2 is approached from both adjacent T1s for eight movement sequences per target plane. **C.** Trial sequence illustrating T1 and T2 onset and idealized tangential velocity profiles.

Movement sequences (i.e. combinations of T1 and T2) were performed with full visual feedback throughout the movement (visual (V) condition) or without visual feedback following movement onset (non-visual (NV) condition). Each trial began with the illumination of the starting position (Fig. 4.2C). This cue also defined the depth at which the subsequent targets would appear. Between trials, subjects had ample time (1.5 sec) to visually align their hand with the starting position. After a 350 ms holding period within the starting window, T1 would appear, cueing the first movement. Upon leaving a predetermined window (r = 4.5 cm) around the starting position, T1 would disappear and an adjacent T2 would appear, cueing the second movement. The size of this window was chosen such that T2 appeared very close to peak hand velocity to T1. This was done to ensure subjects immediately perceived the target jump by minimizing the effects of saccadic suppression (Prablanc et al., 2003), which was not the focus of the present research and a potential confound to analysis. On NV trials, coincident with the appearance of T1, the visual feedback of the moving hand was removed for the duration of the trial. On V trials, vision of the hand was always allowed. For each trial, the feedback condition (V, NV), depth plane, and the locations of T1 and T2 were all pseudo-randomly selected such that each combination of variables was sampled seven (7) times. The subject had no prior knowledge of any of these trial parameters prior to trial onset.

Selection of target positions was randomized both within and across depth planes on a trial by trial basis. In addition, subjects were instructed to move as quickly and accurately as possible to the presented targets. These aspects of the

63

experiment design were incorporated to accentuate planning and execution related noise processes rather than to minimize them, thereby allowing a characterization of their interaction. Subjects were also instructed to avoid correcting their position at the end of a sequence. Knowledge of results was provided by means of an auditory tone that signaled that subjects were in an acceptable window around the target (+/- 5 cm along each axis) but this information could not be used to further adjust endpoint position. The trial was considered a success if the subject moved to T2 in under 1400 msec and remained within the target window for 350 ms.

Data Analysis. Analysis focused on movement errors at the end of each sequence (i.e. at each T2). Movement endpoints were defined as the point at which the tangential movement velocity fell below 10% of its peak value for movements to T2. To assess accuracy, constant errors were calculated by subtracting the known target center (T) from the measured endpoint of the hand (h) on each trial. More specifically, constant errors along a given axis were calculated as:

$$e_d = \frac{1}{n_d}\sum_{i=1}^{n_d} h_d^i - T_d \qquad (1)$$

where T_d is the location of the target at depth plane d, h_d^i is the endpoint position of the hand for this target for trial i, and n_d is the corresponding number of trials. Similarly, precision was assessed by calculating the variable errors along a given axis for each target position as follows:

$$\sigma_d = \frac{1}{n_d}\sqrt{\sum_{i=1}^{n_d}(h_d^i - \overline{h_d})^2} \qquad (2)$$

where $\overline{h_d}$ represents the mean endpoint position for a given target at a particular workspace depth.

Movement endpoints were arranged according to subject, feedback condition, target sequence, and depth plane. Levene's test (a conservative test of equality of variances) was used to analyze the separate effects of workspace depth, feedback condition, and movement direction on the endpoint variability along each axis (for a given sequence). Where sample sizes were larger (e.g. after grouping endpoints across workspace depths for a given sequence) Bartlett's test of uniformity was applied. This also allowed us to assess more specific differences in variability (e.g. lesser or greater variance).

Principal components analysis (PCA) was used to quantify the size, shape and orientation of the endpoint distributions. For this analysis we first calculated the 95% tolerance ellipsoids associated with each endpoint distribution as follows (McIntyre et al., 1998; Morrison, 1990):

$$T_{95\%} = q \frac{(n+1)(n-k)}{n(n-q-k+1)} F_{0.05,q,n-q-k+1,} H \qquad [3]$$

where the dimensionality $q=3$, the number of target positions $k=1$, F refers to the 95% confidence F-statistic wit 3 and 3 degrees of freedom, and H is the covariance matrix of endpoint position h. Eigenvalues and eigenvectors were determined from the matrix T. The eigenvalues determined the size of the distributions, the ratio of the eigenvalues associated with each eigenvector determined the shape of the distributions and the eigenvectors themselves determined the orientation. A χ^2 test of the form used by Morrison (1990), and

McIntyre et al. (1997), was used to test whether any two eigenvalues were significantly different from each other, in order to ascertain whether the distributions were isotropic or anisotropic. For visualization purposes, 95% confidence ellipses and ellipsoids were calculated for the endpoint distributions using Matlab code based on the Khachiyan algorithm (Khachiyan, 1996; Khachiyan & Todd, 1993), as implemented by Nima Moshtagh.

In a recent examination of the role of execution noise in movement variability, it was observed that movement variability (endpoints and initial movement directions) varied systematically with movement direction (van Beers et al., 2004). Moreover, when movements in a single direction but different distances were examined, endpoint ellipses were better aligned with the last part of the movement trajectory than with the straight line joining the starting position to the target, a finding attributed largely to execution noise. In order to estimate the contribution of execution noise in the present experiment we consequently related endpoint variability to both the 'total' movement vector between T1-T2 (vector connecting T1 and T2 endpoints), as well as the 'terminal' movement vector, i.e. the difference between the T2 endpoint and the hand position 200 msec prior to the end of movement. More specifically, to evaluate the degree of alignment between execution and endpoint variability we calculated the angle in space (α) between the movement vector (both total and terminal) and the first eigenvector derived from PCA.

Results

Subjects generally produced stereotyped reaching trajectories under both feedback conditions. Figure 4.3 shows endpoint positions and average movement paths for clockwise sequences in the frontal plane. Data for a single subject at each workspace depth are shown. Though movements in both conditions were very stereotyped, movements in the NV condition (red) often undershot T1 and were then followed by a slightly more curved and variable movement to T2. In contrast, when vision was available (blue), subjects moved completely to T1, then executed the movement to T2 in a more direct and consistent manner. This behavior is consistent with previous findings under similar feedback conditions (Prablanc et al., 1979).

Temporal aspects of the movement trajectories also differed somewhat between feedback conditions but, as with the movement paths, these differences were consistent across depths. Peak velocities to T1 in the NV condition were significantly slower than their V counterparts for many sequences ($p < 0.05$). The reduced velocities and durations on NV reaches suggest a misestimation of the movement amplitudes required to reach T1. With respect to movements to T2 (which remained visible throughout), there were no significant differences in peak velocities and movement times between the V and NV conditions. Regarding workspace depth, no significant effect of depth on peak velocities and movement times to T2 was noted for either condition.

Endpoints in the V condition were in general more accurate and less variable than those in the NV condition. However, in both feedback conditions,

variability was generally most pronounced along the depth axis. This can be readily appreciated in Fig. 4.4, which shows a top-down view of the movements and endpoints shown in the "Middle" plot of Fig 3. Variable errors were larger along the depth axis than along the horizontal for both the upper (left panel) and lower (right panel) T2s. This was true in both feedback conditions, though the endpoint distributions were larger without vision. The mean of the endpoint distributions (constant errors) were also occasionally biased outside the target plane though the nature of this bias (under or overshoot) was both target and subject dependent. Such idiosyncratic behavior with regard to constant errors has been reported elsewhere (Berkinblit et al., 1995; Darling & Miller 1993; Foley & Held 1972; Soechting & Flanders 1989a) thus these errors were not explored in detail. Instead, we will focus our discussion on the variable errors, which provide more direct information about planning and execution-related noise. We first consider the endpoint variability in the V condition and then consider these errors in the absence of visual feedback.
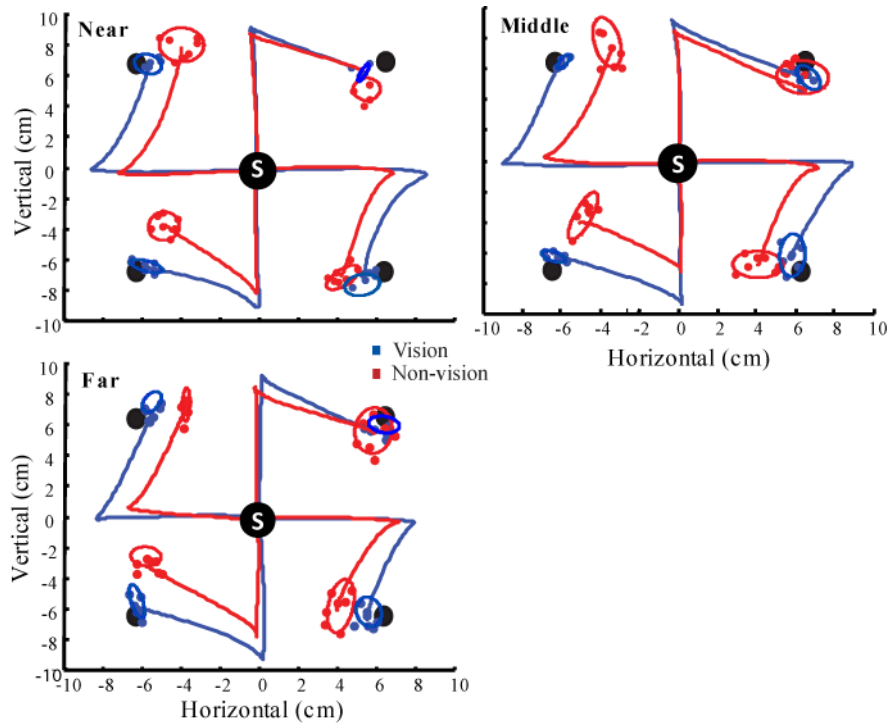
Figure 4.3. Mean trajectories and endpoint positions to clockwise T2s. Each depth

is represented for one subject. Each colored dot represents the endpoint for a

single trial to the target in a given feedback condition. Open ellipses represent

95% confidence ellipses for the endpoint distributions in each feedback condition.

Filled black circles refer to target locations. Performance generally varied

between V and NV conditions, but did not vary with depth for a given T1-T2

sequence.
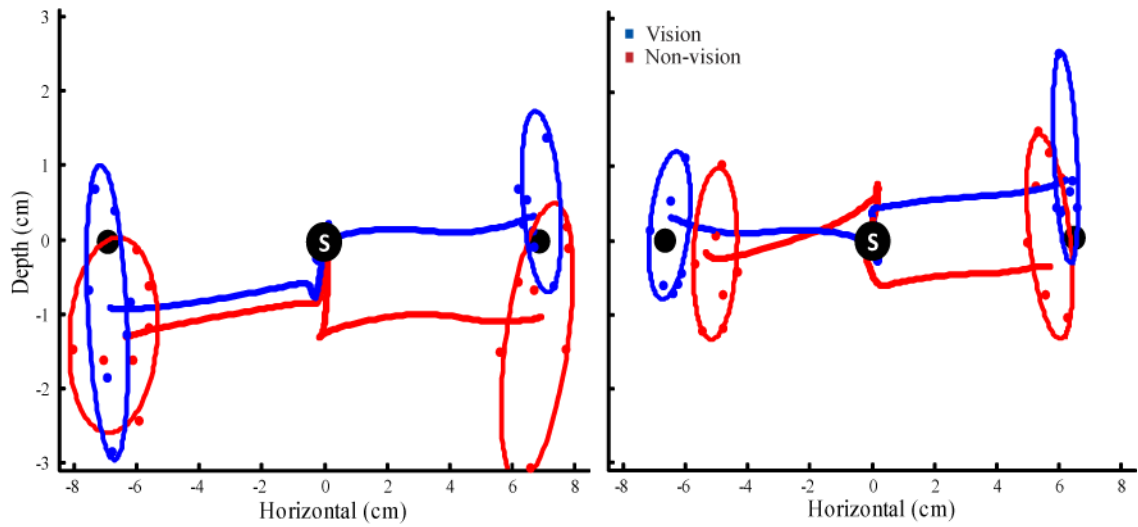
Figure 4.4. Mean trajectories and endpoint positions in the horizontal plane to
upper (left) and lower (right) T2s for the movements shown in the 'middle'
workspace depth of Fig. 4.3. Other figure conventions as in Fig. 4.3. Variability
along the depth axis was generally similar in magnitude between V and NV
conditions.

Endpoint variability under visual feedback. The pattern of endpoint variability associated with a given movement sequence was relatively consistent across workspace depths and subjects. Figure 4.5 shows bar plots of the variable errors along each axis for the clockwise movement sequences in a single subject (the same subject as in Fig. 4.4). Data for identical movement sequences (i.e. same T1-T2 combination) executed at different workspace depths are shown in each panel. As indicated above, variable errors tended to be larger along the depth axis than along the horizontal or vertical axes; this is most evident for $T2_{135}$ and $T2_{225}$. In addition, the relative distribution of endpoint variance associated with a given movement sequence was generally consistent across depths. This was quantitatively assessed by comparing the variance along a given axis as a function of workspace depth. When data from all subjects and sequences were analyzed, only 14 out of 168 (8%) sequences showed an effect of workspace depth (Levene's test, $p < 0.05$). Thus, we conclude that the endpoint variability associated with identical movement sequences was not significantly affected by changes in workspace depth in this experiment.

For planar arm movements, patterns of endpoint variability have been shown to be better related to the terminal phases of the hand trajectory (which include any curvature), than to the vector connecting the initial hand position to the target (van Beers et al., 2004). This has been used to argue that endpoint variability is better related to execution than planning noise. Thus, a key question concerns how well the orientations of terminal movement vectors in the present experiment can explain the observed patterns of endpoint variability. To aid in

71

comparing the terminal movement vector with the distribution of observed variable errors we used PCA. The first eigenvector typically accounted for 60-75% of the total variance in endpoint position and the first two eigenvectors typically accounted for nearly 95% of the variance, consistent with other studies of endpoint variability in 3D space (McIntyre et al., 1998; 1997). To assess the role of execution-related noise, we used the first eigenvector as our estimate of the orientation of endpoint variance and compared that to the orientation of both the total movement vector and the terminal movement vector (see Methods). The rationale is that if execution related noise were largely responsible for producing the anisotropic distribution of errors observed in this task, then the first eigenvectors and movement vectors should be roughly aligned in 3D space.

Visual inspection of movement paths suggested that neither the total movement vector nor the terminal vector could account for the generally large out-of plane (depth) component of the first eigenvectors. This can be appreciated from Fig. 4.6 which illustrates for a single subject the average movement paths (blue lines) and 95% confidence ellipsoids for sequences in the middle plane. Black lines cutting through each ellipsoid represent the first eigenvector for that sequence, centered on the mean endpoint. In the frontal plane (Fig. 4.6a), ellipsoids and eigenvectors suggest some degree of elongation of the endpoint variability along the mean T1-T2 path. This is consistent with our expectation that execution noise plays a role in determining endpoint variability, especially when visual planning uncertainty is reduced. However, for most sequences, only a small portion of the eigenvector is observed to project onto the frontal plane. Instead,

for many sequences the first eigenvector was oriented *perpendicular* to the plane

containing the starting position and targets. This is most evident in Fig. 4.6b,

which shows top-down views of the same movements and ellipsoids. For both

upper (top) and lower (bottom) T2s, the orientations of the ellipsoids and

eigenvectors were clearly biased along the depth axis. Moreover, they are clearly

not well aligned with the average movement paths, which were largely

horizontally directed.

Figure 4.6 suggests that the principal axis of movement variability was not

well explained by the orientation of either the total or terminal movement vectors

in this experiment. This was generally the case. First, on average, the 1st

eigenvector had a significantly larger component along the depth axis than along

the horizontal and vertical axes (Kruskal-Wallis test, $p<0.001$; Fig. 4.7a). In

contrast, the components of the mean terminal movement vector were not

significantly different from each other, which suggests that eigenvectors and

terminal movement vectors were often misaligned. To verify this we calculated

the angle (α) between the total/terminal movement vector and the first eigenvector

for each sequence. For the terminal vector, the mean angular difference across

sequences was 58˚ (+/- 21), much larger than one would expect if the movement

vector (and therefore execution-related noise) were largely responsible for the

observed anisotropy in endpoint position. With respect to the total movement

vector, a mean α of 69˚ (+/- 19) was observed, indicative of even poorer

alignment. The terminal movement vector was better than the total vector at

explaining patterns endpoint variability in virtually all analyses and in both

73

conditions. As a result we will focus the rest of our discussion of execution noise on this vector.

It is important to emphasize that the movement vector *did* affect endpoint variability in this experiment, it just did so in an axially-dependent manner. This was ascertained by correlating α with the degree of movement along each axis. Since a given movement sequence resulted in largely identical patterns of movement variability at each workspace depth we combined the variable errors for identical sequences across depths for this analysis. This also served to increase our statistical power. For the terminal vector, α was uncorrelated with movement along the vertical axis (r = 0.06; p = 0.66) and was only weakly correlated with horizontal movement (r = 0.426; p < 0.01). However, α was strongly correlated with movement along the depth axis (r = -0.643; p < 0.001; Fig. 4.7c). In fact, when the component of the terminal movement vector was greater than 0.75 (i.e. when it was oriented largely along the depth axis) then α was on average 36˚ (+/- 17), indicating a relatively high degree of alignment. Note that although we combined data across workspace depths for this analysis, these basic trends were clearly observable without such grouping. Thus, in this condition, anisotropies in endpoint position appear to be largely related to misestimating the final position in depth, with a smaller contribution from execution-related noise processes.

We also assessed the influence of execution noise by comparing the endpoint distributions for pairs of movement sequences associated with different T1s but the same T2. The average angle between terminal movement vectors to a common T2 was 85º (+/- 32.5). Given this disparity, we predicted that a strong

74

influence of execution noise would result in significant differences in the endpoint variability associated with different movements to the same T2. We found that for 43% (12/28) of the possible comparisons, endpoint distributions differed significantly along at least one axis (Bartlett's test, $p<0.05$). This indicates that the movement path did affect endpoint distributions to some degree in this experiment, which could reflect the influence of execution-related noise.
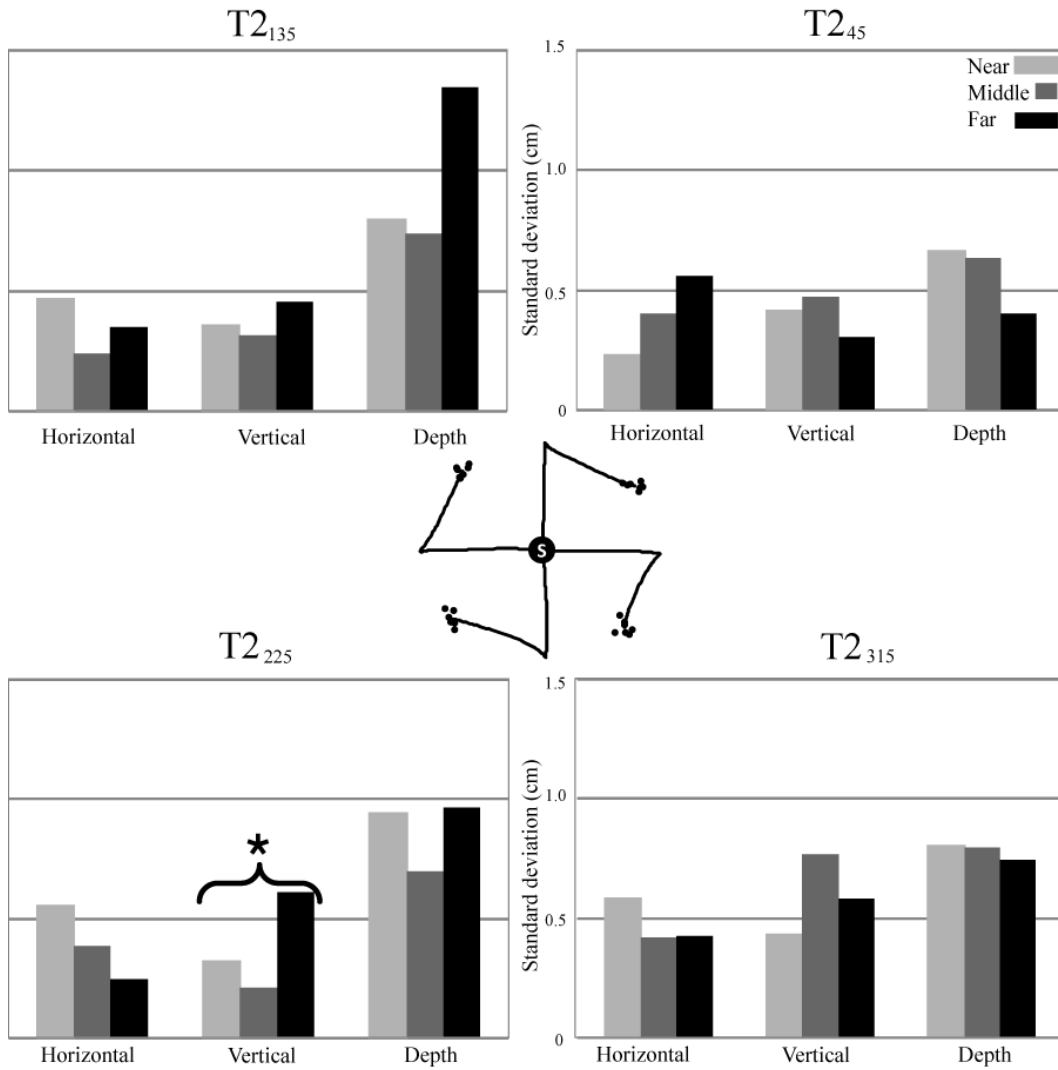
Figure 4.5. Single subject variable errors for clockwise sequences performed at each workspace depth. Axis-specific errors were compared across workspace depths for identical sequences using Levene's test. Stars demarcate statistically significant differences ($p<0.05$). A significant result along any one axis resulted in the entire sequence being classified as being 'workspace dependent'. When all subjects and sequences were considered only 8/168 sequences (~5%) were classified in this way.

Figure 4.6. Mean trajectory and 95% confidence ellipsoids in the V-condition. **A.**
Frontal plane view of the mean trajectories and endpoint positions for clockwise
sequence in the middle workspace. Data from one subject in the V condition are
shown. Also shown are 95% confidence ellipsoids for each endpoint distribution
and the first eigenvectors derived from principal components analysis of these
distributions (black lines). In this view ellipsoids appear to be aligned to some
degree with the mean trajectory. **B** Top-down view of the same movements
shown in **A** for the upper (top) and lower (bottom) T2s. Eigenvectors and ellipses
appear largely oriented along the depth axis and not with the mean trajectory.

77
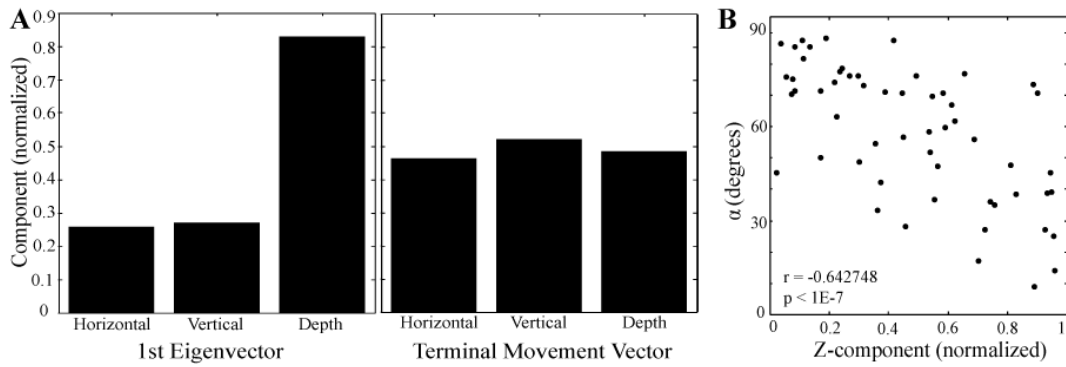
Figure 4.7. Comparison of eigenvectors and terminal movement vectors. **A.** Axial components of the 1st eigenvector (left) and terminal movement vector (center), averaged across all subjects and sequences. Eigenvectors were significantly biased along the depth axis (p<0.001) whereas terminal movement vectors were not biased along any axis. **B.** Scatterplot of the depth component of the terminal movement vs. α (the angle between the 1st eigenvector and the terminal movement vector). Significant negative correlation indicates that larger components of movement in depth resulted in greater alignment of movement and eigenvectors.

Endpoint variability without online visual feedback. Similar to the V condition, patterns of endpoint variability in the NV condition were relatively consistent across workspace depths and subjects. In this condition we did not observe as strong a tendency for variable errors to be elongated along the depth axis. That is, neither the average terminal movement vector nor the average 1st eigenvector were biased along a particular axis. However, patterns of endpoint variability associated with a given sequence were still generally similar across workspace depths. That is, when data from all subjects and sequences were analyzed, only 15 out of 168 sequences (9%) showed an effect of workspace depth (Levene's test, $p < 0.05$). Thus, similar to the V condition, endpoint variability associated with identical movement sequences was not significantly affected by changes in workspace depth.

Figure 4.8 illustrates average movement paths and 95% confidence ellipsoids for a single subject in the NV condition. Here, ellipsoids appear larger and more isotropic than those in the V condition. This is consistent with the prediction that an increase in sensor uncertainty would lead to more variability overall. Similar to the V condition, first eigenvectors in this condition had large components in depth. However, this was less consistently observed than for movements with visual feedback. Also similar to the V condition was the tendency for the eigenvectors and movement vectors to be misaligned. This can be seen in both the frontal (Fig. 4.8a) and horizontal plane views (Fig 8b). These observations are consistent with the idea that the removal of visual feedback results in an increase in sensor uncertainty (and therefore planning noise).

Consequently, more isotropic patterns of movement variability were observed in this condition than when vision of the hand was available. The overall increase in planning noise was such that evidence of execution related variability was less evident in the observed endpoint distributions in this condition.

The above observations regarding endpoint variability in the NV condition were consistent across subjects and for the majority of sequences. In general, endpoint distributions were more isotropic without hand vision and the first eigenvectors describing these distributions were still generally not aligned with the terminal movement vector. These conclusions were based on the following: first, as stated above, the components of the mean eigenvector across subjects and sequences were not significantly different from one another in this condition, which indicates a lack of consistent anisotropy in the endpoint data. Mean movement vectors were also not biased along a given axis. In addition, the angle between the between the terminal movement vector and first eigenvector was still generally quite large (54˚, +/- 23), illustrating the lack of consistent relation between the orientations of the terminal movement vectors and the primary axis of movement variability. Similar to the V condition, alignment between the first eigenvectors and movement vectors was not correlated with the degree of movement along the vertical axis ($r = -0.003$; $p = 0.98$) and was only weakly correlated with horizontal movement and movement in depth ($r = 0.314$; $p < 0.05$, and $r = -0.420$; $p < 0.01$, respectively).
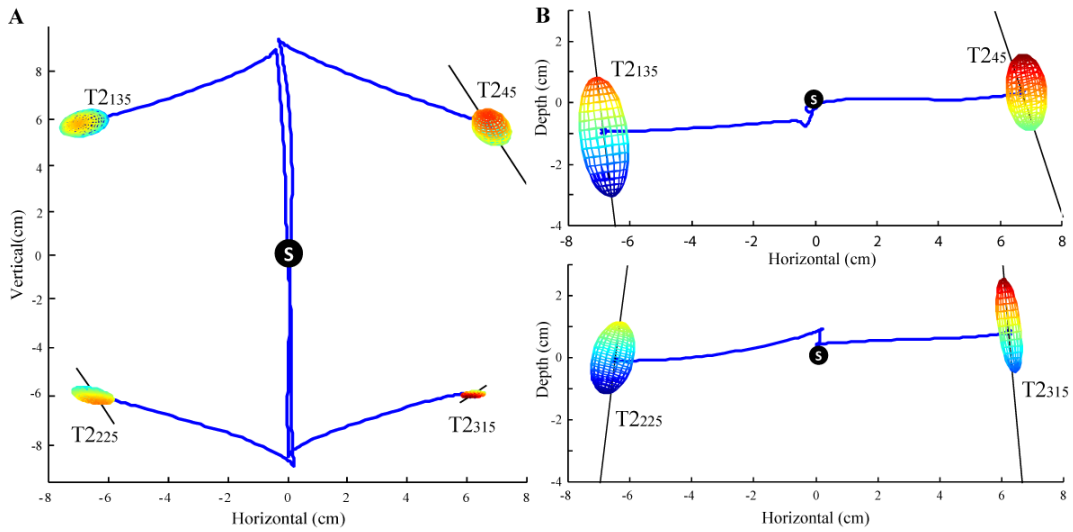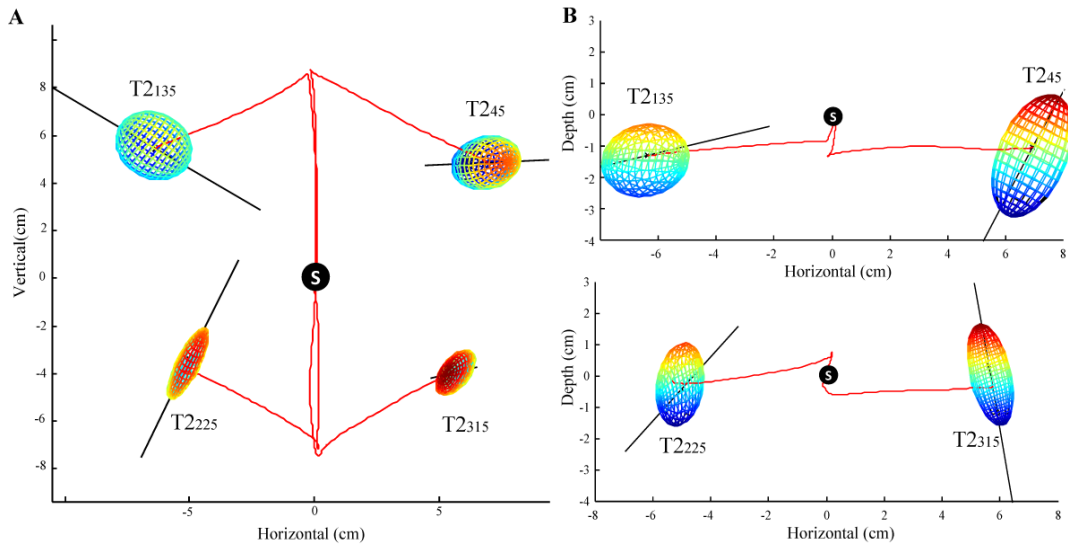
Figure 4.8. Mean trajectory and 95% confidence ellipsoids in the NV-condition.

A. Frontal plane view of the mean trajectories and endpoint positions for clockwise sequence in the middle workspace (NV condition). Figure conventions as in Fig. 4.6. Ellipsoids are generally larger and more isotropic than those of the V condition (Fig. 4.6). **B**. Top-down view of the same movements shown in **A** for the upper (top) and lower (bottom) T2s. As in the V condition, eigenvectors and ellipsoids appear largely oriented along the depth axis and not with the mean trajectory.

Effects of online visual feedback. These results may also be interpreted with respect to the role of vision in the online control of arm movements in 3D space. To evaluate the effect of online visual feedback, we compared endpoint variable errors between the two visual feedback conditions. Since we rarely observed a significant effect of workspace depth on variable errors, endpoints were combined across workspaces for identical sequences. Figure 4.9 illustrates the variable errors in both conditions for clockwise sequences from a single subject. In general, endpoint variability in the V condition was significantly reduced along the vertical and horizontal axes but not along the depth axis (Bartlett's test, $p<0.05$). This pattern was consistently observed across sequences and subjects. This observation suggests visual feedback reduces sensor and planning noise along the horizontal and vertical axes (relative to NV conditions), but does not reduce sensory uncertainty in depth, consistent with observations obtained in studies of hand position estimation in the horizontal plane (van Beers et al., 1998).
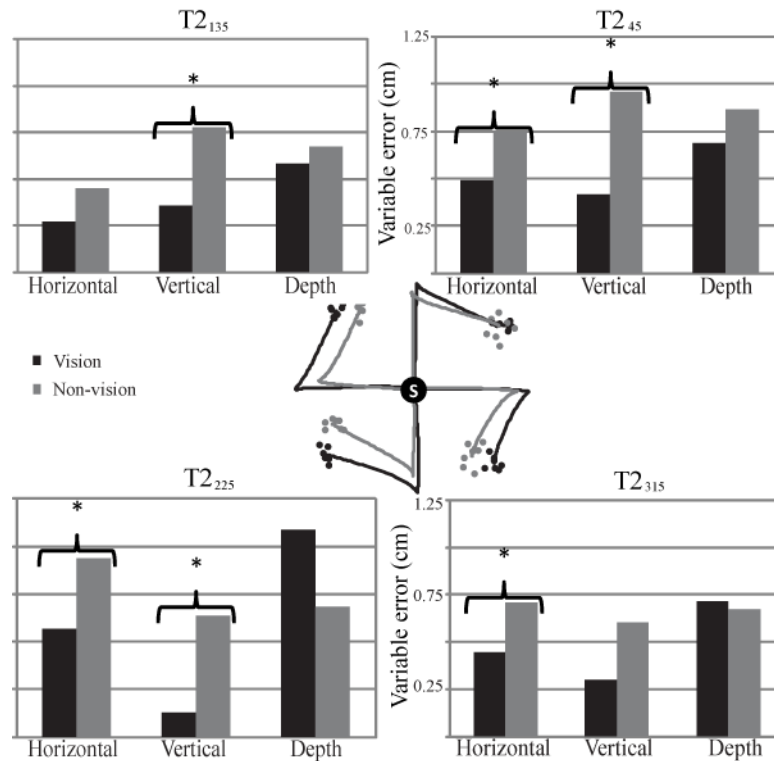
Figure 4.9. Single subject variable errors along each axis for clockwise sequences in both conditions. Endpoints were combined across depths for each sequence prior to calculating errors. Bartlett's test of uniformity was used to determine whether vision reduced variable errors along a given axis (stars). Variability in the NV condition was significantly larger along the horizontal and vertical axes for almost all sequences. Variable errors along the depth axis did not vary significantly between feedback conditions.

83

Interestingly, despite allowing subjects over 1 second to visually align their hand with the starting position, we observed a similar pattern of variability at this position. While variability was smaller overall at the starting position, subjects were slightly less precise at positioning their hands along the depth axis compared to either the horizontal or vertical axes. In addition, the variability along the horizontal and vertical axes was similar in magnitude. Given that subjects acquired this position under conditions where execution-related noise was relatively reduced, we interpret this finding as further evidence that the observed endpoint variability was largely a product of sensor/planning

Coordinate frames. Analyses of endpoint variability are often used to infer the reference frame or frames used to plan movements (Gordon et al., 1994; McIntyre et al., 1998; 1997; Vindras & Viviani, 1998). The bias in errors along the depth axis begs the question as to whether their orientation supported movement planning in an eye/head or trunk/arm based reference frames. To probe this we again combined our data across workspace depths for identical sequences and examined the orientation of the resulting ellipses and eigenvectors. As illustrated in Figure 4.10, when viewed in both the sagittal and horizontal planes these eigenvectors appeared to have their largest components along the depth axis, as previously discussed. This is consistent with reduced visual precision along this axis and could be interpreted as supporting an eye-centered reference frame for movement planning. However, in the sagittal plane these vectors did not in most cases point toward the nominal sight line (i.e. inferiorly for upward targets, superiorly for lower targets). In the horizontal plane these eigenvectors also did

84

not appear to converge toward the sight line nor were they rotated in the direction

of the shoulder of the pointing (right) arm, a key element of the most prominent

body-centered scheme (Flanders et al., 1992). Thus, patterns of endpoint

variability in this experiment likely reflect the influence of multiple reference

frames, a point we discuss further below.
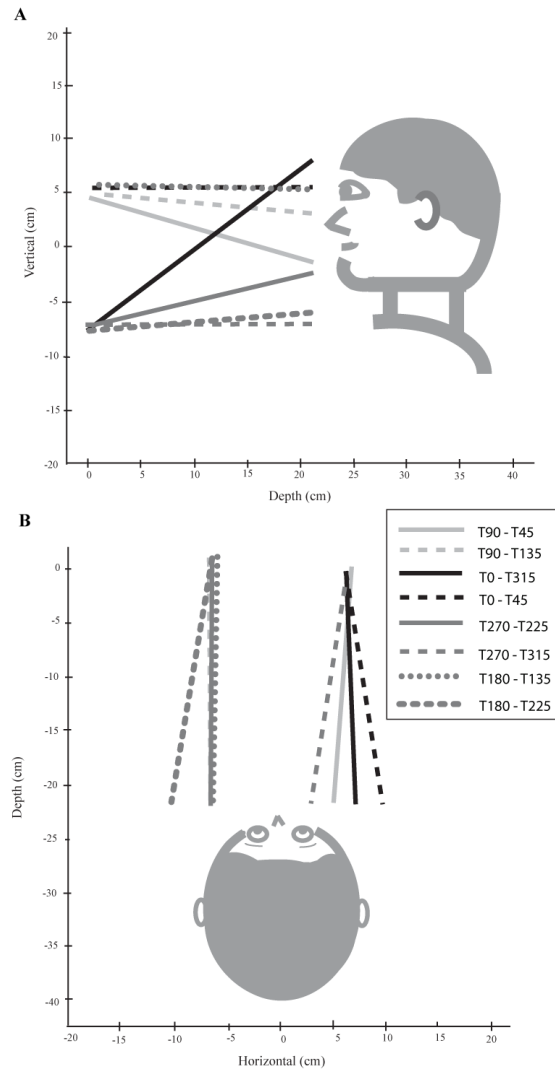
Figure 4,10. Principle eigenvectors of endpoint distributions for movement sequences in the V condition from a single subject. Error distributions for each sequence were collapsed across depths prior to PCA. Each eigenvector originates from the mean error of its endpoint distribution relative to the average target distance from the subject. Vectors were elongated to aid in visualization. **A.** Projection of eigenvectors onto the sagittal plane. **B.** Projections onto the horizontal plane. Neither view suggests a single frame of reference underlies the endpoint distributions.

Discussion

Subjects produced movement sequences to targets arranged in three vertical planes separated in depth, approaching each target from two different directions. These movements were conducted with visual feedback (V condition) and without vision (NV condition). This design provided a means to probe the interaction of execution noise and planning noise with respect to reaching variability. Endpoint variable errors in the V condition were relatively small along the horizontal and vertical axes but were elongated along the depth axis, consistent with previously reported characteristics of visual reliability (McIntyre et al., 1997; van Beers et al., 1998; van Beers et al., 2002b; Viguier et al., 2001). Errors in the NV condition were generally larger and more isotropically distributed in space than those in the V condition but were similar in magnitude along the depth axis to those in the V condition. The large component of error in depth in both conditions suggests a prominent role for planning noise in determining endpoint variability for movements in three dimensions. We propose that this arises from visual uncertainty associated with localizing targets in depth or noise associated with combining target position with hand position to determine the required movement vector. This effect is likely compounded by execution noise when the terminal movement vector is also along this axis. Therefore, we conclude that patterns of endpoint errors across the workspace arise from the interaction of anisotropically distributed visual planning noise with noise related to execution. That is, the spatial interaction of these sources of variability

occurs in a direction-dependent manner defined by the characteristics of noise arising within each process.

Relation to previous findings. The elongated pattern of endpoint errors in depth described here is reminiscent of the findings of McIntyre and colleagues (1997, 1998). In these experiments, subjects made movements from starting positions near the body to targets located further away from the body surface. The resulting endpoint distributions were consistent with a misestimation of endpoint position in depth and were interpreted as evidence for a 'viewer-' or eye-centered planning frame during visually guided movements (McIntyre et al., 1998; 1997). More recently, van Beers et al. (2004) reported that for center-out reaching movements in the horizontal plane, endpoint variability was well accounted for by noise in the motor command. This noise resulted in patterns of variability that were elongated along the movement direction near the end of the trajectory. As a result, for movements directed toward or away from the body these errors appeared to be elongated in depth. Thus, the patterns of variability described by McIntyre and colleagues could conceivably be explained as arising from either planning noise, execution noise or both processes, as the axes along which these noise sources are expected to dominate were nearly collinear in these latter experiments.

Here we observe significant, distinct effects of planning noise and execution on endpoint distributions, something many previous works in either planning or motor variability have not described. However, unlike these previous studies, our task is designed specifically to enhance both planning and execution

noises during the movement. One way this was achieved was through use of the double-step paradigm. This required subjects to make larger total movements and likely increased the amount of execution dependent noise over that of a single movement. Additionally, the differences in direction between movement vectors from separate paths to a common T2 were much greater than in previous works. Lastly, by arranging targets in the vertical plane, we decorrelate movement direction from visual noise, whereas many previous works have left these largely collinear. These characteristics likely made sensory and movement dependent effects somewhat more pronounced than has been shown in previous studies of single movement reaches to targets in depth.

While planning and execution noise have traditionally been evaluated independently, the two inherently interact during the production of movement. Further, these interactions can lead to ambiguity in interpreting patterns of movement variability, for reasons stated above. The present task, which involved randomized target positions, workspaces and visual conditions as well as unpredictable changes in target location, was designed to accentuate both planning and execution related noise processes. In addition, by keeping starting positions in the same vertical plane as the targets, thereby requiring planned movements to be largely perpendicular to the depth axis, we sought to disentangle the contributions of planning and execution related noise to endpoint variability. Indeed, we found that even though required movement directions were roughly orthogonal to the sight line in this experiment, patterns of endpoint variability

were still largely elongated in depth, in agreement with previous findings obtained for movements in 3D space (McIntyre et al., 1998; 1997).

Interaction between execution and planning noise. Recently, it has been argued that planning and execution related noise combine "near optimally" in the temporal domain (Faisal & Wolpert, 2009). These investigators demonstrated that overall task variability could be predicted from the sum of time-dependent sensory and motor variability. That is, when sensing times were small, and sensor uncertainty was therefore large, task variability was high. However, when sensing uncertainty was smaller (due to longer sensing times) variability became more indicative of the level of execution noise (Faisal & Wolpert, 2009). Extending this scheme to the spatial domain, one would predict that the shape of a given endpoint distribution would reflect the relative amount of noise due to planning and execution, as well as the spatial distribution of each noise source. The latter is believed to be determined by the natural coordinate axes of the relevant sensors and effectors (the eyes and arm, respectively).

In the V condition, vision of the hand was available at all times. Since visual estimation of hand position has been shown to be highly precise along the horizontal and vertical axes, planning noise throughout movement should have been relatively low in the vertical plane in the V condition. As a result, one might predict that patterns of variability in the vertical plane would reflect largely execution related noise in this condition. While execution noise was not the dominant source of variability in this experiment, its influence *was* most apparent in the vertical plane in the V condition, as suggested by the slight elongation of

the confidence ellipsoids along the average movement direction in Fig. 4.6. In contrast, endpoint distributions appeared more isotropic in the NV condition when viewed in the vertical plane (Fig. 4.8). This would be expected if planning noise in this plane was considerably larger without visual feedback of the hand, a premise supported by previous findings (Carrozzo et al., 1999). Thus, the observed patterns of variability in the two feedback conditions appear to arise from differences in the relative levels of planning noise between conditions as well as the differing spatial distributions of uncertainty arising from planning and execution noise.

An important corollary to this discussion is that when both levels of noise are similar and their underlying coordinate axes are aligned, then their respective contributions to endpoint variability should be more difficult to distinguish. This was in fact the case in this experiment. In general, the principal axes of movement variability were better explained by known anisotropies in visual planning noise than by the orientation of the movement vector. However, as Fig. 4.7 indicates, when movements involved a significant depth component, endpoint distributions *were* relatively well aligned with the movement vector. This arises from the fact that when movements are directed in depth, the coordinate axes of visual uncertainty and execution noise are largely collinear, and therefore contribute together to the elongated shape of endpoint distributions in depth.

A more quantitative estimation of the relative contributions of execution and planning noise, as has recently been performed in a different context (van Beers 2009), would require an in depth analysis of the variability associated with

movement sequences performed along all three axes in space. Experiments of this nature could be a fruitful avenue for future investigations. Similarly, probing the nature of visual planning noise will require more advanced experimental paradigms as well. As suggested by Fig. 4.1, this noise could arise at several stages of the planning process, including during the estimation of target and/or hand position as well as during computation of the required movement vector. The similar levels of variability along the depth axis in the V and NV condition suggest that estimation of hand position is not a major determinant; this could be a reflection of the more dominant role of proprioception in estimating hand position along this axis (see *Cue integration* below). Instead, the large variability in depth reported here more likely resulted from visual uncertainty of target locations in depth or during the computation of movement vectors, which includes coordinate transformations and subsequent vector subtraction. Future experiments will seek to distinguish among these various possibilities.

Workspace dependence. Previous work has shown that proprioceptive reliability decreases as the hand moves further from the body (van Beers et al., 1998). Visual reliability on the other hand is relatively constant, at least for distances within the workspace of the arm (Viguier et al., 2001). As a result we hypothesized that the weighting of vision and proprioception might vary with workspace depth, resulting in different patterns of errors for identical movement sequences performed in different depth planes. Contrary to our initial hypothesis, increasing workspace depth did not generally affect the endpoint variability

92

associated with different movement sequences. This suggests that the interaction of planning and execution noise was generally consistent across the workspace.

The fact that planning noise did not appear to change with workspace depth may be partially related to our experimental design and apparatus. Our use of a shield to block view of the arm prevented evaluation of hand positions closer than approximately 20 cm from the body, where proprioception should be most precise (van Beers et al., 1998). In addition, we did not explore positions near the limits of the reaching workspace, where proprioception might be expected to show a sudden decrease in precision (Scott & Loeb, 1994; Wilson et al., 2008). In other words, in this study we may have explored a region of space where the reliability of somatic feedback (like visual feedback) is relatively constant, leading to only minor effects on movement planning. These small changes in somatic reliability along this axis might also have been masked by the additional but larger visual uncertainty associated with target localization along this axis.

Cue integration. As previously mentioned, we observed similar degrees of error in depth in both feedback conditions. In fact, variability along this direction was almost always greater than variability along the horizontal or vertical axes. We attribute this to the increased planning noise associated with localizing targets in depth (McIntyre et al., 1997; Viguier et al., 2001). However, variability along the horizontal and vertical axes differed greatly between conditions, with errors being significantly smaller with hand vision than without. This suggests an anisotropic effect of vision in this experiment, as predicted by recent "optimal" cue integration schemes. Recent work in cue integration has

argued that multiple sensory cues are combined in such a way that the contribution of each input is proportional to its reliability (the inverse of uncertainty) (Ernst & Banks 2002; Jacobs 1999; Knill & Saunders 2003; Kording & Wolpert, 2004; van Beers et al., 1999). Vision is highly reliable along the horizontal and vertical axes, but less so in depth. Proprioception, on the other hand, exhibits the opposite tendency. Thus, an "optimal" integration of these senses would manifest as a stronger weighting of visual information along the horizontal and vertical than in depth. Our observation that vision assists hand localization in the horizontal and vertical axis but has little effect on reliability in depth is precisely the pattern predicted for a system executing "optimal" integration strategies.

Frames of reference. Variable errors and constant errors have historically been analyzed as a means to understand movement planning, particularly the reference frame or frame in which movements are planned. The rationale behind using variable errors is that the coordinate system used to encode endpoint positions would reveal itself as a lack of correlated variance along a set of coordinate axes that are linked to key 'nodes' in the sensorimotor chain. Behavioral evidence supporting hand, body, and eye-centered coding of reach endpoints has previously been presented (Flanders et al., 1992; Gordon et al., 1994; McIntyre et al., 1998; 1997; Vetter et al., 1999; Vindras & Viviani ,1998). More recently, behavioral studies suggest that under many circumstances reaching errors reflect the influence of distinct movement related processes and/or sensory signals that are encoded in correspondingly distinct reference frames (Ghez et al.,

2007; McGuire & Sabes, 2009), observations which have support in both the modeling and neurophysiological literature (Buneo et al., 2002; Deneve et al., 2001). These schemes typically invoke a mixture of reference frames, e.g. eye-centered coordinates with limb or body-centered ones, with the weighting being determined by the statistical properties of the signals being integrated (McGuire & Sabes 2009) or, more generally, the task conditions (Heuer & Sangals 1998).

The present results are partially supportive of this general scheme. That is, principal eigenvectors in this experiment were influenced in part by the direction of hand movement, which could be interpreted as reflecting a movement plan in hand-centered coordinates. The influence of an eye-centered reference frame is implied by the elongation of variable errors along the depth axis (consistent with reduced visual precision along this axis). However, as Fig. 4.10 suggests, we did not find strong evidence for a convergence of the eigenvectors, as would be expected for eye-centered coding (assuming subjects were fixating the target, which is reasonable). In addition, when viewed in the sagittal plane, these eigenvectors did not always point along the sight line, which is also inconsistent with an eye-centered coding scheme. Strong evidence for the encoding of endpoints in a single body-centered reference was also not found, as mentioned in Results. Thus, interpreted in the context of the coordinates of movement planning, the present results point to a role for both relative (hand) and absolute (eye/body) coordinates, though the origin of the latter is equivocal.

CHAPTER 5

CONTRIBUTION OF EXECUTION NOISE TO ENDPOINT

VARIABILITY IN 3D SPACE

Introduction

Noise pervades every stage of sensorimotor processing and contributes to

movement variability, a hallmark of human motor behavior (Faisal et al., 2008).

This noise can be attributed in part to neural processes associated with

transforming sensory signals into motor commands ('planning noise') and to

processes associated with transforming motor commands into movements

('execution noise')(van Beers et al., 2004). Planning noise includes noise arising

during the initial sensing of limb and target position, as well as noise that arises

during the central integration of these signals, and is thought to result in

variability in movement direction and amplitude, as well as speed (Churchland et

al., 2006a; Churchland et al., 2006b; Gordon et al., 1994; McIntyre et al., 1998;

1997; Vindras & Viviani, 1998). Execution noise also arises from both peripheral

and central mechanisms and can have profound effects on movement variability

(Buneo et al., 1995; van Beers et al., 2004). Understanding how planning and

execution-related noise interact is critical not only for explaining movement

variability that is observed in neurologically intact human subjects but also for

comprehending the exaggerated variability that arises following nervous system

damage (Contreras-Vidal & Buch, 2003; Hermsdorfer & Goldenberg, 2002;

Longstaff & Heath, 2006; Thies et al., 2009). In addition, the effects of this

interaction are relevant to understanding such diverse sensorimotor functions as

position estimation (van Beers et al., 1999; 1998; van Beers et al., 2002b), cue integration (Kording & Wolpert, 2004), and motor adaptation (van Beers, 2009).

The effect of noise manifests differently depending upon whether it is execution or planning based. For example, noise associated with execution is thought to result in movement variability that is most pronounced along the direction of movement, particularly its terminal component (van Beers et al., 2004). In contrast, noise associated with sensing the position of the limb (a component of movement planning) has different spatial characteristics which arise from the unique properties of the sensors. For example, localization of the hand by proprioception is reportedly more precise when the hand is closer to the body and is also more precise in depth than in azimuth (van Beers et al., 1998; van Beers et al., 2002b). Vision is also more precise for positions closer to the eyes/body but is more precise in azimuth than in depth. These differing workspace dependencies predict that patterns of movement variability arising from planning noise will depend on whether hand position is sensed through proprioception alone or via both senses (Shi & Buneo 2009). In either case, the effects of this noise will be both movement direction and arm configuration dependent (Shi & Buneo 2009).

As a result of the different behavioral consequences of execution and planning-related noise, determining the source or sources of movement variability that arises during a particular experiment can be problematic. For instance, patterns of variability following movements made from a starting position near the body to targets further away in depth have often been found to be significantly

97

elongated along the depth axis (Carrozzo et al., 1999; McIntyre et al., 1998; 1997; van Beers et al., 2004). These results could be interpreted as resulting from noise in execution (van Beers et al., 2004), noise in visual estimation of the target and/or hand (van Beers et al., 1998; Viguier et al., 2001) or both processes. This is due to the fact that the axes along which execution noise and visual planning noise are thought to dominate (the terminal movement axis and depth axis, respectively) are aligned when movements are directed in depth. Additionally, the elongated pattern of variability could also arise due to noise associated with other aspects of movement planning (McIntyre et al., 2000; McIntyre et al., 1998; 1997).

In most instances, however, movement variability likely arises from the interaction of noise sources (Thaler & Todd, 2009). In support of this idea, sensory and execution noise have been shown to interact 'near-optimally' in the temporal domain to determine overall levels of behavioral variability (Faisal & Wolpert 2009). In a recent study of unconstrained reaching movements to targets in the frontal plane, we argued that this may also be the case in the spatial domain (Apker et al., 2010). In particular, we showed that visually-related planning noise played a dominant role in determining patterns of endpoint variability in 3D space, with execution noise contributing to this variability in a direction dependent manner (i.e. along the movement vector). However, since movements in this experiment were designed to be confined largely to the frontal plane, it was unclear if planning and execution noise interacted in the same way for movements requiring large components along the depth axis. In addition, in these

experiments, the role of uncertainty in hand position estimation in determining patterns of movement variability in 3D could not be adequately determined. That is, although we found that patterns of endpoint variability were larger and more isotropic in the absence of hand vision, due to the use of predominantly frontal plane movements we were unable to fully interpret the roles of execution and planning noise in shaping these distributions.

In the present investigation we studied the interaction of planning and execution noise during the performance of movement sequences with or without a substantial terminal component in depth. As in Apker et al. (2010), planning and execution noise were accentuated by randomizing target positions from trial to trial and by switching the final target position during movement, which required rapid, online changes in movement planning and execution. The switching of targets was performed in such a way that the resulting sequences of two reaches were either both chiefly contained within a frontal plane ('frontal sequences') or involved an initial reach within the frontal plane and a second that was directed toward or away from the subject ('depth sequences'). In addition, on half of the trials movements were made without visual feedback of the hand, a manipulation designed to increase uncertainty in hand position estimation (Franklin et al., 2007). We hypothesized that variability would be more anisotropic and more strongly aligned with the depth axis when the dominant axes of execution noise and visual planning noise were more aligned, i.e. during depth sequences. We found that when visual feedback was available, patterns of endpoint variability were for the most part anisotropic, with the principal axes of variability being

closely aligned with the depth axis regardless of sequence type (and therefore movement axis). In the absence of visual feedback, variability associated with depth sequences exhibited similar spatial characteristics while movements made primarily within the front plane were considerably more isotropic and were more strongly influenced by the primary axis of movement. These results confirm previous suggestions that anisotropically distributed visual planning noise plays a dominant role in determining patterns of arm movement variability in 3D space. In addition, the findings suggest that in the absence of vision, increased uncertainty in hand position estimation results in patterns of endpoint variability that are more influenced by execution noise than those with visual feedback.

Methods

     Subjects. Ten (10) subjects (3 women, 7 men) between the ages of twenty-one and twenty-seven were recruited to perform the experiment. The experiment complied with and was approved by the Arizona State University Institutional Review Board (IRB) prior to subject recruitment and data collection. All subjects read and signed an IRB approved informed consent form prior to participating. Subjects were briefed on the experimental procedures and what to expect when moving within the virtual environment but were naïve to the purpose of the study.

     Apparatus. An experimental apparatus was constructed to allow control of task parameters during 3-D movements; the arrangement of the different components of this setup is illustrated in Fig. 5.1A. A large, standing frame supported a stereoscopic 3-D monitor (Dimension Technologies Incorporated,

Rochester, NY) which projected images onto a mirror that was visible to the subjects. The mirror was embedded within a metal shield, which was oriented at a 45 degree angle with respect to the monitor. This shield also served to block the arm from view. During the experiment, subjects were seated with their head positioned on a chinrest in such a way that the eyes were aligned with the center of the mirror.

Motion tracking. An active-LED based motion tracking system was used to track movements of the fingertip (Visualeyez ™ VZ-3000 motion tracker (Phoenix Technologies Inc., Burnaby, British Columbia); 150 Hz sampling rate; 0.5 mm spatial resolution). During the experiment, a single LED was positioned on the subject's fingertip and its position was fed back to the subject in near real-time via a virtual reality (VR) environment developed in Vizard® (WorldViz LLC. Santa Barbara, CA). Fingertip position, target positions and the starting position were displayed on the 3-D monitor as green spheres and were ~5 cm in diameter when presented in the vertical plane defined by the starting position and T1 target positions. To aid in depth perception, a wireframe cube was also rendered in the virtual environment. The cube was centered on the starting position but was large enough that all of the targets and movements were completely contained within it. An examination of the efficacy of the depth cues in our environment indicated that subjects can perceive depth with an accuracy and precision similar to that exhibited by subjects in real environments (Viguier et al., 2001) over the range of target depths used in this study.
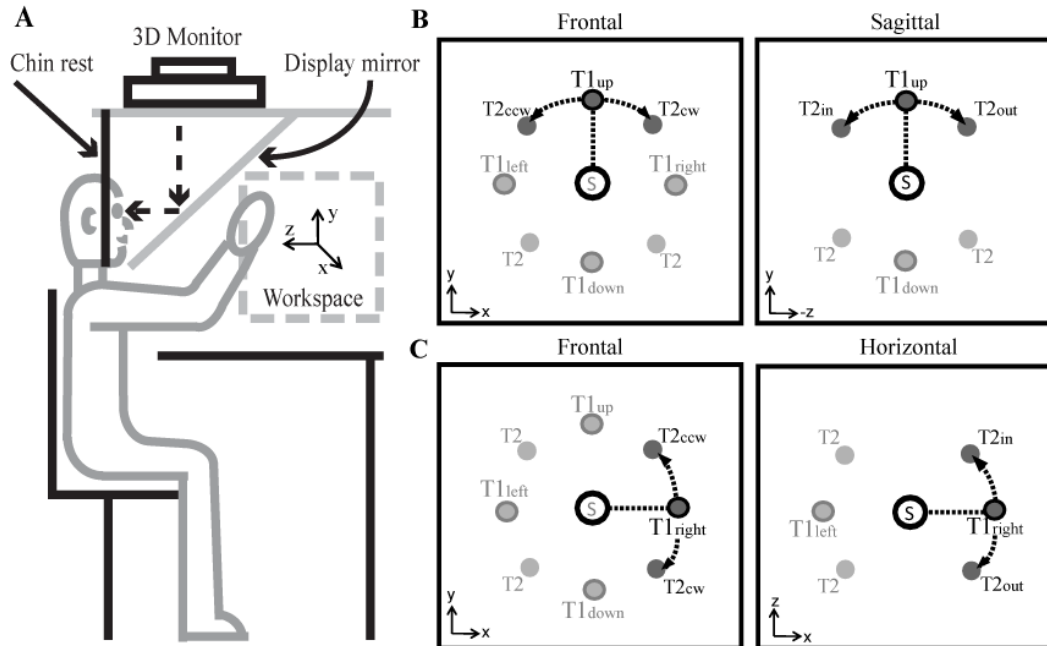
Figure 5.1. Experimental apparatus and target layout. **A:** Experimental apparatus.

B: Frontal and sagittal plane views of the 4 potential movement sequences

associated with $T1_{up}$. The second movement in the sequence was directed to one

of four secondary targets located clockwise ($T2_{cw}$), counterclockwise ($T2_{ccw}$),

inward ($T2_{in}$), or outward ($T2_{out}$) from its associated T1. **C:** Frontal and

horizontal plane views of the 4 potential movement sequences associated with

$T1_{right}$.

Experimental design. The task was to execute a sequence of two reaches to targets that were arranged on the surface of an 18 cm diameter sphere centered on a single starting position. There were four primary targets (T1), located along the x (lateral) and y (vertical) axes cutting through the center of the sphere. Each T1 was associated with four potential secondary targets (T2) located 45° clockwise, counterclockwise, closer in depth (inward) or further in depth (outward) from a given T1 and at a straight-line distance of approximately 6.4 cm (see Figs. 1B, 1C). As a result of this target arrangement, the second movement in a sequence was either largely contained with the same frontal plane as the first movement (in the case of clockwise/counterclockwise movements) or had a large component parallel to the depth axis (for inward/outward movements). This allowed a more comprehensive examination of the interactions between execution noise and planning noise than was previously attempted (Apker et al., 2010). Movement sequences were performed either with visual feedback of fingertip position throughout the movement (visual (V) condition) or without visual feedback (non-visual (NV) condition). Prior to the start of the experiment, subjects were given ample time to acclimate to the virtual environment and did not proceed with the experiment until they self-reported familiarity with moving within our virtual reality.

Individual trials began with the illumination of the starting position which cued the subjects to visually align their fingertip with this position (visual feedback was always present during this epoch). After holding for 350 ms within a 4 cm window centered on the starting position, a T1 would be illuminated,

103

cueing the first movement. Coincident with the fingertip leaving the start position window, T1 would disappear and an adjacent T2 would appear cueing the second movement. Note that the size of the start position window was chosen such that this target jump occurred very close to peak hand velocity to T1, which was designed to obviate saccadic suppression, ensuring subjects were immediately aware of the target jump. On V trials, vision of the fingertip was available throughout the movement. On NV trials however, coincident with the appearance of T1, visual feedback of the fingertip position was removed for the duration of the trial. Feedback condition (V, NV), and target location (T1, T2) were pseudo-randomly selected on a trial by trial basis. Each combination of variables was sampled fifteen (15) times.

Subjects had no knowledge of the trial parameters prior to trial onset and were instructed to move as quickly and accurately as possible to the presented targets. Subjects were also instructed to avoid adjusting their fingertip position at the end of a sequence. These aspects of the experiment design were incorporated to accentuate planning and execution related noise processes rather than to minimize them (as in some previous studies), thereby facilitating a characterization of their interaction. Trials were considered successful if the subject moved to the target quickly and remained within an acceptable window around the target (5 cm radius along each axis) for 350 ms. Knowledge of results was provided in terms of an auditory tone that signaled that subjects were successful but this information could not be used to further adjust endpoint position. When the endpoints did not fall within this window, the trial was aborted

and repeated later during the session. If a subject was having repeated difficulty acquiring a particular target, the 5cm window was temporarily enlarged for that target so that the requisite number of trials could be completed. The decision to increase the window radius in these limited cases was based on concerns that the length of the experimental session would lead to increased difficulty in elevating the limb off of the table and that this fatigue would affect performance on subsequent trials. Only position data for successful trials were retained for analysis.

Data analysis. Movements were first sorted according to subject, feedback condition, and target sequence (i.e. combination of T1 and T2). Movement data were then smoothed offline using a digital low-pass filter (5-point moving average) and the instantaneous tangential velocity was calculated by differentiating the position data along the movement path. Movement endpoints were identified as the point at which the tangential movement velocity fell below 5% of its peak value for movements to T2. In a limited number of instances, recorded movement endpoints were allowed to fall outside of the 5cm target window during data acquisition, in order for subjects to complete a full set of trials to each target location. However, these trials were excluded from analysis, and only amounted to a very small fraction of total trials (26/4800 trials; 0.5%).

To assess movement accuracy, constant errors were calculated by subtracting the known T2 target position from the measured endpoint of the hand. However, since constant errors tend to be idiosyncratic (Berkinblit et al., 1995; Darling & Miller, 1993; Foley & Held, 1972; Soechting & Flanders, 1989a) we

105

did not explore their nature in detail here. Instead, analysis focused on the variable errors, which provide more direct information about planning and execution-related noise (McIntyre et al., 1998; Carrozzo et al., 1999; van Beers et al., 2004). Variable errors associated with a given axis and T2 position (σ_t) were calculated as follows:

$$\sigma_t = \frac{1}{n_t}\sqrt{\sum_{i=1}^{n_t}(h_t^i - \overline{h}_t)^2} \qquad (1)$$

where $\overline{h}_t$ represents the mean endpoint position for a given T2 position t, h_t^i represents the corresponding endpoint position on trial i, and n_t represents the number of trials.

Principal components analysis (PCA) was also used to analyze the endpoint distributions associated with frontal and depth sequences. The 95% tolerance ellipsoids associated with each endpoint distribution were first computed as follows (McIntyre et al., 1998; Morrison, 1990):

$$T_{95\%} = q\frac{(n+1)(n-k)}{n(n-q-k+1)}F_{0.05,q,n-q-k+1},H \qquad (2)$$

where the dimensionality $q=3$, the number of target positions $k=1$, and H is the covariance matrix. The resulting eigenvalues and eigenvectors (obtained from the matrix T) were used to quantify the sizes, shapes and orientations of the endpoint distributions (see below). For visualization purposes, 95% confidence ellipses and ellipsoids were calculated using Matlab code based on the Khachiyan algorithm (Khachiyan, 1996; Khachiyan & Todd, 1993), as implemented by Nima Moshtagh.

Endpoint distributions associated with frontal and depth sequences were compared by analyzing differences in the sizes, shapes and orientations of their corresponding tolerance ellipsoids. The size of each ellipsoid was quantified by its volume (V):

$$V = \frac{4\pi}{3} abc \tag{3}$$

where a represents the radius of the major axis of the 95% confidence ellipsoid and b and c represent the radii of the minor axes. The aspect ratio was used to characterize the shape of each ellipsoid, defined as the ratio of the radius of the major axis of the ellipsoid to the sum of the radii of the minor axes. Lastly, the general orientation of each ellipsoid was defined by the absolute values of the components of the first eigenvector derived from the PCA (Carrozzo et al., 1999; McIntyre et al., 1998; 1997).

Statistical analyses. In order to determine whether the distributions derived from PCA were isotropic or anisotropic a χ^2 test of the form used by Morrison (1990) and McIntyre et al. (1997) was used, which determined whether any two eigenvalues were significantly different from each other. The non-parametric Mann-Whitney U test was used to test whether individual components (lateral, vertical, or depth) of the 1st eigenvectors differed between endpoint distributions. Lastly, ellipsoid volumes and ellipsoid aspect ratios associated with frontal and depth sequences were compared using 2-way ANOVAs with factors 'sequence type' (frontal vs. depth) and T1 location. The latter factor was chosen to assess any differences that may have arisen due to differences in the initial and

107

final movement directions in a sequence. The significance level for all statistical tests used in this study was $\alpha=0.05$.

Results

      Variable errors with visual feedback. Figure 5.2 illustrates average movement paths and individual movement endpoints for the four sequences associated with each T1. Ellipses represent 2-D projections of the 95% confidence ellipsoids calculated for each endpoint distribution. Data from a single subject are shown and are viewed from the bottom up for $T1_{up}$ and $T1_{down}$ and from the subject's left for $T1_{left}$ and $T1_{right}$. These plots show that, although endpoint distributions appeared to vary somewhat in size and shape for the different sequences, these distributions were generally anisotropic in the V condition. In addition, for many of the distributions, the largest component of variability appeared to be aligned with the depth axis. This is most evident for the distributions associated with inward and outward sequences (red), where the average movement paths were also largely parallel to the depth axis. However, this trend can also be observed for some of the distributions associated with clockwise and counterclockwise sequences (black), most notably those associated with $T1_{up}$. This is despite the fact that the average movement paths for these frontal plane sequences were roughly orthogonal to the depth axis. These trends were consistent across subjects in the V condition; across the population, variable errors were largest along the depth axis for 99% of the inward/outward sequences (79/80) and 95% of the clockwise/counterclockwise sequences (77/80).

The tendency for movement variability to be particularly large along the depth axis can be best appreciated from the orientations of the 1st eigenvectors derived from PCA. Figure 5.3 shows the size of each component of these eigenvectors for each type of movement sequence, grouped by T1. Data for a single subject are shown (the same subject shown in Fig. 5.2). The proportion of variance accounted for by the 1st eigenvector (indicated by the numbers at the upper left of each plot) was typically large for this subject and was also reasonably consistent across the different types of movement sequences (mean: 74% +/- 15%). Although the variance accounted for was often higher for inward/outward sequences for this subject, this was not a consistent finding across the population (see below). Figure 5.3 also illustrates that the orientations of these eigenvectors were very consistent. That is, these vectors generally had their largest components along the depth axis for both the clockwise and counterclockwise sequences as well for as the inward and outward sequences. The lone exception to this observation is the counterclockwise sequence associated with $T1_{down}$ which had its largest component along the lateral axis. The fact that the clockwise and counterclockwise sequences typically had their largest components of movement variability along the depth axis might seem surprising as by design these sequences did not require significant movement components in depth. However, this observation is consistent with the findings of Apker et al. (2010), which were obtained under similar conditions. Moreover, these investigators showed that this trend was not related to the orientation of the terminal components of the average, executed movements in the frontal plane,

109

which were largely orthogonal to the depth axis in that study and the present one (see Fig. 5.2).

The main findings illustrated in Fig. 5.3 were also observed at the population level. Figure 5.4 shows the average size of the components of the 1st eigenvectors associated with each type of endpoint distribution. As with the single subject shown in Fig. 5.3, the average proportion of variance accounted for by the 1st eigenvector was generally large and very consistent across subjects and sequence types (mean: 77% +/- 4%), consistent with other studies of endpoint variability in 3D space (Apker et al., 2010; McIntyre et al., 1998; 1997). In contrast to the single subject data, there was little difference between the average amount of variance accounted for by the eigenvectors for the clockwise/counterclockwise sequences and the eigenvectors for the inward/outward sequences (78% and 76%, respectively) Figure 5.4 also clearly shows that at the population level the 1st eigenvectors were strongly biased along the depth axis: looking across all sequence types, the mean component of the eigenvector along this axis was never less than 0.8. Interestingly, even though the clockwise and counterclockwise sequences (and likewise the inward and outward sequences) were directed along axes that differed somewhat in orientation (due to the fact that targets were on the surface of a sphere), the average components of their associated eigenvectors were typically very similar. This was confirmed statistically as well: no statistically significant differences were found between the magnitudes of the individual eigenvector components associated with clockwise and counterclockwise sequences (Mann Whitney U test conducted separately on

the lateral, vertical and depth axes, $p<0.05$). Similarly, no differences were found between the magnitudes of the individual eigenvector components associated with inward and outward sequences (Mann Whitney U test, $p<0.05$).

Size, shape, and orientation of endpoint distributions with visual feedback. Given previous findings (Apker et al., 2010), we hypothesized that in the V condition, endpoint distributions associated with depth-directed movements (i.e. inward/outward sequences) would be more anisotropic and more strongly aligned with the depth axis than endpoint ellipsoids associated with frontal plane movements (clockwise/counterclockwise sequences). Instead, our analysis of the 1st eigenvectors associated with individual endpoint distributions suggested that the orientations of these distributions were very similar at the population level. To further examine the similarities and differences between the different types of sequences, we also compared their endpoint distributions in terms of their sizes (volumes) and shapes (aspect ratios), which take into account variability along axes other than those defined by the 1st eigenvector. Since the 1st eigenvectors for counterclockwise and clockwise sequences were statistically indistinguishable from each other at the population level for each T1 (see above), we combined the distributions corresponding to these sequences together for this analysis and refer to the combined error distributions as 'frontal sequences'. Similarly, distributions for the inward/outward sequences (which were also statistically indistinguishable from each other at the population level) were grouped together for this analysis and are referred to as 'depth sequences'.
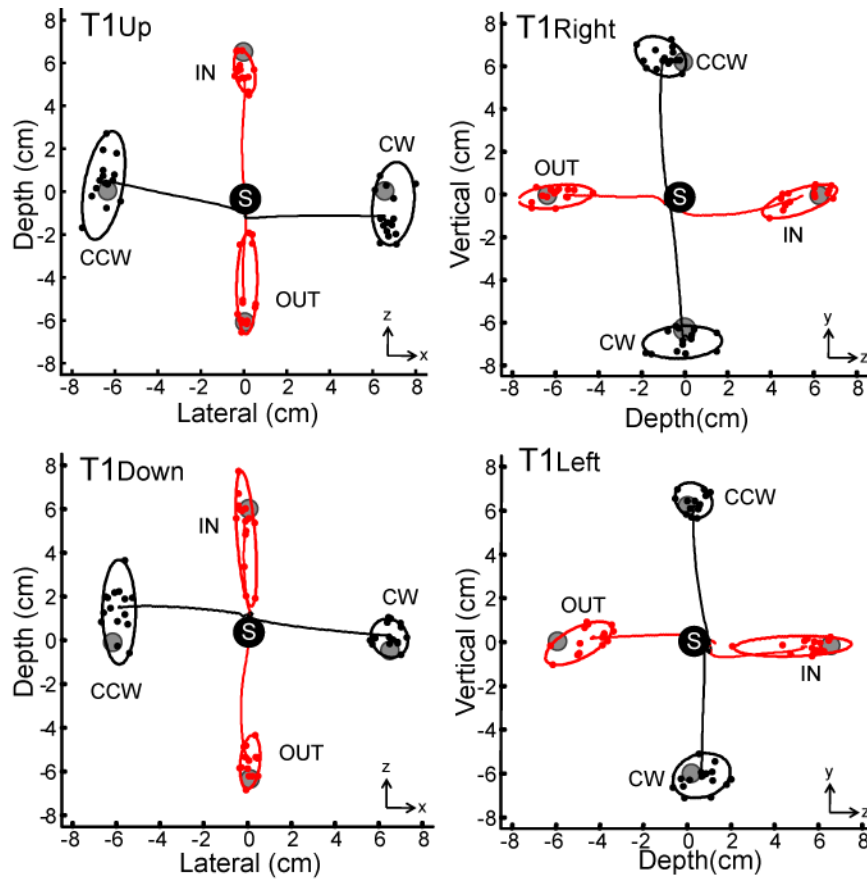
Figure 5.2. Movement endpoints, confidence ellipses, and average trajectories in the V condition for a single subject. Data are viewed from the bottom up for $T1_{up}$ and $T1_{down}$ and from the subject's left for $T1_{left}$ and $T1_{right}$. Ellipses represent 2-D projections of the 95% confidence ellipsoids calculated for each endpoint distribution. Solid black circles denote the starting position, and gray circles denote the location of the T2s. Most endpoint distributions appear elongated along the depth axis, particularly those associated with inward and outward sequences (red).
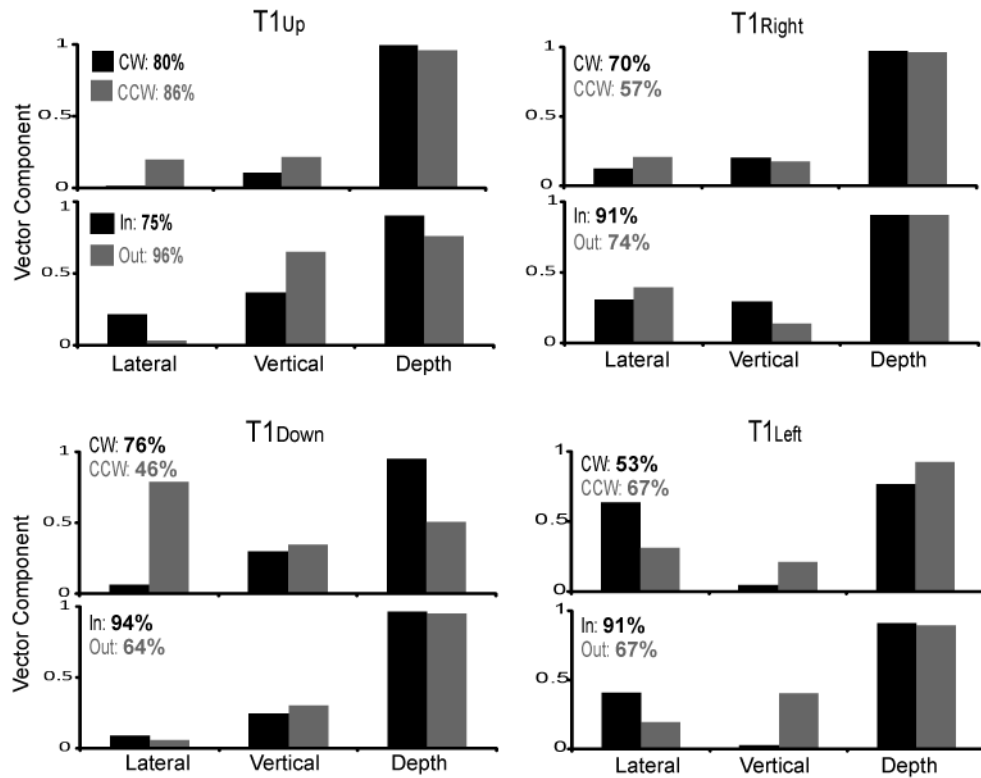
Figure 5.3. Lateral, vertical, and depth components of the 1ˢᵗ eigenvectors derived from a principal components analysis of each endpoint distribution. Data for a single subject in the V condition are shown, grouped by T1 location. Percentages to the left of each plot show the proportion of variance accounted for by the 1ˢᵗ eigenvector. Components were largest along the depth axis for most sequences.
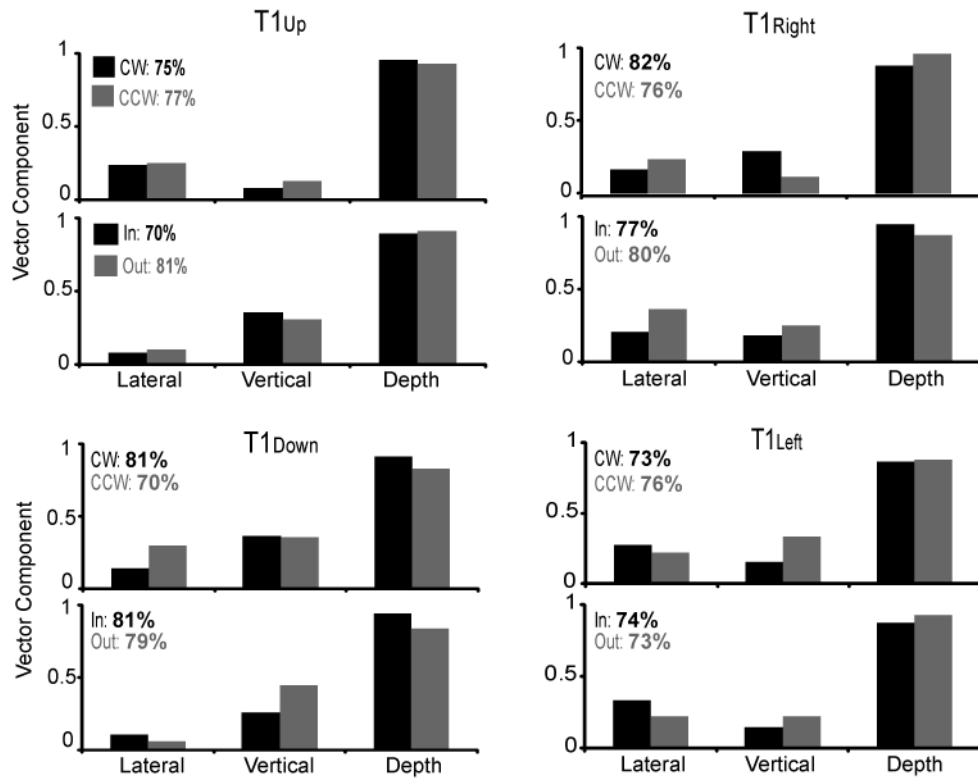
Figure 5.4. Mean 1st eigenvectors for the population (N=10) in the V condition. Figure conventions as in Fig. 5.3.

Figure 5.5A shows a horizontal plane view of the population ellipsoids and 1st eigenvectors for the frontal and depth sequences associated with each T1. The main axes of the ellipsoids, as well as the 1st eigenvectors appear to be strongly aligned with the depth axis, as would be expected given the results shown in Figs. 5.2-4. In addition, the ellipsoids appear fairly consistent in size (volume) and shape across the different T1s and types of sequences. To further illustrate the consistency in volumes, Fig. 5.5B plots the average ellipsoid volumes associated with frontal and depth directed sequences for the population, grouped by the different T1s. This figure shows that ellipsoid volumes were typically small in the V condition, averaging between 15 and 20 cm^3 (approximately equivalent to the volume of a golf ball). Ellipsoid volumes were also generally consistent across the different T1s and between sequence types. At the population level we found no statistically significant effects of T1 location, sequence type (depth vs. frontal), or their interaction on ellipsoid volume (2 factor ANOVA; p=0.71, p=0.35, and p=0.75 respectively). Thus, for the most part 3D endpoint distributions associated with frontal and depth sequences did not appear to differ in size (volume) when vision of the hand was available throughout movement.

Endpoint distributions associated with frontal and depth sequences were also similar when analyzed in terms of their shapes. Figure 5.5C shows the aspect ratios of the ellipsoids associated with frontal and depth-directed sequences, grouped by T1. These aspect ratios reveal that, on average, variability along the 1st eigenvector (which is proportional to the length of the longest radius of the

115

ellipsoid) was ~1.5 times greater than that along the other eigenvectors for both

types of sequences. Similar to the analysis of ellipsoid volume, Fig. 5.5C also

shows that the shapes of the ellipsoids were similar between frontal and depth-

directed sequences and across the different T1s. This was confirmed statistically

as well: here again we found no statistically significant main or interaction effects

of T1 location or sequence type on ellipsoid aspect ratio (2 factor ANOVA,

$p=0.51$, $p=0.91$ and $p=0.42$, respectively). We conclude therefore that the shapes

of the endpoint ellipsoids also did not vary in a consistent manner between frontal

and depth sequences in the V condition.

The similarities in ellipsoid volumes and shapes extended to the ellipsoid

orientations. Figure 5.5D shows the average components of the 1st eigenvectors of

the endpoint distributions associated with frontal and depth sequences, grouped

by T1. This figure strongly suggests that both types of sequences had their largest

components along the depth axis, in agreement with the analyses shown in Figs. 3

and 4. This was in fact the case; depth components of the 1st eigenvectors were

significantly different from both the lateral or vertical components for both the

frontal and depth sequences (Mann Whitney U tests, $p<0.05$). Some small but

significant differences were observed between components for some axes (Mann

Whitney U test, $p<0.05$). For example, lateral components were somewhat larger

for the frontal sequences for $T1_{up}$ and $T1_{down}$, while for $T1_{right}$ the opposite trend

was observed (there was no difference in these components for $T1_{left}$). These

differences likely reflect the influence of execution noise, a point we will return to

later. Overall however, Fig. 5.5 and its associated statistical analyses strongly

suggest that in the presence of visual feedback, endpoint distributions associated with frontal and depth-directed movement sequences did not appear to differ substantially in size, shape, and orientation. In addition, the results suggest that for both sequence types, variability was predominantly anisotropic and strongly aligned with the axis along which uncertainty associated with planning and updating visually-guided movements would be expected to dominate, i.e. along the depth axis.
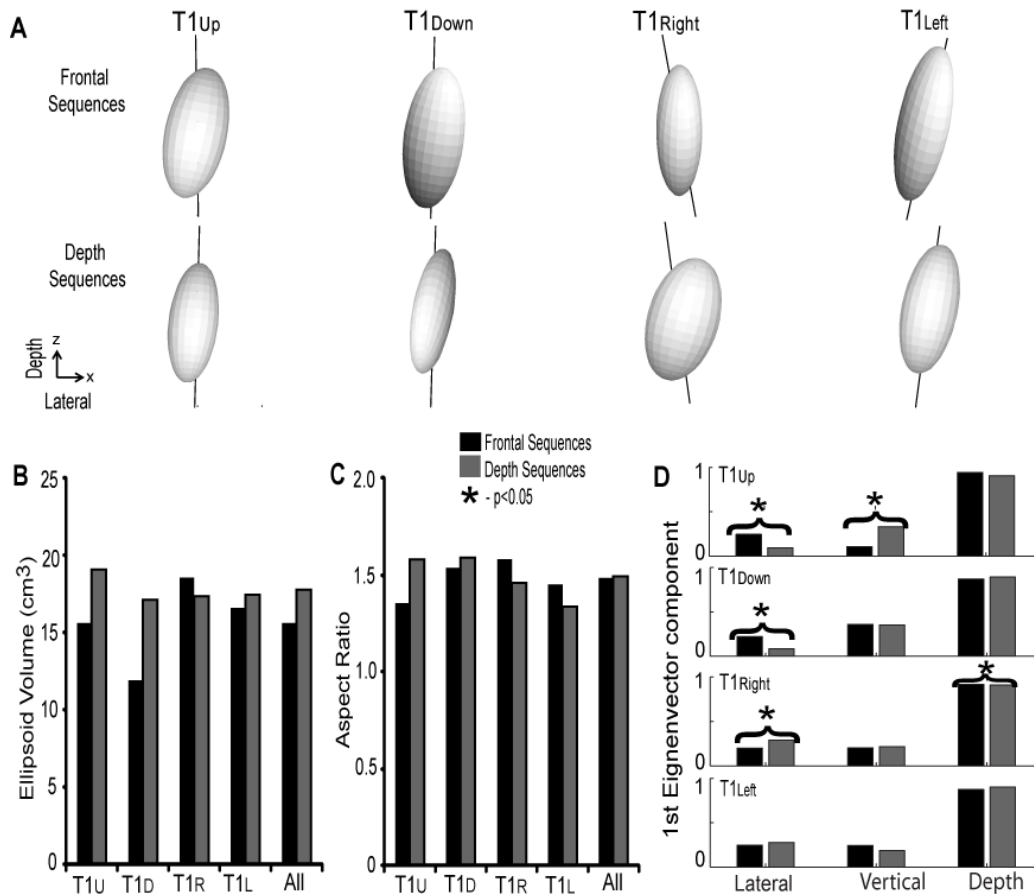
Figure 5.5. Analysis of endpoint ellipsoids associated with frontal and depth

sequences in the V condition. **A:** Horizontal plane views of the ellipsoids and 1st

eigenvectors associated with each T1. All ellipsoids are plotted on the same scale.

Coordinate axes at the lower left also serve as scale bars (2cm). **B:** Ellipsoid

volumes (sizes), for frontal and depth sequences associated with each T1. **C:**

Aspect ratios of the endpoint ellipsoids (shapes) for frontal and depth sequences

associated with each T1. **D**: Average absolute values of the axial components of

the 1st eigenvectors (orientations) associated with each T1. In general, volumes,

aspect ratios, and ellipsoid orientations did not vary substantially between frontal

and depth sequences in the V condition.

118

Variable errors without visual feedback. As in Fig. 5.2, Fig. 5.6 shows

average movement paths, individual movement endpoints, and confidence ellipses

for the four endpoint distributions associated with each T1. Data from a single

subject in the NV condition are shown. As expected, endpoint distributions were

often larger in this condition, which likely resulted from the increased uncertainty

associated with estimating the position of the hand in the absence of visual

feedback. In comparison to the V condition, variable errors in the NV condition

appeared to be somewhat less anisotropic and the nature of this anisotropy also

appeared to differ among the different types of sequences. That is, although the

variability associated with depth-directed sequences (red) still appeared to have a

very large component along the depth axis, this was less consistently observed for

the frontal sequences (black). In Fig. 5.6 these observations are most evident for

sequences associated with $T1_{down}$ and $T1_{right}$. Here the distributions for the

inward/outward sequences appear anisotropic and aligned with the depth axis,

while the distributions for the clockwise and counterclockwise sequences appear

either isotropic or do not appear to be aligned with the depth axis.

Figure 5.7 shows the average 1st eigenvectors associated with each type of

endpoint distribution in the NV condition, grouped by T1. There are noticeable

differences between these eigenvectors and those in the V condition. First, the

proportion of variance accounted for by the 1st eigenvector was typically smaller

in this condition (mean: 66% +/- 5%) and was somewhat smaller for the frontal

sequences than for the depth-directed sequences (61% vs. 72%), a finding which

was not observed in the V condition. These observations suggest that the endpoint

119

distributions were in fact more isotropic in this condition, particularly those

associated with frontal sequences, as was also suggested by Fig. 5.6. Regarding

the components of the eigenvectors, for virtually all sequence types the average

magnitudes of the lateral, vertical and depth components were more similar in this

condition than in the V condition. This was particularly true for the clockwise and

counterclockwise sequences. For example, although the eigenvectors for the

clockwise and counterclockwise sequences associated with $T1_{right}$ and $T1_{left}$

showed a slight tendency toward having larger components in depth this was not

the case for $T1_{up}$ and $T1_{down}$. In fact for $T1_{down}$, these components were relatively

uniform in magnitude for both the counterclockwise and clockwise sequences.

Thus there was not a consistent pattern of variability between sequence types in

the NV condition, unlike what was observed in the V condition.

Figure 5.7 shows that the inward/outward sequences *did* tend to have their

largest components along the depth axis, as was observed in the V condition.

However, the lateral and vertical components were relatively larger in this

condition than in the V condition, suggesting the endpoint distributions were not

as well aligned with the depth axis in the absence of hand vision. Overall, Figs. 6

& 7 suggest that movement variability in the NV condition, rather than being

dominated by visual planning noise, more strongly reflected the effects of

execution noise and/or an interaction between execution noise and visual planning

noise. This appeared to be particularly true for the movement sequences

performed in the frontal plane where the endpoint distributions were more

isotropic and apparently less clearly aligned with the depth axis.

120
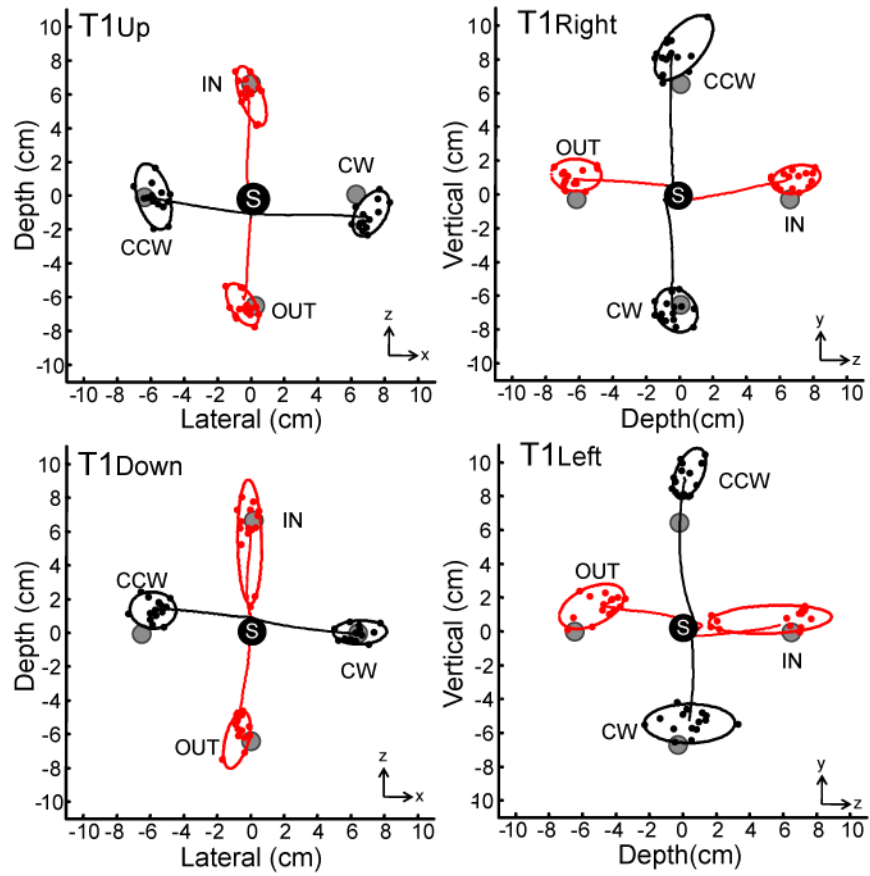
Figure 5.6. Movement endpoints, confidence ellipses, and average trajectories in the NV condition for a single subject. Figure conventions as in Fig. 5.2. Endpoint distributions were generally larger than those in the V condition and were less consistently elongated in depth.
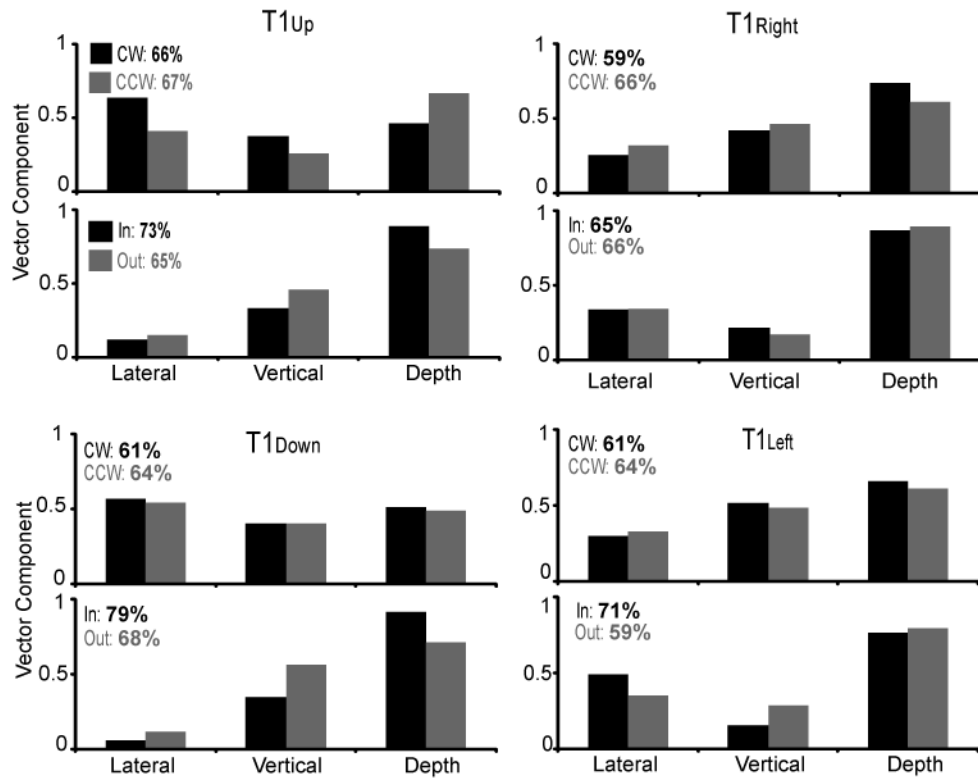
Figure 5.7. Mean 1st eigenvectors for the population in the N V condition. Figure conventions as in Figs. 5.3 & 5.4.

Size, shape, and orientation of endpoint ellipsoids without visual feedback. As was the case in the V condition, the 1st eigenvectors for counterclockwise and clockwise sequences at each T1 in the NV condition were statistically indistinguishable from each other at the population level (Mann Whitney U test applied along each axis, $p<0.05$). This was also true for the inward/outward sequences in the NV condition. As a result we again grouped the data together for the clockwise and counterclockwise sequences at each T1 ('frontal sequences') and also grouped the data together for inward and outward sequences ('depth sequences'). Figure 5.8A shows a horizontal plane view of the resulting population ellipsoids and 1st eigenvectors for the frontal and depth sequences associated with each T1. In contrast to the ellipsoids in the V condition, these appeared to differ somewhat in size and shape between sequence types (e.g. for T1$_{up}$ and T1$_{down}$). The most striking difference however was with regard to the orientations of the ellipsoids. Although the ellipsoids and eigenvectors for the depth sequences were strongly aligned with the depth axis (as in the V condition), this was not the case for the frontal sequences. For T1$_{up}$ and T1$_{down}$ these appeared to be oriented largely laterally, reflecting the fact that the clockwise and counterclockwise sequences associated with these T1s had large lateral components of movement. For T1$_{right}$ and T1$_{left}$, the eigenvectors and ellipsoids appear to be rotated out of the horizontal plane to some degree, consistent with the fact that the clockwise and counterclockwise targets associated with these T1s had large *vertical* components of movement.

123

As in the V condition, we quantified the sizes, shapes and orientations of the endpoint ellipsoids associated with the frontal and depth sequences in the NV condition and compared them. Figure 5.8B shows the average ellipsoid volumes. Ellipsoid volumes were generally much larger in the NV condition than in the V condition, averaging between 50 and 100 cm^3. Figure 5.8A suggested that the ellipsoid volumes for the frontal sequences were larger than those for the depth sequences, particularly for $T1_{up}$ and $T1_{down}$. Although some slight differences in the average ellipsoid volumes can be observed both across T1s and between sequence types in Fig. 5.8B, ellipsoid volumes tended to be quite variable across subjects. As a result, these differences were not statistically significant at the population level (2 factor ANOVA, $p=0.68$, $p=0.31$, and $p=0.35$ for main effects of T1, main effects of sequence type and interaction effects, respectively). Thus, similar to the V condition, endpoint distributions associated with frontal and depth sequences did not differ significantly in volume in the NV condition.

Figure 5.8C shows the average aspect ratios of the endpoint ellipsoids in the NV condition, grouped again by T1 and sequence type. Some similarities and some differences can be observed between the results of this analysis and the analogous one shown in Fig. 5.5. In terms of similarities, aspect ratios were generally consistent in magnitude across the different T1s, as they were in the V condition. However, aspect ratios were somewhat smaller under NV conditions, averaging between 1 and 1.25. (In contrast, the average aspect ratio in the V condition was ~1.5). This again suggests that endpoint variability was more isotropic without hand vision than with hand vision, as was also suggested by

124

Figs. 6 and 7. Another difference between the V and NV conditions was the tendency for aspect ratios to be somewhat larger for depth sequences than for frontal sequences in the NV condition. In Fig. 5.8C this can be observed for nearly all the T1s (the exception being $T1_R$) and is consistent with Fig. 5.7, which indicated that the proportion of variance accounted for by the 1st eigenvector was typically less for the frontal movement sequences than for the depth sequences. When examined statistically, although no significant main effect of T1 location on aspect ratio was found, a significant main effect of sequence type (frontal vs. depth) was identified (2 factor ANOVA; p=0.66 and p=0.04, respectively; p=0.22 for interaction effects). Post-hoc tests (Tukey's HSD) indicated that this difference arose largely due to differences associated with $T1_{down}$, though again Fig. 5.8C suggests that aspect ratios for most of the other T1s were trending in that direction. Overall, these results suggest that in the NV condition, depth sequences were associated with slightly more elongated endpoint distributions than those associated with frontal sequences and that both types of sequences were less elongated than those in the V condition.

Substantial differences were observed between the orientations of the endpoint distributions in the NV condition. Figure 5.8D shows the average components of the 1st eigenvectors derived from PCA for the frontal and depth sequences, grouped by T1. This figure suggests that depth sequences had their largest components of variability directed along the depth axis, as in the V condition. Statistical analyses confirmed that the depth components of the 1st eigenvectors differed from both the lateral or vertical components for all of the

125

T1s (Mann Whitney U test, p<0.05). However, this was not the case for the frontal sequences: only for $T1_{right}$ was the depth component significantly different from both the lateral and vertical components.

Not surprisingly then there were differences between the two sequence types along certain axes and, moreover, these differences were larger than those in the V condition and more consistent in nature. For example, lateral components were larger for the frontal sequences for $T1_{up}$ and $T1_{down}$ and vertical components for the frontal sequences were larger for $T1_{right}$ and $T1_{left}$ (Mann Whitney U tests, p<0.05). These differences were consistent with differences in the required movement axes used to approach the final target positions. That is, for frontal sequences, $T1_{up}$ and $T1_{down}$ were associated with large lateral terminal components of movement while those for $T1_{right}$ and $T1_{left}$ were associated with large vertical components. In contrast, depth sequences were not generally associated with either large lateral or vertical terminal movement components. Therefore, we conclude that in the absence of visual feedback, endpoint distributions differed in orientation (and to a lesser degree shape) between frontal sequences and depth sequences. These differences in orientation appear to reflect differences in the directions of the movement vectors used to approach the final target positions, suggesting an enhanced role for execution noise in determining patterns of endpoint variability when vision of the hand is unavailable.

Comparisons between feedback conditions yielded results that were similar in many ways to those described in Apker et al. (2010) but with several important additional findings. That is, a t-test performed on the combined data for

all T1s found that endpoint distributions (ellipsoid volumes) in the NV condition were larger than their V condition counterparts for both sequence types (p<0.05). In addition, aspect ratios of ellipsoids in the V condition were significantly larger than those in the NV condition for both sequence types (p<0.05). These results were similar to those described in Apker et al. (2010). Regarding differences in orientation, the orientation of the ellipsoids of depth sequences were generally similar between feedback conditions. That is, of the 12 comparisons made between axial components of the eigenvectors across all T1s, only 1 difference (8%) was found between feedback conditions. In contrast, for frontal sequence ellipsoids, 9/12 components (75 %) differed significantly between the V and NV conditions across all T1 location , including significantly differing depth components for each T1 location (Mann-Whitney U test, p<0.05). As a result, ellipsoids in the NV condition were more strongly biased along the lateral and/or vertical axes, consistent with a greater effect of the movement vector on these endpoint distributions.

Start-position corrected endpoint analysis. Variability in finger position at the starting position was analyzed to ensure that differences in endpoint variability did not arise from differences in variability at the starting position between frontal and depth sequences. A Levene's test confirmed that variability in the starting position was not significantly different along any axis between the frontal or depth sequences associated with a given T1; this was the case for both feedback conditions (p>0.05). As an added measure, we also reran our statistical analyses using start-position-corrected endpoint positions. The results of only

127

2/32 (6%) of our statistical tests differed following this correction: Differences in the 1st eigenvector components along the horizontal and depth axes for $T1_{right}$ in the V condition, which were previously shown to be statistically significant, were not significant following correction. Importantly, these exceptions do not alter the conclusions of this study; in fact they strengthen the conclusion that frontal and depth sequences were similar in the vision condition.
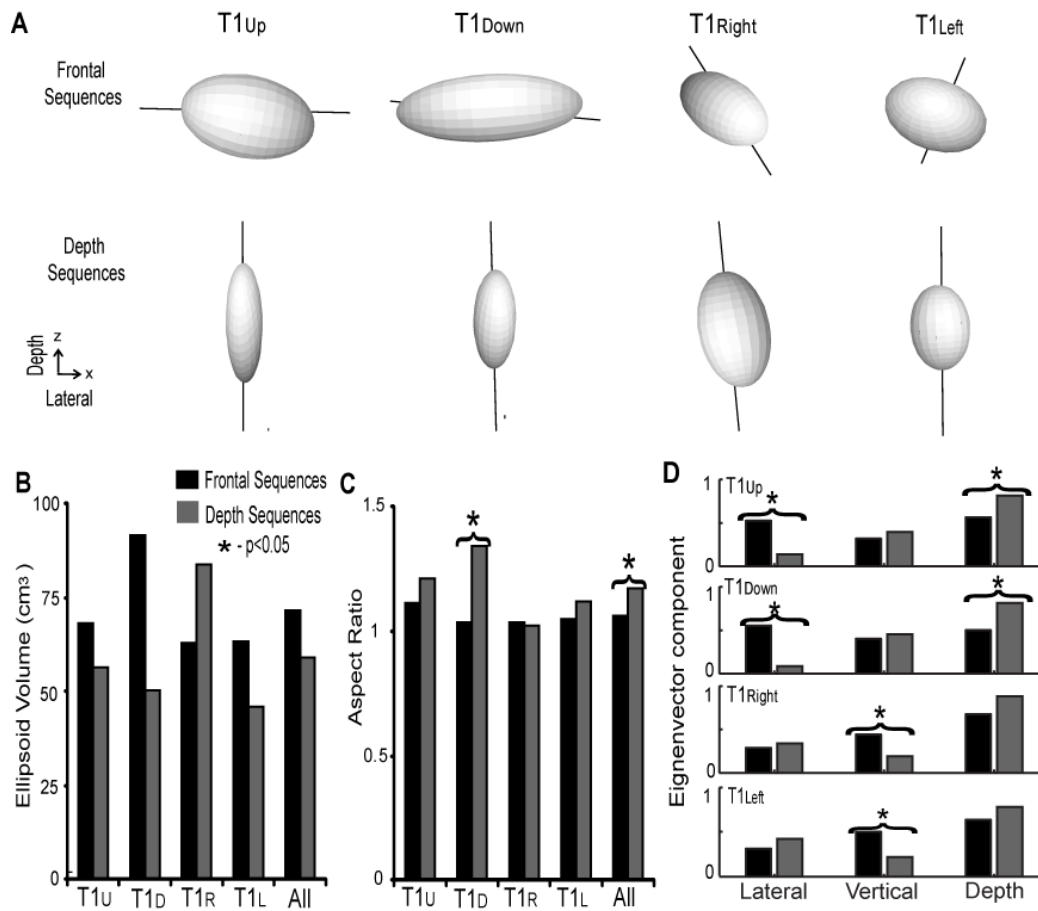
Figure 5.8. Analysis of endpoint ellipsoids associated with frontal and depth sequences in the NV condition. Figure conventions as in Fig. 5.5. Orientations (1st eigenvectors) varied substantially between frontal and depth sequences in this condition.

Discussion

      In this experiment, we quantified patterns of endpoint variability associated with movement sequences performed in the frontal plane and compared these patterns to those associated with sequences containing a large movement component in depth. For both types of sequences, movements were performed with and without vision of the hand. We hypothesized that for both visual conditions endpoint distributions would be more elongated and more aligned with the depth axis for sequences containing large movement components in depth. We found that when visual feedback of the hand was available, patterns of variability at the endpoint of both sequence types were highly anisotropic, with the primary axis of variability being strongly aligned with the depth axis, suggesting that the executed movement direction (and therefore execution noise) played only a minor role in shaping endpoint distributions in this condition. However, when visual feedback of the hand was not available, patterns of endpoint variability differed significantly for the two types of sequences. More specifically, while endpoint distributions associated with depth sequences were very similar to those observed with visual feedback of the hand, endpoint distributions for frontal sequences were more isotropic and not generally well aligned with the depth axis. These results emphasize the primacy of visual planning noise in determining patterns of endpoint variability in 3D space and also suggest that the removal of visual feedback (and resulting increased uncertainty in estimating hand position) *effectively* unmasks the effects of execution-related noise (and planning noise as well) leading to patterns of

variability which can differ substantially for movements performed along different axes in 3D space.

Relation to previous findings. Although previous studies have examined the relations between movement variability and sensing noise (Osborne et al., 2005; Shi & Buneo, 2009; van den Dobbelsteen et al., 2001; Vindras et al., 1998), planning noise (Churchland et al., 2006a; Gordon et al., 1994; McIntyre et al., 1998; 1997; Vindras & Viviani, 1998), and execution noise (Buneo et al., 1995; van Beers et al., 2004), the relative importance of these noise sources in determining patterns of arm movement variability in 3D space remains a matter of debate. For planar (2D) arm movements, it has been argued that movement variability is dominated by noise associated with execution (van Beers et al., 2004). In a previous study of 3D arm movement sequences performed in the frontal plane (Apker et al., 2010) we argued that patterns of arm movement variability were largely determined by visually-derived noise associated with planning movements in depth. That is, endpoint distributions were aligned with the depth axis and were only minimally influenced by the executed movement directions, suggesting a lesser role for execution noise. However, the fact that movement directions were predominantly orthogonal to the dominant axis of visual planning noise in this study made it difficult to distinguish the effects of execution noise from uncertainty in hand position, as each would be expected to manifest in roughly similar ways for these types of sequences.

The findings of Apker et al. (2010) were reminiscent of those of McIntyre and colleagues (1997, 1998) who also demonstrated that for point to point reaches

131

initiated from starting positions near the body to targets further away in depth, endpoint distributions were highly anisotropic and strongly aligned with the depth axis. In these studies, the primary axis of variability even converged toward the sight-line for movements performed in different workspaces with respect to the body, providing strong evidence that these patterns of variability arose from noise associated with visual estimation of the hand and/or target. The present findings for the V condition, and for the depth sequences in the NV condition, are consistent with the findings of both Apker et al. (2010) and McIntyre and colleagues (1997, 1998). However, the observation that endpoint distributions for frontal sequences were strongly influenced by the primary axes of movement in the NV condition suggests that execution noise can play a more significant role in determining patterns of endpoint variability when visual feedback of the hand is unavailable (Gordon et al., 1994; van Beers et al., 2004).

To ascertain the specific role of hand vision in determining patterns of variability in 3D space, Carrozzo et al. (1999) analyzed movement endpoints as human subjects made reaching movements with and without vision of the hand but with full vision of the target (achieved via a virtual reality paradigm). These investigators observed that patterns of endpoint variability in the presence of hand vision were consistent with those reported here for the V condition, i.e. they were highly anisotropic and strongly aligned along the depth axis. In the absence of hand vision patterns of variability were more isotropic and less aligned with the depth axis, consistent with the NV endpoint distributions for the frontal sequences in the present study but not with those for the depth sequences. These

132

observations can be explained by certain methodological differences between the two studies. In the study of Carrozzo et al. (1999), movements were similar to the frontal sequences in the present study in that final target positions were approached largely using varying degrees of vertical and lateral movements. It is not surprising therefore that the endpoint distributions in the two studies had some similar properties. In Carrozzo et al. (1999) movements also had components in depth, but these were very different from the depth-directed sequences used here. In the present study subjects were required to pass through (or near) an intermediate target that was at the same lateral and vertical position on the way to the final target. As a result, final target positions were approached using movements with much larger depth components than those in Carozzo et al. (1999), which likely explains why the depth-directed sequences were more aligned with the depth axis in the present study.

Interaction between planning and execution noise. Since movement directions were designed to be orthogonal to the depth axis in Apker et al. (2010) it was unclear if the interaction of execution and planning noise would manifest in a similar way for movement sequences that were directed *along* the depth axis. Given our previous results, as well as those of McIntyre and colleagues (1997, 1998) we hypothesized here that endpoint distributions would be more anisotropic and more aligned with the depth axis under these conditions, reflecting the fact that the dominant axes of execution noise and visual planning noise were aligned. In fact when visual feedback was present, endpoint distributions associated with both frontal plane and depth-directed sequences *were* anisotropic and aligned

133

predominantly with the depth axis and did not differ in terms of their overall sizes (volume), shapes or orientations. Thus, even when execution noise was directed along the depth axis, it did not appear to significantly alter overall patterns of movement variability. This supports the idea that uncertainty associated with planning and updating visually-guided movements plays a dominant role in determining patterns of endpoint variability in 3D space.

While the effect of execution noise was only minimally apparent in the V condition its effect could be easily observed in the NV condition, particularly during the performance of frontal plane movement sequences. Endpoint distributions appeared relatively isotropic for frontal plane movement sequences in the NV condition and were also not well aligned with the depth axis, appearing to be more strongly influenced by the primary axes of movement. Note that this also appeared to be the case in Apker et al. (2010), though due to the fact that only frontal plane movement sequences were used in that study we were unable to fully explain these patterns. In contrast, endpoint distributions for depth sequences in the NV condition more closely resembled those in the V condition, being largely anisotropic and oriented in depth. Based on these differences, we believe that patterns of endpoint variability in the absence of online visual feedback results from increased uncertainty in estimating the position of the hand, which effectively unmasks the effects of execution-related noise and planning noise.

The removal of visual feedback would be expected to result in greater uncertainty in estimating hand position as estimates that depend only on a single sense (proprioception in this case) are generally less precise than those derived

through multisensory integration (van Beers et al., 2002a). This increased uncertainty would be expected to have two effects. First, movement planning would be adversely affected, resulting in errors in planned movement directions and extents (Buneo et al., 1995; Franklin et al., 2007; Shi & Buneo, 2009). These errors would be compounded by noise associated with visual estimation of the targets as well as central planning noise, with the resulting effects on behavior being difficult to predict. However, it is likely that variability would be increased along all axes leading to generally more isotropic distributions. Second, in the absence of online visual feedback increased hand position uncertainty near the end of the movements would be expected to effectively increase the influence of execution noise (by failing to mitigate it, as when vision is available), thereby elongating the endpoint distributions along the movement direction (van Beers et al., 2004). For frontal sequences, this would result in endpoint distributions that reflected a combination of enhanced execution noise and visual planning noise, which was observed in the present study (see Fig. 5.8D). For depth sequences, this interaction would be less apparent, as the executed movement directions were not orthogonal to but aligned *with* the primary axis of visual planning noise. Even so, the observation that ellipsoids were larger and less elongated under these conditions is consistent with effectively increased levels of both planning and execution noise during performance of these sequences.

Given that endpoint distributions of 3D movements are highly dependent on planning noise, it would be interesting to know if this endpoint variability arises due to planning noise at the beginning of movement or is more related to

135

uncertainty towards the end. The influence of execution noise is most dependent

on the terminal phases of movement (van Beers et al., 2004); it may also be the

case therefore that the influence of planning noise largely reflects feedback

conditions nearer the end of movement. This could be tested by removing visual

feedback at various times throughout the movement. Conversely, it would also be

of interest to observe the effect of returning visual feedback at various points in

the terminal movement. Recently, Faisal & Wolpert (2009) demonstrated that

temporal characteristics of sensory and execution noises integrate in a 'near

optimal' manner. Varying the timing and/or duration of visual feedback would

help integrate this finding with the present results to develop a better sense of the

spatiotemporal nature of the influence of planning and execution noises.

CHAPTER 6

MULTIMODAL FEEDBACK CONTROL OF REACHING UNDER

ANISOTROPIC FEEDBACK NOISE

Introduction

Variability in goal oriented reaching performance is an inevitable product

of human sensorimotor control. This is due to noise in the neural signals

underlying both the planning and execution phases (Faisal et al., 2008,

Churchland et al., 2006). Planning variability is largely attributable to uncertainty

in sensory feedback estimates of limb position, while execution noise arises from

variability in the motor commands and muscle contraction (van Beers et al.,

2004). A growing body of evidence suggests an important function of the brain is

to minimize perceptual and behavioral variability (Wolpert et al., 1995, Kording

& Wolpert, 2004). To accomplish this, brain would need to employ a mechanism

to minimize the effects of noise in planning and execution phases of movement.

Given the perceived origins of variability, optimizing performance

requires minimizing the noise in sensorimotor processes. Statistically speaking,

minimizing signal noise can be accomplished by integrating information weighted

by its noise level relative to other related information. Indeed, sensory integration

has been found to be related to the relative signal reliability of the constituent

feedback modalities (Earnst & Banks 1993, Kording & Wolpert 2002, Gu et al.,

2008). In fact, this strategy of integration has been shown to operate on a

direction-dependent basis, weighting feedback differently for each direction

depending on the specific spatial characteristics of sensory uncertainty (van Beers

et al., 1999, van Beers et al., 2002b). By minimizing uncertainty this scheme of integration also subsequently minimizes planning noise, thereby reducing behavioral variability (Wolpert et al., 1995, Shi and Buneo, 2009). Thus, the ultimate influence of planning noise on movement variability depends on the anisotropic properties of the feedback, as well as on the result of their direction-dependent integration.

During movement, afferent sensory signals can significantly lag behind the real-time position of the hand, limiting their efficacy for online control (Rumelhart & Jordan, 1992). To overcome this, the brain uses a copy of the efferent motor commands to generate their predicted outcome to enhance and update the estimate provided by noisy, time-lagging sensory signals into a real-time estimate of limb position for online control (Wolpert et al., 1995; Todorov & Jordan, 2002; Mulliken et al., 2008; Moran & Schwartz, 1999). However, like sensory signals, the motor commands provide a somewhat unreliable source of limb information as the execution of them is corrupted by noise. This results in a discrepancy between predicted and actual outcome of the motor command. Thus, there is an inherent interaction between planning and execution noise during the control. While extensive work has resulted in a keen awareness of how each noise process independently affects movement, many questions remain regarding the contribution and interaction of planning and execution noise in movement variability (Apker et al., 2010, Apker & Buneo, 2012).

Recent evidence suggests the brain learns the statistical properties of the signal noise associated with sensorimotor control (Kording & Wolpert, 2004, van

Beers et al., 2009). As a result, it has been suggested that the behavioral

variability we observe can be modeled as the optimal integration of the noisy

processes underlying sensorimotor control (Todorov & Jordan, 2002, Wolpert et

al., 1995, Guigon et al., 2008). This framework provides a means to model the

interaction of planning and execution noise and generate predictions about how

this may be observed in behavior. With respect to the control of reaching,

Todorov & Jordan (2002) established optimal feedback control as an effective

model of normal non-visually guided reaching. Also simulating non-visual

reaching, Guigon et al. (2008) probed whether control was optimal with respect to

the entire movement or just terminal control using isotropically distributed

feedback noise. Saunders & Knill (2004) also employed a feedback controller that

minimizes endpoint variability to model sensory-motor integration during a visual

perturbation task. In that work, the authors used established properties of

variability in visual estimation in the feedback control model (Saunders & Knill,

2004). However, this model did not include a somatic feedback signal nor did it

account for the spatial anisotropy associated with visual feedback (van Beers et al.

1998, 2002; Viguer et al., 2006). To gain a more complete picture of how noise in

the neural processing underlying sensorimotor affects behavioral variability an

important step is to incorporate both visual and proprioceptive feedback into an

optimal feedback control model of reaching.

We developed a stochastic feedback control model augmented with a

Kalman filter to evaluate the influence of anisotropic feedback noise on the

interaction of planning and execution noise. As illustrated in Figure 6.1A, the

139

model is essentially the "optimal observer" model as described by Wolpert (2007) designed to integrate multiple feedback inputs with an internal estimate of limb position derived from the motor commands. Thus, this model more faithfully represented the processes and integration underlying sensorimotor control that result in behavioral variability. The model was used to generate predictions of endpoint variability under a variety of unimodal sensory feedback control conditions. The results of these simulations clearly demonstrate a significant influence of the spatial anisotropy of feedback noise on patterns of endpoint variability in optimal control. In addition, simulations of multimodal feedback control indicated that the combined influence of both sensory modalities yields unique patterns of predicted variability that could not have been predicted on the basis of any previous evidence. These results suggest that spatial dependencies of sensory feedback noise affect the behavior and predictions of both uni- and multimodal feedback control and thus should be considered when developing models of human movement.
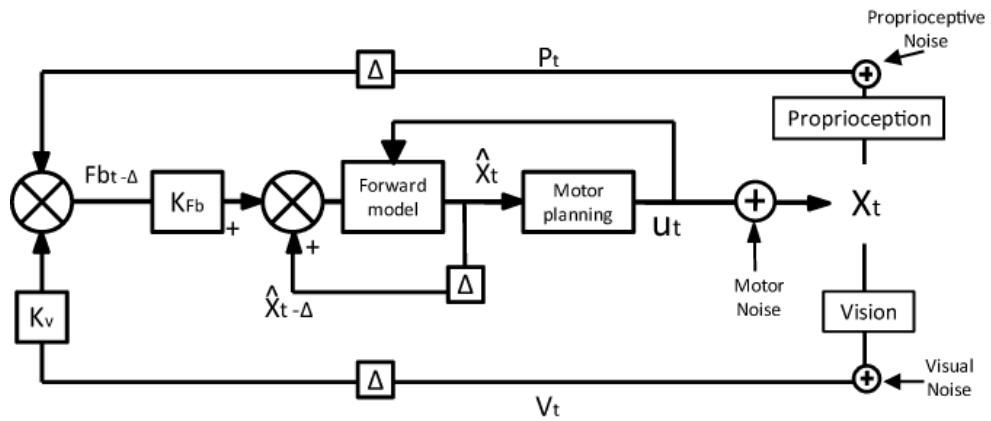
Figure 6.1. Block diagram of a multimodal feedback control model for reaching.
X_t represents the true state of the limb endpoint. $\hat{X}_t$ represents the internal
estimate of X_t developed by the brain from the combination of visual and
proprioceptive feedback along with previous knowledge of the position of the
hand and a forward estimate derived from stored motor commands.

Methods

      Model development. To emulate the sensorimotor control of reaching, we

have developed a multimodal feedback control model expanded from the

feedback controller proposed by Arbib & Hoff (1993), with similar adaptation

employed by Saunders & Knill (2004) to yield an optimal feedback control

model. In this model, the control of the limb is corrupted by multiple independent

sources of Gaussians noise; noise associated with the sensory estimates of the

position of the hand which affect the specification of the motor commands

('sensory/planning noise') and noise in the execution of those commands

('execution noise'). We assume the state of the reaching system is defined as the

lateral (x) and depth (y) components of position, velocity, and acceleration of the

limb endpoint, as well as the position of the target along these two axes at any

given time. In the model, this is represented by a vector X_t, which represents the

actual state of the system at time t:

$$X_t = \{x, \dot{x}, \ddot{x}, y, \dot{y}, \ddot{y}, T_x, T_y\}^T, \tag{1}$$

where $x, \dot{x}, \ddot{x}$ and $y, \dot{y}, \ddot{y}$ represent position, velocity and acceleration along the

lateral and depth axis respectively, and T_x, T_y represent the position of the target

along the lateral and depth axis respectively. The process model by which the

state is expected to evolve over time is given by:

$$X_{t+1} = AX_t + u_t + \sum_i \gamma_{t,i} C_i u_t + \varepsilon, \tag{2}$$

where ε is a signal independent process noise with covariance matrix R_ε, u_t is the

motor command at time t, $\sum_i \gamma_{t,i} C_i u_t$ is the signal dependent process/execution

noise with random noise $\gamma_{t,i}$, and matrix C_i which scales the magnitude of the

noise with the size of the motor command, and A is the evolution matrix which

proprigates the previous state forward in time:

$$A = \begin{bmatrix} 1 & \partial & 0 & 0 & 0 & 0 & 0 & 0 \\ 0 & 1 & \partial & 0 & 0 & 0 & 0 & 0 \\ 0 & 0 & 1 & 0 & 0 & 0 & 0 & 0 \\ 0 & 0 & 0 & 1 & \partial & 0 & 0 & 0 \\ 0 & 0 & 0 & 0 & 1 & \partial & 0 & 0 \\ 0 & 0 & 0 & 0 & 0 & 1 & 0 & 0 \\ 0 & 0 & 0 & 0 & 0 & 0 & 1 & 0 \\ 0 & 0 & 0 & 0 & 0 & 0 & 0 & 1 \end{bmatrix} \tag{3}$$

where ∂ is the time-step between filter iterations; $\partial = 1$ millisecond for all

simulations

As the process evolves, the controller, in this case the brain, attempts to

form an estimate of the state of the system simultaneously from its previous

internal estimate and motor commands which can be augmented with feedback

carrying information of the actual state. In the algorithm, the noisy, internal

estimate is modeled as:

$$\hat{X}_t = \{x, \dot{x}, \ddot{x}, y, \dot{y}, \ddot{y}, T_x, T_y\}^T \tag{4}$$

The estimate of the system, e.g. the perceptual state of the limb developed in the

brain, resembles the real state minus process noise:

$$\hat{X}^-_{t+1} = A\hat{X}_t + u_t \tag{5}$$

To simulate the motor command, we employ a model of the minimum jerk

principle as proposed by Arbib and Hoff (1993), where u_t defined is:

$$u_t = L_t\hat{X}_t \tag{6}$$

where L is derived from the minimum jerk hypothesis, given by:

$$L_t = \begin{bmatrix} 0 & 0 & 0 & 0 & 0 & 0 & 0 & 0 \\ 0 & 0 & 0 & 0 & 0 & 0 & 0 & 0 \\ -60/D^3 & -36/D^2 & -9/D & 0 & 0 & 0 & 60/D^3 & 0 \\ 0 & 0 & 0 & 0 & 0 & 0 & 0 & 0 \\ 0 & 0 & 0 & 0 & 0 & 0 & 0 & 0 \\ 0 & 0 & 0 & -60/D^3 & -36/D^2 & -9/D & 0 & 60/D^3 \\ 0 & 0 & 0 & 0 & 0 & 0 & 0 & 0 \\ 0 & 0 & 0 & 0 & 0 & 0 & 0 & 0 \end{bmatrix} \qquad (7)$$

where D is the time remaining before the end of the movement. The resulting

motor command, u_t, is a single column vector with values which define the

change in acceleration needed to reach the target smoothly on the basis on the

current state of the limb and target.

As mentioned previously, neural processes are inherently noisy, limiting

the accuracy and reliability of internal estimates. We assume that the level of

noise associated with the evolving process is relatively stable and further there is

evidence that the brain has also information related to the reliability of its

estimate. We can approximate the computation done by the brain by developing

the *a priori* error covariance of the estimated state at the next time step based on

the size of the motor command:

$$\Sigma_{t+1}^- = A\Sigma_t A^T + \sum_i C_i L_t \hat{X}_t \hat{X}_t^T L_t^T C_i^T + R_\varepsilon \qquad (8)$$

In addition to the predictive estimates of the limb position based on motor

commands, the brain is also provided with sensory feedback of the actual state. If

we assume a single feedback signal, F_t, is used to augment the state estimate, then

the optimal integration of this input is derived from:

$$\hat{X}_{t+1} = AK_{est}(F_t - H\hat{X}_t) \qquad (9)$$

144

where K_{est} is the Kalman gain for the state estimate and is derived from the state covariance matrix and combined feedback covariance, R_{fb}, which is derived from the properties of the feedback signal or signals (see below) :

$$K_{est} = \left[(H\Sigma_t H^T + R_{fb})^{-1} H\Sigma_t \right]^T \tag{10}$$

where *H* is term which maps feedback estimates to the state estimates. This estimate is then advanced in time with the stored motor commands (see Knill & Saunders 2004) to provide an optimal estimate of limb position for the next time step, $\hat{X}_{t+1}$.

Given the additional information from the sensory feedback, the a posteriori error covariance estimate is generated from the prior error estimate:

$$\Sigma_{t+1} = (1 - AK_{est}H)\Sigma_{t+1}^- \tag{11}$$

Multi-modal feedback signals and integration. In most situations, multiple sensory sources of information of limb and target position are available to the brain during estimation and control. Specifically, the brain appears to rely most heavily on visual and proprioceptive feedback. However, this feedback is inherently noisy. Furthermore, the noise properties of sensory feedback are anisotropic and modality specific. For the purposes of this model, we will assume vision and proprioception only provide an estimate of the position and velocity of the hand and that the feedback can be modeled as:

$$V_t = HX_t + \eta_{v,t}$$

$$P_t = HX_t + \eta_{p,t} \tag{12}$$

145

where H is a term which maps the state estimate at time t into the visual, V_t, and proprioceptive, P_t, sensory feedback signals. $\eta_{v,t}$ and $\eta_{p,t}$ are the noise/uncertainty in the visual and proprioceptive systems with covariance matrix R_v and R_p, respectively.

Statistically optimal sensory feedback integration is believed to follow from maximum likelihood integration of sensory estimates (for a review, see Kording & Wolpert, 2006). That is, the weighting of the proprioceptive feedback signal is derived from its variability, σ_P^2, relative to that of the visual signal, σ_V^2:

$$Weight_p = \frac{\sigma_V^2}{\sigma_P^2 + \sigma_V^2}. \tag{13}$$

This equation is reminiscent of the development of the Kalman Gain. Ergo, we also calculate a Kalman gain to determine the optimal integration of visual and proprioceptive feedback using the covariance of their respective feedback noise:

$$K_{vis} = \frac{R_p}{R_v + R_p} = \left[\left(R_V + R_p \right)^{-1} R_p \right]^T. \tag{14}$$

With this, the optimal integration of the feedback estimate follows a similar form as Eq. 9:

$$F_t = P_t + K_{vis}(V_t - P_t) \tag{15}$$

where F_t is the integrated feedback signal used in Eq. 9. This method defines the combined variability of the estimate according to:

$$\sigma_{combined}^2 = \frac{\sigma_V^2 \sigma_P^2}{\sigma_P^2 + \sigma_V^2}. \tag{16}$$

Thus, the combined feedback signal covariance used in the filter model is equivalent to:

$$R_{fb} = \frac{R_p R_v}{R_v + R_p} = (R_p R_v)(R_v + R_p)^{-1} \tag{17}$$

Sensory noise parameters. Noise in both visual and proprioceptive estimation has been shown to have anisotropic localization properties (van Beers et al., 1998, McIntyre et al., 1997, Viguier et al., 2001). This anisotropy has been quantified in the horizontal plane, as illustrated in Figure 6.1B. Thus, position estimation noise for both feedback inputs were configured to reproduce this behavior along the lateral and depth axes (van Beers et al., 1998, van Beers et al., 2002b).

$$\sigma_{V,x} = 0.1 cm, \quad \sigma_{V,y} = 0.4 \ cm$$

$$\sigma_{P,x} = 1.0 \ cm, \quad \sigma_{P,y} = 0.5 \ cm \tag{18}$$

where $\sigma_{V,x}$ and $\sigma_{V,y}$ represent visual position noise and $\sigma_{V,x}$ and $\sigma_{V,y}$ represent proprioceptive position noise.

Visual and proprioceptive motion noise were derived from previously reported properties. In the case of vision, the relative relationship between position noise and motion noise in the direction of movement was preserved (Saunders & Knill, 2004), although the specific values were scaled to be consistent with the direction-dependent characteristic of position variability (described in Eq. 18). Similarly, the respective relationship of position-to-motion variability in proprioceptive guidance as described in Guigon et al.'s (2008) optimal feedback controller was preserved. Thus motion noise in each feedback modality was also direction dependent, yielding standard deviations of motion noise:

$$\sigma_{V,\dot{x}} = 0.3 \frac{cm}{msec}, \quad \sigma_{V,\dot{y}} = 3 \frac{cm}{msec}, \tag{19}$$

$$\sigma_{P,\dot{x}} = 10 \frac{cm}{msec}, \quad \sigma_{P,\dot{y}} = 5 \frac{cm}{msec}, \tag{20}$$

where $\sigma_{V,\dot{x}}$ and $\sigma_{V,\dot{y}}$ represent visual motion noise and $\sigma_{V,\dot{x}}$ and $\sigma_{V,\dot{y}}$ represent proprioceptive motion noise. These parameters define the position and motion noise for the feedback noise terms η_v and η_p. In all simulations, the target was assumed to be visible throughout the reach; thus, feedback of the target position was assumed to have noise properties similar to that of visual position noise.

Execution noise parameters. Signal independent and signal dependent characteristics of execution noise were configured to be similar with those previously derived for the minimum jerk-model. Specifically, parameters which were empirically derived from human reaching and implemented in the feedback control model of Saunders & Knill (2004) were also used in the present model to derive the total variability from execution noise, σ_{exe}:

$$\sigma_{exe} = 0.5 \frac{cm}{msec^2} + 0.05u_t \tag{21}$$

The signal independent term was used in the ε term and the coefficient of the signal dependent term was used to populate the appropriate diagonals of the C matrix. The signal independent terms was also used to fill the appropriate positions of the R_ε matrix. These coefficients were then scaled to better reproduce previously observed patterns of execution variability for planar reaching of similar movement durations (van Beers et al., 2004).
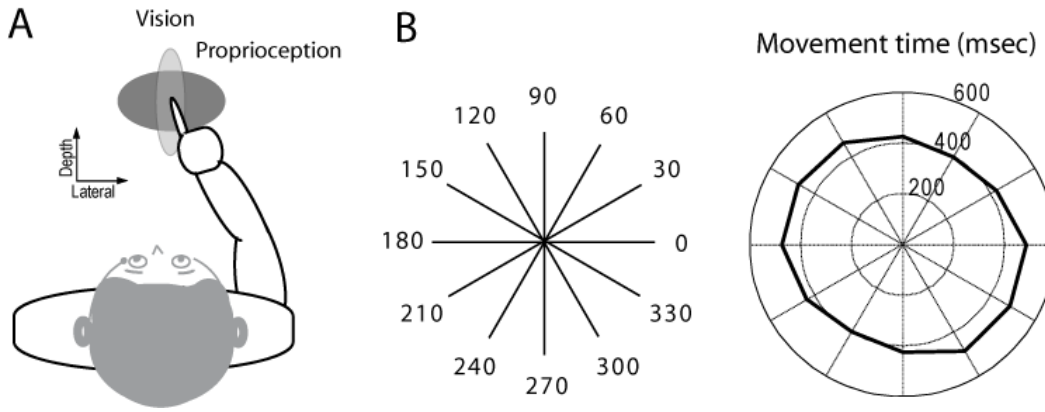
Figure 6.2. Simulation parameters. **A.** Cartoon illustrating the spatial

characteristics of sensory uncertainty in localization. These characteristics were

used to simulate visual and proprioceptive unimodal feedback control, as well as

multimodal feedback control assuming the optimal integration of the two sensory

estimates. **B.** Movement directions to be simulated and associated direction

dependent movement times used during simulation. Movement times are

consistent with those reported for movements of similar magnitude in van Beers

et al. (2004).

Simulations. Reaches were simulated from a central starting to position to each of twelve (12) targets positioned eight (8) cm from the starting position. There is evidence which suggests that average movement time is strongly influenced by inertial forces acting on the limb, producing direction dependent movement times in the horizontal plane (Gordon et al., 1994). The predictions of the motor output from the minimum jerk model used here are sensitive to changes in movement time, therefore, movement times inputted into the model were direction dependent, to be consistent with known characteristics of reaching in the horizontal plane from a natural posture (van Beers et al., 2004). The movement times used for each direction are illustrated in Figure 6.1C. This pattern of movement time was applied to all simulations. A feedback delay of 100msec was used for all simulations.

As means to evaluate the contributions and interaction of execution and sensory/planning noise in an optimal feedback control framework, the above model was configured to simulate movement under a variety of sensorimotor contexts. The first such scenario entailed the elimination of feedback noise entirely, such that the only source of variability was attributable to execution noise (henceforth referred to as "Execution-Only" model). This was achieved by setting both sensory noise terms, $\eta_{v,t}$ and $\eta_{p,t}$, to zero as well as configuring the Kalman Gain, K_{est}, to equal 1 as would be expected under perfect feedback reliability. A second simulation scenario was designed to evaluate the effects of feedback noise with spatial characteristics uniformly distributed in space (referred to as "Isotropic Feedback Noise" model). This was accomplished by simulating

150

feedback control with a single modality (e.g. vision) with isotropic equal noise levels along both the lateral and depth axes, with specific values such that the total variance would commensurate with previously quantified visual uncertainty (see Figure 6.1B):

$$\sigma_{V,x|y} = 0.45 \; cm, \qquad \sigma_{V,\dot{x}|\dot{y}} = 1.35 \; \frac{cm}{msec}. \tag{22}$$

Both the feedback signal and feedback covariance matrix were set to equal those of the visual feedback modality thereby obviation the proprioceptive input.

Reaching was also simulated assuming a single feedback source with natural noise characteristics tailored to approximate the amount of uncertainty of biological sensory feedback. Movements were simulated under three conditions of sensorimotor control with natural feedback noise characteristics: visual guidance alone ('Visual Feedback Noise'), proprioceptive guidance alone ('Proprioceptive Feedback Noise'), and control guided by the optimal integration of the sensory modalities ('Multimodal Feedback Noise'). Comparison of these models with those described above was used to evaluate the relative contributions and interaction of feedback and motor noise in the context of optimal feedback control of reaching movements.

Data analysis. For each simulation condition five hundred (500) independent movements were simulated to each target position. As described in Apker et al. (2010) and Apker & Buneo (2012), movement endpoints were identified as the point at which the tangential movement velocity fell below 5% of its peak value for each simulated movement. Analysis focused on the variable errors, which provide more direct information about planning and execution-

related noise (McIntyre et al., 1998; Carrozzo et al., 1999; van Beers et al., 2004). Principal components analysis (PCA) was also used to analyze the endpoint distributions associated with frontal and depth sequences. The 95% tolerance ellipsoids associated with each endpoint distribution were first computed as follows (McIntyre et al., 1998; Morrison, 1990):

$$T_{95\%} = q \frac{(n+1)(n-k)}{n(n-q-k+1)} F_{0.05,q,n-q-k+1} H , \qquad (24)$$

where the dimensionality $q=3$, the number of target positions $k=1$, and H is the covariance matrix. The resulting eigenvalues and eigenvectors (obtained from the matrix T) were used to quantify the sizes, shapes and orientations of the endpoint distributions (see below). For visualization purposes, 95% confidence ellipses and ellipsoids were calculated using Matlab code based on the Khachiyan algorithm (Khachiyan, 1996; Khachiyan & Todd, 1993), as implemented by Nima Moshtagh.

Endpoint distributions associated with frontal and depth sequences were compared by analyzing differences in the sizes, shapes and orientations of their corresponding tolerance ellipsoids. The size of each ellipsoid was quantified by its total variance:

$$Total\ Var. = ab\pi, \qquad (25)$$

where a represents the radius of the major axis of the 95% confidence ellipsoid and b represents the radii of the minor axes. The aspect ratio was used to characterize the shape of each ellipsoid, defined as the ratio of the radius of the major axis of the ellipsoid to the sum of the radii of the minor axes. Lastly, the

general orientation of each ellipsoid was defined by the absolute values of the components of the first eigenvector derived from the PCA (Carrozzo et al., 1999; McIntyre et al., 1998; 1997).

Statistical analysis. To assess whether spatial properties of feedback noise significantly affected the patterns of variability predicted by the optimal feedback control model, correlation analysis was applied between the simulations to determine whether the calculated total variance, aspect ratio, or orientation deviation of 95% confidence ellipses followed the same patterns across all the reaching directions. The rationale for this is as follows: depending upon the spatial characteristics of the modeled sensory variability, the expected influence of the feedback signal would also be direction dependent, resulting in weak correlation between the predicted patterns of variability of different feedback models. On the other hand, if two simulations are found to be significantly correlated, the differences in noise properties can be assumed not to have significantly affected the model's predictions of reaching performance. To compare between simulation results, non-parametric Mann-Whitney U tests were applied to the above characteristics of endpoint variability for each target position. For all tests, a significance threshold of $p = 0.05$ was used.

Results

Execution-only model. Figure 6.3 illustrates simulated endpoint positions and calculated 95% confidence ellipses generated from the predicted endpoints of movements simulated without variability in estimation of the hand or target, i.e. zero planning noise. Ellipses appear elongated almost entirely along the direction

153

of movement, consistent with the anticipated effects of execution dependent variability (van Beers et al., 2004). As illustrated in Figure 6.4, average peak movement velocity varied between 31.3 and 38.0 cm/sec across the movement directions. As expected, movement time and peak velocity were strongly correlated (R = -0.995, p<0.05) for these simulations, with shorter movement times resulting in increases in peak velocities, consistent with the need to generate stronger motor commands for those directions. The length and size of the ellipses in figure 6.3 appear slightly larger for movements in the first and third quadrants, consistent with those directions with the greatest peak velocities.

Figure 6.4B-D illustrates the total variance, aspect ratio and orientation deviation of the 95% confidence ellipses, respectively, calculated for simulated endpoints for each movement direction. Total variance arising solely from execution noise was found vary between 71.7 and 101.3 mm^2. Aspect ratio varied between 3.5 and 2.5, and a significant correlation was found between aspect ratio and movement velocity (R=0.912, p<0.05). The predicted values of total variance and aspect ratio, including the relationship between aspect ratio and movement speed, are all consistent with previously observed contributions of signal dependent motor noise to reaching variability for movements of a similar size and speed (van Beers et al., 2004). Lastly, the deviation between movement vector and ellipse orientation is nearly zero for all directions. This suggests that the orientation of simulated endpoint ellipses was largely along the direction of movement, again in agreement with the anticipated effects of execution related noise (van Beers et al., 2004).

154
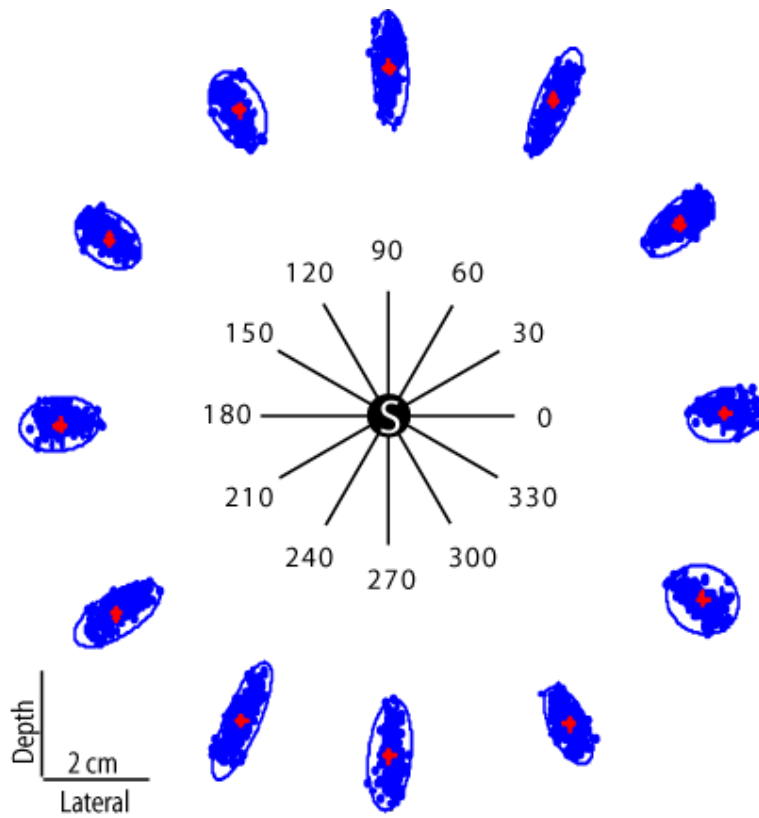
Figure 6.3. Predicted endpoints of feedback control model with zero feedback

noise. Predicted endpoint positions (blue dots) for all movements simulated with

95% confidence ellipsoids (blue lines). The average endpoint position for a given

direction is shown as a red cross at the center of each distribution. Inset scale

relates endpoint distributions but not distance from the central starting position to

a given endpoint.
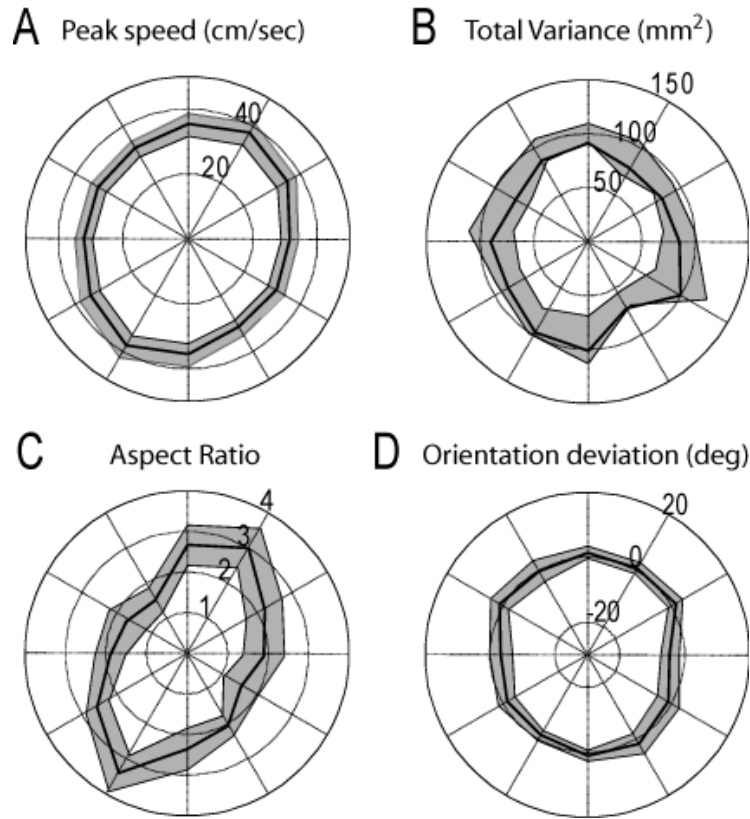
Figure 6.4 Size, shape, and orientation of predicted endpoint ellipses for the
feedback control model with zero feedback noise . **A.** Polar plot of the average
peak velocity of simulated movements. Black curves here and below represent
mean values and the surrounding shaded areas represents the 95% confidence
interval. Peak velocity was inversely related to movement time (R= -0.995,
p<0.05). **B.** Total variance in predicted endpoint distributions. **C.** Aspect ratio of
endpoint ellipses. **D.** Orientation deviation of ellipses from the movement
direction. Near zero degree deviations suggest endpoint ellipses varied
systematically with movement direction.

Isotropic vs. anisotropic feedback noise. The results of the isotropic feedback noise model are illustrated in Figure 6.5A. In general, the patterns of endpoint variability were very similar to those observed for the zero-planning noise model. In fact, the patterns of aspect ratio were significantly correlated to those of the model of execution variability alone (R=0.832, p< 0.05), as was the pattern of deviation off the movement vector (R=0.819, p<0.05). This suggests that isotropic noise has little effect on the patterns of endpoint variability attributed to execution processes. Patterns of total variance patterns were also similar to the execution-only model, only slightly larger values due to the increased feedback uncertainty. This suggests that under isotropic properties of sensory/planning noise, patterns of endpoint variability appear to be largely dependent upon the characteristics of execution noise.

Figure 6.5 also illustrates the predicted patterns of variability for simulations with visual feedback noise only (Fig. 6.5B) as well as proprioceptive noise only (Fig. 6.5C). In each of these conditions, the predicted patterns of endpoint variability often differed significantly from those of the isotropic feedback noise. For instance, while the average total variance was similar between the isotropic and visual noise models, neither total variance nor the aspect ratios were strongly correlated with the isotropic model predictions (R=0.346, p=0.24 and R=0.48, p=0.1, for total variance and aspect ratio, respectively) and significantly differed for all 12 directions (Mann-Whitney U-test, p<0.05).

157

For the visual model, Fig. 6.5 B shows that endpoint ellipses were most elongated along the depth axis in this condition (the direction in which visual noise was also elongated as illustrated in the left-most column). The increased influence of spatial patterns of feedback noise was also apparent in the patterns of ellipse orientation deviation from the movement direction and lack of correlation with the results from the isotropic noise model. Orientation of the endpoint ellipses under visual feedback noise were often askew from the movement vector, with the exception being those movements along the depth axis, where the principle axis of feedback noise (i.e. the depth axis) and execution noise (movement direction) were well aligned.

In the proprioceptive noise model, overall total variance of endpoint variability significantly increased compared to previous simulations, consistent with increased sensory uncertainty associated with proprioceptive feedback (Mann-Whitney U-test, $p<0.05$), and was not correlated with any other noise model. In addition, aspect ratios were generally dissimilar to the visual and isotropic noise models and significantly differed from these models along all 12 directions (Mann-Whitney U test, $p<0.05$). In this case, aspect ratio was greatest for those movements most aligned with the lateral axis, the axis of greatest proprioceptive feedback noise. Lastly, the orientation deviation of endpoint ellipses varied from the movement vector for many directions, but was near zero when the movement direction was along the lateral axis.
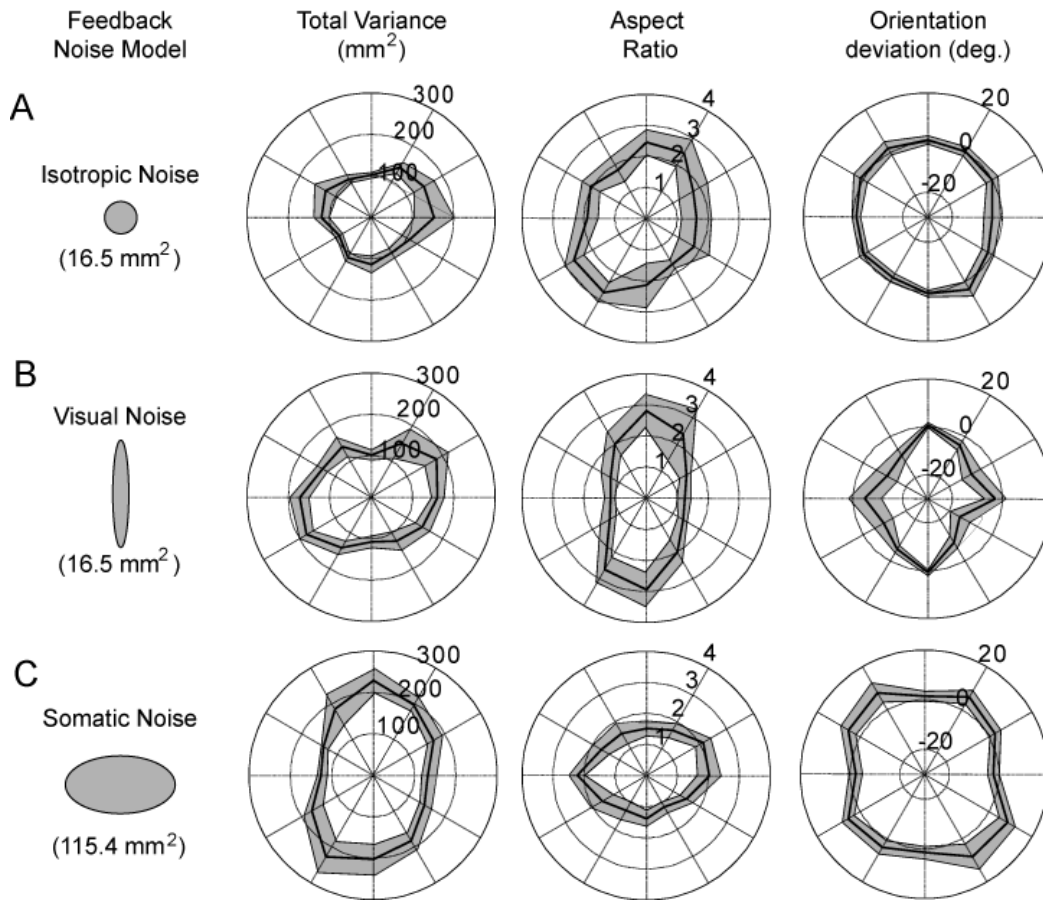
Figure 6.5. Comparison of the predicted patterns of endpoint variability between unimodal feedback control models. Format of polar plots is similar to that in Fig. 6.4. Cartoons on the left illustrate the spatial characteristics of the **A** isotropic, **B** visual, and **C** proprioceptive feedback noise used in the model to generate the predictions illustrated in the same row. Predicted total variance, aspect ratio, and orientation deviation of endpoint ellipses varied among the unimodal models. In all cases anisotropic noise models yielded anisotropic patterns of variability which differed significantly from the predictions of the isotropic feedback noise model.

Multimodal feedback. Finally, feedback control of reaching was simulated with a feedback signal derived from the maximum likelihood integration of two feedback sources with noise properties similar to those of visual and proprioceptive uncertainty. The results of these simulations are shown in Figure 6.6. In general, the patterns of simulated endpoint variability appear to be most similar to those observed in the simulations of visual feedback. For instance, aspect ratios are greater for movements along the depth axis, consistent with the patterns of visual noise. In fact, aspect ratios of ellipses generated from the multimodal model were significantly correlated with only those of the unimodal simulation with visual feedback-like noise (R=0.902, p<0.05). Similarly, the orientations of these predicted ellipses were also somewhat similar the unimodal simulations with anisotropic visual noise characteristics. It should be noted, however, that aspect ratios and orientations were not identical to those observed in the unimodal visual feedback model and were not significantly correlated with those of any other simulated feedback condition. Similarly, total variance was not significantly correlated with any other model predictions of endpoint variability. In all cases, the predictions of the multimodal model significantly differed from those of the other feedback models along many of the movement directions (Mann-Whitney U test, p<0.05).

These differences between multimodal feedback simulations and other simulations are related to the combined influence of the two feedback modalities. That is, while the predicted endpoint variability of the multimodal model were generally similar to those of the visual feedback model, the contribution of

proprioceptive feedback resulted in a few significant disparities between them. For instance, aspect ratios for more lateral movements are greater than those calculated under the unimodal visual feedback back model. This suggests a decrease in feedback variability off the lateral axis (i.e. in depth) under multimodal conditions. This decrease may be attributable to the integration of proprioceptive input which provides a more reliable estimate of the limb position along the depth axis. Thus, optimal integration of sensory feedback with noise properties consistent with visual and proprioceptive feedback will yield different patterns of endpoint variability than of any of the unimodal conditions. While these patterns are somewhat similar to that of the unimodal visual feedback control, the entirety of the predicted endpoint variability could not have been predicted based any combination of unimodal model results.
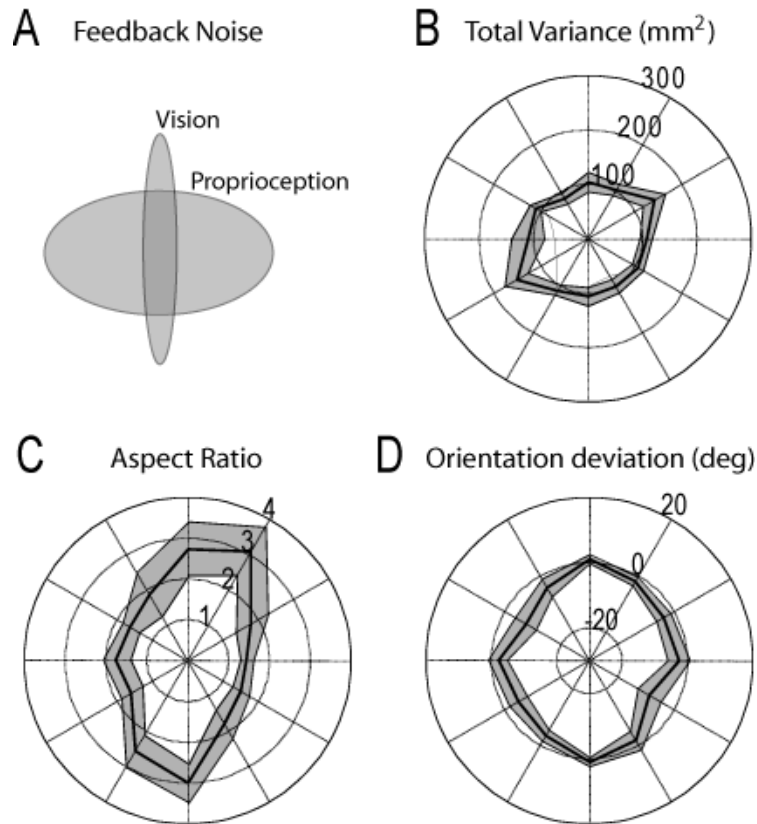
Figure 6.6. Predicted patterns of endpoint variability under multimodal feedback control. Format is consistent with Fig. 6.4 and 6.5. **A.** Simulated visual and proprioceptive feedback noise are overlaid to illustrate their integration. **B.** The direction-dependent patterns of predicted total variance were similar but not identical to visual unimodal model. **C.** Aspect ratio varied with movement direction similar to that of the visual unimodal model, but was rotated clockwise to a small degree. **D.** Orientation deviation was in general smaller than for the anisotropic feedback models, but was non-zero for many directions.

Discussion

Here we developed a feedback control model used to predict movement variability due to noise in planning/sensing and execution of movements. Multiple forms of feedback noise were inputted into the model, in order to evaluate the influence of anisotropic noise properties and multimodal sensory integration on the predicted movement variability. As expected, feedback noise with isotropic properties did not appreciably affect patterns of endpoint variability from those predicted without feedback noise whatsoever. Conversely, unimodal feedback control with visual or proprioceptive feedback noise characteristics yielded disparate patterns of endpoint variability. The specific differences depended largely upon the spatial patterns of feedback noise itself, indicative of the influence of the spatial anisotropy in feedback uncertainty on control. When the visual and proprioceptive inputs were combined into an integrated feedback estimate, the model produced patterns of variability which were different from either unimodal prediction. Specifically, while a heavy bias for visual feedback was observed, there was a clear contribution of proprioception in the patterns of endpoint variability. These results emphasize the importance of spatial characteristics of feedback uncertainty in the basis of reaching variability. This is of particularly relevance when simulating or interpreting movement during such reaching conditions as those involving a misalignment or removal of one source of feedback.

Validity of model results. The patterns observed in the execution-only simulations are consistent with previous behavioral results. In a 2004 work, van

163

Beers and colleagues attempted to predict behavioral variability resulting from execution noise alone. Their results demonstrated that when movements were more rapid, there was increased contribution of execution noise to overall movement variability and more elongated variable ellipses, consistent with evidence of signal dependent contributions of motor noise (van Beers et al., 2004). These observations are consistent with the patterns of endpoint variability predicted by the present simulations. For instance, Figure 6.3 demonstrates an increase in aspect ratio for those directions with shorter movement times. Also consistent with their findings, the present model predicted patterns of endpoint deviation near zero for all movement directions. This suggests that the orientation of simulated endpoint ellipses was largely along the direction of movement, indicative of the strong influence of signal dependent execution noise. Intriguingly, the influence of execution noise parameters was able to largely reproduce the patterns of execution variability described in van Beers et al., 2004, despite not explicitly modeling the biomechanical properties of the arm. This may suggest that the conversion from joint space to Cartesian coordinates does not result in unique patterns of behavioral variability during 2D reaching.

The modeling results offer several clear predictions for behavioral investigations of the integration of sensory/planning and execution noise. These predictions can be used to evaluate how well human behavior conforms to principles of optimal control. For instance, the model suggests that when there is little or no planning noise, patterns of execution noise dominate; a prediction consistent with previous behavioral results (Faisal & Wolpert 2009, van Beers et

164

al. 2004). Conversely, if execution noise was very low (i.e. during slow movements or static estimation), one would expect endpoint variability to largely resemble the spatial patterns of sensory feedback uncertainty. In fact, this has been observed for the case of static localization of the hand via proprioception and vision (van Beers et al. 1998, Faisal & Wolpert 2009).

Influence of sensory noise on variability. The influence of sensory uncertainty and planning noise on movement variability has been widely reported in both behavioral and neurophysiological studies. For instance at the neural level, noise in the sensory feedback and the planning stages have been shown to account for a significant amount of variability in motor behavior (Osborn et al., 2005, Churchland et al., 2006a; Churchland et al., 2006b) Behaviorally, the anisotropic nature of sensory feedback uncertainty has been shown to affect both the process of sensory integration as well as limb position estimation and endpoint control (van Beers et al., 2002; Apker et al., 2010; Apker & Buneo, 2012). The present model takes these behavioral observations into consideration in its design. As a result, the model generates predictions which indicate a significant influence of the spatial patterns of feedback noise. In this way, the predictions of the model further support the suggestion that human behavioral variability may be the result of an optimal integration of sensory feedback and forward processing.

The model results also suggest that the relative levels of planning and execution noise along a given movement direction are important to the patterns of reaching variability. This is particularly evident in the differences in the total variability plots in Figs. 6.2-5. In essence, these figures describe the amount of

165

total uncertainty at the end of the movement resulting from the integration of direction dependent execution noise and spatial patterns of sensory uncertainty. This is consistent with the findings of Faisal & Wolpert (2009), wherein the authors report that behavioral variability results from the "near optimal" combination of sensory and execution derived uncertainty. In the present study, when planning noise is introduced, total variance increases for all movement directions. However, despite having similar total sensory uncertainty, the isotropic and visual feedback noise models yielded different patterns of total variance. This echoes previous behavioral observations which suggest that integration of feedback and execution noise takes place in a direction dependent manner (Apker et al., 2010; Apker & Buneo, 2011).

Interaction of sensory/planning and execution noise. The spatial characteristics of sensory feedback noise have been shown to affect the patterns of integration and subsequently, endpoint variability (van Beers et al., 2002; McIntyre et al., 1998, Carrozzo et al., 1999). Consistent with this, the influence of the anisotropic feedback noise on endpoint variability is also apparent in patterns of all three metrics of endpoint ellipses. For instance, total variability predicted for each model with anisotropic noise yielded different direction dependent patterns, suggesting that shape of sensory feedback noise played an important role in determine endpoint uncertainty. Interestingly, the direction-dependent nature of the total variance suggests that the total variance is greatest when the movement direction is largely orthogonal to the direction of maximum noise in the feedback estimate (See Fig. 6.5). This suggests that the combined effect is most noticeable

166

when sensory/planning noise affects the direction rather than amplitude of movement, a finding reminiscent of recent behavioral research which suggests separated controllers of amplitude and direction in movement coordination (Sainburg et al., 2003; Sarglena & Sainburg, 2007). Alternatively, this may be interpreted as the total variability being predicted to be greatest when movements are orthogonal to the orientation of feedback noise. This is consistent with the 'near-optimal' integration described by Faisal & Wolpert (2009) as each noise contributes along a different axis, rather than be combined and reduced along a common direction, as their model predicts (Faisal & Wolpert, 2009).

The calculated aspect ratios in the three unimodal modals also demonstrate the direction dependent influence of feedback noise on the shape of behavioral variability. Specifically, the movement directions associated with the greatest aspect ratios coincides with cases where movement direction (i.e. execution noise) and sensory noise orientation (i.e. depth axis for vision and lateral axis for proprioception) are more aligned. In fact, it appears that ellipse aspect ratio is proportional to the degree to which these two noise sources are aligned. This is evidence of the model's prediction of the interaction between execution and sensory/planning noise processes. In fact, this prediction is very consistent with the observed interaction of planning and execution noise during reaching movements in 3D (Apker & Buneo, 2012).

The influence of sensory noise properties is also apparent from the differences in orientation deviation predictions across unimodal simulations. Interestingly, in both the visual and proprioceptive models the predictions of

orientation deviation are non-zero for nearly all directions except for those cases where the movement direction and noise orientation are well aligned (i.e. depth axis for vision and lateral axis for proprioception). This suggests sensory noise resulted in variability independent of the movement vector. Our results are again consistent with observations have found evidence for 'near optimal' combination of temporally derived sensory and execution noise, extending the scheme of integration into the spatial domain (Faisal & Wolpert, 2009). Specifically, the present model predicts that the combination of noise occurs on an axial dependent basis (Apker et al., 2010).

Multimodal vs. unimodal feedback control of reaching. Removing or perturbing visual feedback during movement is a common psychophysical approach to probe sensorimotor control. In fact, this was the application of the model described in Saunders & Knill (2004). In this work, the authors applied the predictions of visual feedback control without the aid of proprioceptive feedback to observations of human behavior following a mid-reach visual perturbation. However, both visual and proprioceptive feedback have been shown to contribute to the estimation of hand position and improved reaching performance (Prablanc et al., 1979; Rossetti et al., 1995; Desmurget et al., 1995; Vindras et al., (1998); Carrozzo et al., 1999; McIntyre et al., 1998; Battiglia-Mayer et al., 2003). As a result, one would expect a contribution of proprioceptive feedback throughout their reaching task, affecting estimation (and thus control) of the limb during the periods without visual feedback as well as when it was present, having particular impact during the period of visual perturbation. The results of unimodal and

168

multimodal simulations described here indicate a significant effect of both visual

and proprioceptive feedback during reaching. Thus the present model may be

better suited to predict sensorimotor control and behavior under feedback

conditions in which either visual or proprioceptive feedback is perturbed or

removed at any point during the task.

Future directions. Given the predictions illustrated in Figures 6.3-6., the

next step is to conduct a behavioral experiment wherein subjects perform identical

reaching movements to those simulated by the model. Comparison between these

results and model predictions will be used to make informed adjustments to the

model. Depending upon the results, the necessary adjustments may be as minor as

changes in model parameters, such as visual noise levels, or may be as significant

as requiring changes to fundamental model equations or to the model architecture.

For instance, given that the spatial patterns of proprioceptive uncertainty are

posture dependent, a biomechanical component may be required to more

accurately predict the contribution of proprioception to feedback control. This

element may be particularly important to the process of extending this model to

the simulation of movements in 3-Dimensions. In fact, fixing the relationship

between limb orientation and uncertainty in 3D may offer new insights into

unique patterns of sensory integration during movement planning in the vertical

plane (Apker et al., 2011).

Increasing the simulated movement time will reduce the peak velocity

generated and subsequently decrease the levels of execution noise. Conversely,

simulating more rapid movements would be expected to result in a greater

contribution of execution noise to endpoint variability. However it is not clear to what degree this would affect the apparent contribution of sensing/planning noise to endpoint variability. Thus, in addition to offering a means to improve the execution noise component of the model, comparing the model predictions of differing movement times/speeds to those of actual behavior may also provide insight into how well human behavior conforms to the predictions of optimal feedback control.

It has been suggested that behavioral variability is dependent upon temporal factors related to sensation and movement (Faisal & Wolpert, 2009). Here we characterize their contributions to variability given their variability in space. Both temporal and spatial factors of sensorimotor noise naturally contribute and interact to ultimately shape behavioral variability. The feedback control model presented here is also ideally suited to evaluate the temporal-spatial interactions of sensorimotor feedback control. One potential means to probe the temporal-spatial interactions using the model would be to evaluate how performance depends on the duration of presentation of vision both before and during the movement. For instance, simulating movements where visual feedback is removed at movement onset, 25% into the movement, and 50% into movement will provide insight into the degradation of estimation precision as a function of time and how this manifests in behavior. Characterizing the interaction of spatial and temporal properties of sensorimotor noise and their impact on movement variability is an important step toward a comprehensive model of sensorimotor feedback control.

CHAPTER 7

SUMMARY AND CONCLUSIONS

The work detailed in this volume has focused on the influence of noise in sensory integration and sensorimotor integration. Specifically, we have investigated how this noise affects control of the limb during the planning and execution of goal oriented reaching movements. To this end, several research projects were designed and carried out, each offering unique and novel insights into how the brain plans, coordinates, and controls limb movements in the presence of noise at all levels of sensorimotor control. The results of these works and their contribution to the study of sensorimotor control are briefly summarized below.

Sensory Integration and Movement Planning in 3D-Space

New evidence suggests that additional factors may affect the contribution of sensory feedback in 3D space compared to that observed in 2D (Desmurget et al., 1997; Scheidt et al., 2005; McIntyre & Le Seac'h, 2007). Yet, little work has been done to evaluate workspace dependent and direction dependent effects of sensory integration outside of the horizontal plane. As a first step towards investigating spatial dependencies of integration across the 3D workspace we designed an experiment to assess the process of movement planning for unconstrained movements to vertical targets (see Chapter 3). While the physical relationship of the finger to the targets did not change, the visual feedback of the finger at the starting position was either aligned with the finger's actual position or misaligned by a perturbation in either the lateral or vertical axis in some trials.

By comparing the movement direction between aligned and misaligned

conditions, we could assess the relative contribution of vision to movement

planning in 3D space.

We found that the influence of vision on estimation of fingertip position

was significantly greater along the lateral axis than the vertical axis. In addition,

we observed that when visual and somatosensory cues were dissociated along the

vertical axis in the near workspace, the relative contribution of vision varied

significantly with target location; this trend was also observed following laterally

dissociated visual feedback, however it did not reach significance. This direction

dependent effect may be related to additional factors affecting the relative

contribution of visual feedback for movement planning in 3D space (i.e. sensation

and/or compensation for the effect of gravity).

The results of this study provide several important insights into the nature

of sensory integration and movement planning. Primarily, these results extend

many previously observed principles regarding integration in the horizontal plane

into the 3D workspace. However, we also provide evidence that additional

factors, beyond visual and proprioceptive feedback contribute to the planning and

coordination of vertical movements. Future work will be needed to identify the

nature of the additional factors and their specific influence on sensorimotor

integration. For instance, there is the potential that the perceived limb orientation

versus gravity (a product of a combination of proprioception and information

from the otoliths) and required to compensate for the effects of the gravitational

force) impacts motor planning (Le Seac'h & McIntyre, 2007). Thus, the added

complexity of moving against gravity entails additional sensory estimates as well as alternative computations to be performed during planning.

Contributions of Planning and Execution Noise in Unconstrained Movement

Movement variability arises from a combination of execution noise and planning noise (Thaler & Todd, 2009). The use of task constraints which reduce the complexity of reaching movement is common in the study of sensorimotor processing. Often, these constraints have the effect of artificially minimizing the influence of one or both sources of variability (van Beers et al., 1998; van Beers et al., 2004). As a result, little is known of their relative contribution to reaching variability when both are present at normal levels, as during normal reaching. To begin to assess their relative contributions to natural movement variability, we designed a task to accentuate both planning and execution noise as a means to study their combined effects of during normal, unconstrained reaching. This study is described in detail in Chapter 5, but is summarized below.

Subjects were asked to perform a sequence of two reaching movements and we evaluated their endpoint variability for influences of planning and execution noise. Interestingly, we found that visually-derived planning noise was likely the dominant contributor to endpoint variability. This was inferred from the significant elongation in variability along the depth axis, the direction in which visual uncertainty is greatest; this direction was also largely orthogonal to any movement direction. These results suggest that execution noise plays a relatively minor role in endpoint variability of unconstrained movements. Further, these results are generally consistent with previous evidence of optimal, or 'near-

173

optimal' integration of noise sources in sensorimotor control, however, the nature of their integration and interaction must be more explicitly tested before more firm conclusions can be drawn.

Interaction of Planning and Execution Noise During Unconstrained 3D Movement

As previously mentioned, very little information exists regarding how planning and execution noise manifest in behavior when both sources of noise are unmitigated by task constraints. In the previous work, we investigated the relative contributions of planning and execution noise during normal, 3D movements. However, because movement direction and visual planning noise were largely opposed in the study, characterization of the interaction was relatively limited. To address the nature of their interaction, a subsequent study was performed in which the movement directions were either aligned with, or were orthogonal to, the direction of visually-derived planning noise (see Chapter 5). This design facilitated a comparison of endpoint variability between conditions in which planning and execution noise would be expected to interact minimally (i.e. when they were orthogonal) and maximally (when they were aligned).

We found that when visual feedback of the hand was provided throughout the movement, patterns of endpoint variability did not vary with final movement direction. Conversely, when visual feedback of the hand was withheld throughout the movement, a significant effect of the movement direction on endpoint variability was found. These results suggest that visual feedback essentially masks the influence of execution noise. This is likely due to the acuity of visual feedback

174

of the hand allowing subjects to detect the error in movement and mitigate it before the end of the movement. Thus, this study suggests an even greater role of feedback control for movements in 3D-space, and further emphasizes the role of sensory uncertainty in determining the patterns of endpoint variability.

Multimodal-Feedback Control Model with Natural Feedback Characteristics

Optimal stochastic feedback control has become a popular conceptual and computational framework for sensorimotor control (Wolpert et al., 1995, Harris and Wolpert, 1998). However, previous examples of these models in the literature often consider only a single source of feedback information of the limb during movement, neglecting the potential influence of other sources of information. This simplification has been justified methodologically, e.g. modeling only proprioceptive feedback by assuming a non-visual task (Todorov and Jordan, 2002), or pragmatically, e.g. assuming only visual feedback given evidence of its dominance over proprioception in most contexts (Saunders & Knill, 2004). However, such simplifications greatly limit the predictive capacity of these models to very esoteric scenarios. Moreover, these models often neglect to account for known spatial anisotropies in the sensory feedback noise. While these characteristics significantly affect endpoint control in behavior, the influence of the multimodal and anisotropic nature of sensory feedback on the predictions of optimal sensorimotor control remains unknown.

To begin to address these issues, we developed an optimal stochastic feedback control algorithm with realistic multimodal feedback inputs (see Chapter 6). Simulations were run to predict the influence of sensory feedback with

175

different distributions of noise in space on the characteristics of endpoint variability. Analysis of the predicted endpoints provided a means to determine whether or not these natural anisotropies in sensory feedback would affect reaching performance in an optimal control framework.

Predicted endpoint variability significantly differed between simulations with anisotropic vs. isotropic sensory feedback noise. Further, this model demonstrates that the availability of multiple feedback inputs also significantly affects endpoint variability, and thus both vision and proprioception must be considered when modeling visually guided reaching. These results indicate that the modality-specific anisotropic nature of feedback uncertainty must also be considered when modeling sensorimotor feedback control of the limb. The multimodal nature of the present model represents a significant evolution for optimal feedback control models of sensorimotor control, opening up a host of new possibilities to assess the predictions of optimality in sensory integration and motor control. For instance, a multimodal model could be used to simulate movements which entail a perturbation or complete removal of the visual feedback.

Broader Contribution and Impact of Research

In addition to their individual contributions, this work as a whole offers important insights into many open issues of neuroscience and neural engineering.

Sensory integration across the workspace. In addition to exploring the contributions of vision and proprioception to movement planning in the vertical plane, this work also directly assessed several predictions of workspace and

direction dependent aspects of sensory integration and sensorimotor control. For instance, previous evidence has suggested that proprioceptive uncertainty is significantly reduced as the limb's distance from the body increases (van Beers et al., 1998). This would be expected to result in a significant change in the relative contribution of proprioceptive feedback to limb state estimation, as well as significantly different variability between workspace depths. We tested these predictions in a variety of contexts only to find that the contribution of proprioceptive feedback did not significantly change within a comfortable reaching distance. Importantly, this does not necessarily contradict the observed change in proprioceptive reliability nor does it refute the principles of optimal cue integration. Rather, it suggests that with respect to the integration of proprioception at the perceptual level, the change is not so great as to significantly affect its weighting.

Coordinating 3D movements. Recent evidence suggests that the coordination of unconstrained movements in 3D may be significantly more complex than that for movements restricted to 2D (Desmurget et al., 1997; Scheidt et al., 2005). Thus, without direct evaluation, it is difficult to draw any conclusions *apriori* about sensorimotor feedback control during 3D movements. To study variability in sensorimotor control in a more general, natural context, we asked subjects to execute unconstrained reaching movements to targets throughout the workspace in a number of different tasks and experiments. The findings of these studies provide important insights into how to bridge observations of sensorimotor control in the horizontal plane to control of 3D

177

movements. For instance, we found evidence that suggests similar principles of sensory integration and feedback control of limb movements as those observed in 2D experiments can be observed in 3D coordination. However, we also observed an increased dependency on the characteristics of sensory estimation error and planning variability in the performance of goal oriented reaching. This finding is consistent with previous findings of visually/non-visually guided movements in 3D space (McIntyre et al., 1997; Carrozzo et al., 1999).

Direct assessment of the influence of planning and execution noise in sensorimotor control. In the study of sensory/planning variability, task constraints are often focused on reducing movement related noise or planning noise to examine the effects of execution variability (van Beers et al., 1998; van Beers et al., 2004). As a result, their respective influences during natural movement remain unclear. One reason for this is that in many cases the behavioral consequences of each process can be considerably overlapping. This ambiguity represents a critical weakness in our understanding of sensorimotor control and the origin of behavioral variability. A primary aim of this work has been to evaluate the relative contributions and interaction of planning and execution noise during more natural movements. Towards this end, we have provided strong evidence that the influence of planning noise plays a pivotal role in shaping endpoint variability, both in terms of the anticipated effects of planning noise as well as in modulating the influence of execution noise present in the endpoint distribution.

Specifically, we showed that while visual planning noise is a pervasive part of 3D movement variability, it can also mask the effects of execution noise. This is because visual feedback is precise enough to detect movement errors throughout the reach, such as those due to execution noise, affording the sensorimotor control system the opportunity to compensate for them online. However, when vision is removed, errors due to execution noise go unaccounted for as they may not be detected by relatively imprecise proprioceptive feedback. This suggests a prominent role of feedback control in the coordination of 3D movements when visual feedback is available.

This work has emphasized the importance of the spatial properties of feedback uncertainty on planning noise. This was shown in observed behavior both in terms of its effects on sensory integration as well as in endpoint control during complex 3D reaches. In addition, the importance of the noise properties was also apparent in the predictions of an optimal feedback control model. As a whole, the results of the work detailed in this volume generally support the application of optimal integration and control theories to human behavior and sensorimotor control.

Significance to neurological disorders. Fundamentally, this research is investigating the mechanisms by which the brain combines sensory information and transforms it into a meaningful intention to interact with the surrounding world. Normally, this process is effortless and unperceived. However, optic ataxia, ideomotor apraxia, and asomatoagnosia are only a few examples of pathologies which can manifest in sensorimotor deficits. Often, behavioral

179

variability is an important tool in the characterization and treatment of many sensorimotor disorders. Thus, understanding how planning and execution-related noise would normally interact is critical for interpreting the exaggerated variability that arises following nervous system damage (Contreras-Vidal & Buch, 2003; Hermsdorfer & Goldenberg, 2002; Longstaff & Heath, 2006; Thies et al., 2009). The work detailed in this volume provides important insights into how noise in sensorimotor control manifests during normal behavior and provides a basis for characterizing a deficit as being related to either sensory/planning or motor processing. This information may ultimately be used to determine the most appropriate therapeutic/rehabilitative strategy and provide a means to better quantify recovery.

Insights into the neural control of reaching. While these experiments have been focused on the influence of sensorimotor noise on behavior, the results of these works provide several insights into the neural processes underlying the control of reaching. For instance, in the introduction, area 5 of the parietal lobe and PMd were identified as likely candidates to be the neural substrate for limb state estimation. The results of these studies suggest that at all phases of movement production, encoding of the limb and target position in depth should be the most variable. This hypothesis could be tested in these areas by recording activity of cells in area 5 or PMd while the hand is positioned at various positions within the horizontal plane and attempting to predict the lateral and depth position from the neural activity. The present work suggests that decoding performance for lateral positions should exceed that for depth positions,

consistent with greater uncertainty in encoding this parameter (Ma et al., 2006; Ma & Pouget, 2008).

In addition, the present results potentially offer insight into the process of sensory integration for estimation of limb position. Specifically, when vision is present, encoding of lateral position should become more robust but relatively unchanged in depth. When vision is removed, encoding of lateral position should degrade significantly while the encoding of position in depth should be largely unchanged. Similarly, given the results of the study described in Chapter 3, the relative influence of visual feedback on cell and population activity should be reduced in the encoding of vertical position of the hand relative to that of the lateral position. This can also be evaluated through decoding analysis. Note that our behavioral evidence is generally consistent with the theory of optimal cue integration (van Beers et al., 2002b; Ernst & Banks, 2002; Wolpert, 2007). However, integration during static and dynamic phases of movement may differ substantially (Wolpert et al., 1995; Scheidt et al., 2005). Thus, to study this at the neural level, an effective approach may be to use to a delayed reaching task wherein there is a waiting period between the presentation of the target and the cue to initiate movement. This would allow for the dissociation of activity during initial planning period from that updating and would provide a more controlled basis to evaluate the influence of visual and proprioceptive inputs. Should these neural predictions are confirmed, it would add to an already large body of evidence which suggests the brain has developed a mechanism of integration and

feedback control which minimizes uncertainty and behavioral variability (Deneve et al., 2001; Ma et al., 2006; Ma & Pouget, 2008; Angelaki et al., 2009).

Future Work

Without question, an important next step is to test the predictions of the sensorimotor control model against empirical evidence from actual reaching behavior. The results of this comparison will be used to make informed adjustments to model parameters or equations to better fit empirical data. Following this, new predictions may be generated in a number of sensorimotor contexts, such as control during a visuomotor perturbation or in the presence of periodic visual feedback availability. Comparing the results of the model with those observed from human behavior under identical conditions will provide important insights into the nature of sensorimotor control as well as optimal feedback control as an underlying computational framework.

In general, we found that endpoint variability of 3D movements is largely dependent on the spatial characteristics of planning noise. Recently, Faisal & Wolpert (2009) demonstrated that total variability is also influenced by the integration of temporal characteristics of sensory and execution noises. Thus an important next step is to investigate how the temporal characteristics of sensorimotor noise interact with spatial characteristics to determine total behavioral variability. For instance, it would be interesting to know if this variability is related to planning noise at the beginning or at the end of movement. This could be tested by removing visual feedback at various points throughout the movement. Similarly, it would also be of interest to examine the effect of

returning visual feedback at various points in the movement. The feedback control filter described here is ideally suited to simulate these conditions to probe the spatial-temporal interaction and integration of planning and execution noise from an optimal control standpoint. This can be used to generate predictions of behavior which can be compared to observations from a complementary human reaching study. Experimentally, varying the timing and/or duration of visual feedback during a reaching task in 3D space would provide a means to characterize the spatial-temporal interaction of planning and execution noises.

Additionally, as our understanding of sensorimotor integration expands, it would also be useful to adapt the multimodal sensorimotor model to generate predictions of optimal feedback control in 3D. While undoubtedly a challenging endeavor, the potential insights into the complexity of sensorimotor control one could gain in the process of developing such a model would be of great value. However, this would be extremely challenging, and still a great deal more work must be done to investigate human performance during 3D movements in order to parameterize and populate the model with the appropriate equations. For instance, highlighted in this work and in others, moving in the presence of gravity may have a unique effect on sensory integration, anticipatory motor commands, and ultimately behavior (Le Seac'h & McIntyre, 2007). However, as described above, more research is needed into the specific effects of gravity on reaching, as well as a number of other factors, before such a comprehensive model of 3D sensorimotor control can be developed.

WORK CITED

Angelaki, D.E., Gu, Y., DeAngelis, G.C. (2009). Multisensory integration: psychophysics, neurophysiology,and computation. *Curr Opin Neurobiol, 19* 452-458

Apker, G.A., Darling, T.K., Buneo, C.A. (2010). Interacting noise sources shape patterns of movement variability in 3D space. *J Neurophysiol,104*(5), 2654-2666

Apker, G.A, & Buneo, C.A. (2012). Contribution of execution noise to endpoint variability in three-dimensional space. *J Neurophysiol, 107*, 90-102

Apker, G.A., Karimi, C.P., Buneo, C.A. (2011). Contributions of vision and proprioception to arm movement planning in the vertical plane. *Neuroscience Letters, 503*(3), 186-190

Ashe, J., & Georgopoulus, A.P. (1994). Movement parameters and neural activity in motor cortex and area-5. *Cerebral Cortex*, *4*(6), 590-600

Averbeck, B.B., Chafee, M.V., Crowe, D.A. (2005). Parietal representation of hand velocity in a copy task. *J Neurophysiol, 93*(1), 508-518

Bagesteiro, L.B., Sarlegna, F.R., Sainburg, R.L. (2006). Differential influence of vision and proprioception on control of movement distance, *Exp Brain Res, 171*, 358-370

Batista, A.P., Santhanam, G., Yu B.M., Ryu, S.I., Afshar, A, Shenoy, K.V. (2007). Reference frames for reach planning in macaque dorsal premotor cortex. *J Neurophysiol*. *98*(2), 966-983

Battaglia-Mayer, A., Caminiti, R., Lacquaniti, F. Zago, M. (2003). Multiple levels of representation of reaching in the parieto-frontal network. *Cerebral Cortex, 12*(10), 1009-1022

Battaglia-Mayer, A., Mascaro, M., & Caminiti, R. (2007). Temporal evolution and strength of neural activity in parietal cortex during eye and hand movements. *Cerebral Cortex, 17*(6), 1350-1363.

Bays, P.M., & Wolpert, D.M. (2007). Computational principles of sensorimotor control that minimize uncertainty and variability. *J Physiology,* 578, 387–396

Berkinblit, M.B., Fookson, O.I., Smetanin, B., Adamovich, S.V., and Poizner, H. (1995). The interaction of visual and proprioceptive inputs in pointing to actual and remembered targets. *Exp Brain Res, 107*, 326-330

Blohm, G., Keith, G., Crawford, J.D. (2009). Decoding the cortical transformation for visually guided reaching in 3-D space. *Cerebral Cortex, 19*,1372-1393

Buneo, C.A., Boline, J., Soechting, J.F., Poppele, R.E. (1995). On the form of the internal model for reaching. *Exp Brain Res, 104,* 467-479

Buneo, C. A., & Andersen, R. A. (2006). The posterior parietal cortex: sensorimotor interface for the planning and online control of visually guided movements. . *Neuropsychologia, 44*(13), 2594-2606.

Buneo, C. A., Jarvis, M. R., Batista, A. P., & Andersen, R. A. (2002). Direct visuomotor transformations for reaching. *Nature, 416*(6881), 632-636.

Caminiti, R., Ferraina, S., & Johnson, P. B. (1996). The sources of visual information to the primate frontal lobe: a novel role for the superior parietal lobule. *Cereb Cortex, 6*, 319-328.

Carrozzo, M., McIntyre, J., Zago, M., Lacquaniti, F. (1999). Viewer-centered and body-centered frames of reference in direct visuomotor transformations. *Exp Brain Res, 129*, 201-210,

Cisek, P., & Kalaska, J.F. (2005). Neural correlates of reaching decisions in dorsal premotoro cortex: Specification of multiple direct choices and final selection of action. *Neuron*, *45*(5), 801-814

Churchland, M.M., Afshar, A., Shenoy ,K.V. (2006a). A central source of movement variability. *Neuron 52*, 1085-1096

Churchland, M.M., Yu B.M., Ryu S.I., Santhanam, G., and Shenoy, K.V. (2006b). Neural variability in premotor cortex provides a signature of motor preparation. *Journal of Neuroscience 26*, 3697-3712

Contreras-Vidal, J.L., & Buch, E.R. (2003). Effects of Parkinson's disease on visuomotor adaptation. *Exp Brain Res* 150: 25-32

Darling, W.G., & Miller, G.F. (1993). Transformations between Visual and Kinesthetic Coordinate Systems in Reaches to Remembered Object Locations and Orientations. *Exp Brain Res 93*: 534-547

Deneve, S., Latham, P.E., and Pouget, A. (2001). Efficient computation and cue integration with noisy population codes. *Nat Neurosci, 4*, 826-831

Deneve, S.; Duhamel, J.R., Pouget, A. (2007). Optimal sensorimotor integration in recurrent cortical networks: A neural implementation of Kalman filter *J. Neuroscience, 27*, 5744-5756

Desmurget, M., Jordan, M., Prablanc, C., Jeannerod, M. (1997). Constrained and unconstrained movements involve different control strategies. *Journal of Neurophysiolog,y 77*, 1644-1650

Desmurget, M., & Grafton, S. (2000). Forward modeling allows feedback control for fast reaching movements. *Trends Cogn. Sci., 4*, 423–431

Ernst, M.O., & Banks, M.S. (2002). Humans integrate visual and haptic information in a statistically optimal fashion. *Nature, 415*(6870), 429-433.

Eskandar, E.N., & Assad, J.A. (1999). Dissociation of visual, motor and predictive signals in parietal cortex during visual guidance. *Nat Neurosci, 2*(1), 83-93

Faisal, A.A., Selen, L.P.J., Wolpert, D.M. (2008). Noise in the nervous system. *Nat Rev Neurosci, 9*, 292-303

Faisal A.A., & Wolpert, D.M. (2009). Near optimal combination of sensory and motor uncertainty in time during a naturalistic perception-action task. *J Neurophysiol 101*, 1901-1912

Flanders, M., Helms-Tillery, S.I., Soechting, J.F. (1992). Early stages in a sensorimotor transformation. *Behav Brain Sci 15,* 309-362

Flash, T., Hogan, N. (1985). The coordination of arm movements: An experimentally confirmed mathematical-model. *J Neuroscience, 5*, 1688-1703

Foley, J.M., & Held R. (1972). Visually Directed Pointing as a Function of Target Distance, Direction, and Available Cues. *Percept and Psychophys 12*, 263-268

Lukos, J.R., Lee, D., Poizner, H., Santello, M. (2010). Anticipatory Modulation of Digit Placement for Grasp Control Is Affected by Parkinson's Disease, *Plos One, 5*.

Franklin DW, So U, Burdet E, and Kawato M. (2007) Visual feedback is not necessary for the learning of novel dynamics. *Plos One 2*, 2007.

Gentili, R., Cahouet, V., Papaxanthis, C. (2007). Motor planning of arm movements is direction-dependent in the gravity field, *J Neuroscience 145,* 20-32

Ghez, C., Scheidt, R., Heijink, H. (2007). Different learned coordinate frames for planning trajectories and final positions in reaching. *J Neurophysiol 98,* 3614-3626

Graziano, M. S., Cooke, D. F., & Taylor, C. S. (2000). Coding the location of the arm by sight. *Science, 290*(5497), 1782-1786.

Gordon, J., Ghilardi, M.F., Ghez, C. (1994) Accuracy of Planar Reaching Movements .1. Independence of Direction and Extent Variability. *Exp Brain Res, 99*, 97-111

Gordon, J., Ghilardi, M.F., Cooper, S.E., Ghez, C. (1994). Accuracy of planar reaching movements. II. Systematic extent errors resulting from inertial anisotropy. *Exp. Brain Res, 99*:112-130,

Gu, Y., Angelaki, D.E., DeAngelis, G.C. (2008). Neural correlates of multisensory cue integration in macaque MSTd. *Nature Neuroscience 11*, 1201-1210

Guigon, E., Baraduc, P., Desmurget, M. (2008). Computational motor control: feedback and accuracy. *European Journal of Neuroscience. 27*, 1003–1016

Harris, C.M., & Wolpert, D.M. (1998). Signal-dependent noise determines motor planning. *Nature*, *394*(6695), 780-784

Hermsdorfer, J., & Goldenberg, G. (2002). Ipsilesional deficits during fast diadochokinetic hand movements following unilateral brain damage. *Neuropsychologia 40*, 2100-2115

Heuer, H., & Sangals, J. (1998). Task-dependent mixtures of coordinate systems in visuomotor transformations. *Exp Brain Res 119,* 224-236

Hoff, B., & Arbib, M.A. (1993). Models of trajectory formation and temporal interaction of reach and grasp. *J. Mot. Behav*., *25*, 175–192

Jacobs, R.A. (1999). Optimal integration of texture and motion cues to depth. *Vision Res 39*, 3621-3629

Jordan, M.I., & Rumelhart, D.E. (1992). Forward models – Supervised learning with a distal teacher. *Cognitive Sciecne 16*(3), 307-354

Khachiyan, L.G. (1996). Rounding of polytopes in the real number model of computation. *Math Oper Res 21*, 307-320

Khachiyan, L.G., Todd, M.J. (1993). On the complexity of approximating the maximal inscribed ellipsoid for a polytope. *Math Program 61*, 137-159

Knox, J.J., Hodges, P.W. (2005). Changes in head and neck position affect elbow joint position sense, *Exp Brain Res, 165*, 107-113.

Lacquaniti, F., Guigon, E., Bianchi, L., Ferraina, S., & Caminiti, R. (1995). Representing spatial information for limb movement: role of area 5 in the monkey. *Cereb Cortex, 5*(5), 391-409.

Lateiner, J.E., & Sainburg, R..L. (2003). Differential contributions of vision and proprioception to movement accuracy, *Exp Brain Res 151*, 446-454

Le Seac'h A.B., & McIntyre J. (2007). Multimodal reference frame for the planning of vertical arms movements*, Neuroscience Letters 423,* 211-215

Longstaff, M.G., & Heath R.A. (2006). Spiral drawing performance as an indicator of fine motor function in people with multiple sclerosis. *Hum Movement Sci 25*, 474-491

Kording, K. P., & Wolpert, D. M. (2004). Bayesian integration in sensorimotor learning. *Nature, 427*(6971), 244-247.

Kording, K. P., & Wolpert, D. M. (2006). Bayesian decision theory in sensorimotor control. *Trends Cogn. Sci., 10*(7), 319-326.

Kuo, A.D. (1995). An optimal-control model for analyzing human postural balance. *IEEE Trans. on Biomed. Engin., 42*, 87-101

Ma, W.J, Beck, J.M., Latham, P.E., Pouget, A.G. (2006) Bayesian inference with probabilistic population codes.*Nature Neuroscience 9*, 1432-1438

Ma, W. J., & Pouget, A. (2008). Linking neurons to behavior in multisensory perception: A computational review. *Brain Research, 1242*, 4-12

MacDonald, P.A., & Paus, T. (2003). The role of parietal corext in awareness of self-generated movements: A transcranial magnectic study. *Cerebral Cortex*, *13*(9), 963-967

Mars, F., Archambault, P.S., Feldman, A.G. (2003) Vestibular contribution to combined arm and trunk motion, *Exp Brain Res, 150,* 515-519.

McGuire, L.M.M., & Sabes, P.N. (2009). Sensory transformations and the use of multiple reference frames for reach planning. *Nature Neuroscience, 12*: 1056-U1134

McIntyre, J., Stratta, F., Droulez, J., Lacquaniti, F. (2000). Analysis of pointing errors reveals properties of data representations and coordinate transformations within the central nervous system. *Neural Computation 12*. 2823-2855

McIntyre, J., Stratta, F., Lacquaniti, F. (1997). Viewer-centered frame of reference for pointing to memorized targets in three-dimensional space. *J Neurophysiol 78*, 1601-1618

McIntyre, J., Stratta, F., and Lacquaniti, F. (1998) Short-term memory for reaching to visual targets: psychophysical evidence for body-centered reference frames. *J Neurosci, 18*, 8423-8435

Messier,J., & Kalaska, J.F. (2000). Covariation of primate dorsal premotor cell activity with direction and magnitude during a memorized-delay reaching task. *J Neurophysiol*, *84*(1), 152-165

Moran, D. W., & Schwartz, A. B. (1999). Motor cortical representation of speed and direction during reaching. *J Neurophysiol 82*(5), 2676-2692

Morgan, M.L., DeAngelis, G.C., Angelaki, D.E. (2008). Multisensory integration in macaque visual cortex depends on cue reliability. *Neuron, 59*, 662-673

Morrison D. (1990). *Multivariate Statistical Methods*. Singapore: McGraw-Hill

Mulliken, G.H., Musallam, S., Andersen, R. (2008). Decoding trajectories from posterior parietal cortex ensembles. *J Neurosciene, 28,* 12913-12926

Osborne, L.C., Lisberger, S.G., Bialek, W. (2005). A sensory source for motor variation. *Nature* 437:

Papaxanthis, C., Pozzo, T., McIntyre, J. (2005) Kinematic and dynamic processes for the control of pointing movements in humans revealed by short-term exposure to microgravity, *Neuroscience, 135,* 371-383.

Papaxanthis, C., Pozzo, T., Schieppati, M. (2003). Trajectories of arm pointing movements on the sagittal plane vary with both direction and speed, *Exp Brain Res, 148,* 498-503.

Pesaran, B., Nelson, M. J., & Andersen, R. A. (2006). Dorsal premotor neurons encode the relative position of the hand, eye, and goal during reach planning. *Neuron, 51*(1), 125-134.

Prablanc, C., Desmurget, M., Grea, H. (2003). Neural control of on-line guidance of hand reaching movements. *Prog. In Brain Res.: Neural Control of Space Coding and Action Production, 35*, 183-187

Prablanc, C., Echallier, J.E., Jeannerod, M., Komilis, E. (1979). Optimal response of eye and hand motor systems in pointing at a visual target .2. Static and dynamic visual cues in the control of hand movement. *Biol Cybern 35*, 183-187

Prablanc, C., Martin, O. (1992). Automatic-control during hand reaching at undetected 2-dimensional target displacements, *J Neurophysiol, 67* 455-469.

Proske U. (2005). What is the role of muscle receptors in proprioception? *Muscle & Nerve 31*, 780-787

Rossetti, Y., Desmurget, M., Prablanc C. (1995). Vectorial coding of movement - vision, proprioception, or both?. *J Neurophysiol, 74*, 457-463

Sainburg R.L., Lateiner J.E., Latash M.L., Bagesteiro L.B. (2003). Effects of altering initial position on movement direction and extent, *J Neurophysiol, 89*, 401-415

Sainburg, R., Poizner, H., Ghez, C. (1993). Loss of proprioception produces deficits in interjoint coordination. *J. Neurophysiol*. 70: 2136–2147

Sarlegna F.R., & Sainburg R.L., (2007). The effect of target modality on visual and proprioceptive contributions to the control of movement distance, *Exp Brain Res 176*, 267-280

Saunders, J.A. & Knill, D.C. (2004) Visual feedback control of hand movements. *J. Neurosci., 24,* 3223–3234

Scheidt, R.A., Conditt, M.A., Secco, E.L., & Mussa-Ivaldi, F.A. (2005). Interaction of visual and proprioceptive feedback during adaptation of human reaching movements. *J Neurophysiol, 93*: 3200-3213

Schwartz, A. B., Moran, D. W., & Reina, G. A. (2004). Differential representation of perception and action in the frontal cortex. *Science, 303*(5656), 380-383.

Scott, S.H., & Loeb, G.E. (1994). The Computation of Position Sense from Spindles in Monoarticular and Multiarticular Muscles. *J Neurosci 14,* 7529-7540

Scott, S. H., Sergio, L. E., & Kalaska, J. F. (1997). Reaching movements with similar hand paths but different arm orientations .2. Activity of individual cells in dorsal premotor cortex and parietal area 5. *J Neurophysiol, 78*(5), 2413-2426.

Shi, Y., & Buneo, C.A. (2009). Exploring the role of sensor noise in movement variability. In: *IEEE Engineering in Medicine and Biology Society*. Minneapolis, MN.: 4970-4973

Sober, S. J., & Sabes, P. N. (2003). Multisensory integration during motor planning. *J Neurosci, 23*(18), 6982-6992.

Soechting, J.F.,& Flanders, M. (1989). Sensorimotor representations for pointing to targetsin three dimensional space. *J Neurophysiol 62,* 582-594

190

Soechting, J.F., B. Ross, B. (1984). Psychophysical determination of coordinate representation of human arm orientation, *Neuroscience, 13*, 595-604.

Thaler, L., and Todd, J.T. (2009) The control parameters used by the CNS to guide the hand depend on the visuo-motor task: Evidence from visually guided pointing. *Neuroscience 159*, 578-598

Thies, S.B., Tresadern, P.A., Kenney, L.P., Smith, J., et al. (2009). Movement variability in stroke patients and controls performing two upper limb functional tasks: a new assessment methodology. *J Neuroeng Rehabil* 6

Todorov, E. & Jordan, M.I. (2002) Optimal feedback control as a theory of motor coordination. *Nat. Neurosci.,* 5: 1226–1235

van Beers, R.J. (2009). Motor Learning Is Optimally Tuned to the Properties of Motor Noise. *Neuron 63*, 406-417

van Beers, R.J., Haggard, P., Wolpert, D.M. (2004). The role of execution noise in movement variability. *J Neurophysiol, 91*, 1050-1063

van Beers, R. J., Sittig, A. C., & van der Gon, J. J. D. (1998). The precision of proprioceptive position sense. *Exp Brain Res, 122*(4), 367-377.

van Beers, R. J., Sittig, A. C., & van der Gon, J. J. D. (1999). Integration of proprioceptive and visual position-information: An experimentally supported model. *J Neurophysiol, 81*(3), 1355-1364.

van Beers, R.J., Baraduc, P., Wolpert, D.M. (2002a). Role of uncertainty in sensorimotor control. *Philos T Roy Soc B* 357: 1137-1145

van Beers, R. J., Wolpert, D. M., & Haggard, P. (2002b). When feeling is more important than seeing in sensorimotor adaptation. *Current Biology, 12*(10), 834-837.

van den Dobbelsteen, J.J., Brenner, E., Smeets, J.B.J. (2001). Endpoints of arm movements to visual targets. *Experimental Brain Research, 138*, 279-287

Vetter, P., & Wolpert, D. M. (2000). Context estimation for sensorimotor control. *J Neurophysiol, 84*(2), 1026-1034.

Viguier, A., Clement, G., and Trotter, Y. (2001) Distance perception within near visual space. *Perception, 30*, 115-124

Vindras, P., Desmurget, M., Prablanc, C., Viviani, P. (1998). Pointing errors reflect biases in the perception of the initial hand position. *J Physiology*

Vindras, P., & Viviani, P. (1998). Frames of reference and control parameters in visuomanual pointing. *J Exp Psychol Human 24*, 569-591

Wilson, E.T., Wong, J.D., and Gribble, P.L. (2008). Workspace-dependent differences in proprioception of the human arm. . In: *Program No 4658 Neuroscience 2008 Abstracts,* Washington, D.C.: Society for Neuroscience

Wolpert D. (2007). Probabilistic models in human sensorimotor control. *Human Movement Science*, *26*, 511-523

Wolpert, D. M., Ghahramani, Z., & Jordan, M. I. (1995). An internal model for sensorimotor integration. *Science*, 269(5232), 1880-1882.

Worringham, C.J., Stelmach, G.E., Martin, Z.E. (1987). Limb segment inclination sense in proprioception*, Exp Brain Res, 66*, 653-658.

APPENDIX A

PERMISSIONS

PERMISSIONS FROM SCIENTIFIC JOURNALS

Chapter 3 is a published article a in the *Neuroscience Letters*. It is the policy of the *Neuroscience Letters* and Elsevier Publication Co. that the author of a published article is entitled to reproduced Elsevier copyrighted material in a dissertation on the condition that the full citation of the article is provided. In compliance with this policy, below is the full citation associated with this published work:

Apker, G.A., Karimi, C.P., Buneo, C.A. (2011). Contributions of vision and proprioception to arm movement planning in the vertical plane. *Neuroscience Letters, 503*(3), 186-190

Chapters 4 and 5 are both published articles in the *Journal of Neurophysiology*. It is the policy of the *Journal of Neurophysiology* and American Physiological Association that the author of a published article is entitled to reproduced APA copyrighted material in a dissertation on the condition that the full citation of the article is provided. In compliance with this policy, below are the full citations associated with these published works:

Chapter 4:

Apker, G.A., Darling, T.K., Buneo, C.A. (2010). Interacting noise sources shape patterns of movement variability in 3D space. *J Neurophysiol,104*(5), 2654-2666

Chapter 5:

Apker, G.A, & Buneo, C.A. (2012). Contribution of execution noise to endpoint variability in three-dimensional space. *J Neurophysiol, 107*, 90-102

PERMISSIONS FROM CO-AUTHORS

All co-authors who contributed to the published works reproduced in this volume are aware of and have permitted the use of these works. Specifically, Christopher Buneo and Cameron Karimi have granted me permission to reproduce the work which comprises Chapter 3. Christopher Buneo and Timothy Darling have given me similar consent to reproduce the published work presented in Chapter 4, as has Christopher Buneo regarding the work in Chapter 5.

APPENDIX B

INSTITUTIONAL REVIEW BOARD FORMS

Office of Research Integrity and Assurance

To:	Christopher Buneo
	ISTB1
From:	Carol Johnston, Chair
	Biosci IRB
Date:	04/12/2011
Committee Action:	**Renewal**
Renewal Date:	04/11/2011
Review Type:	Expedited F4
IRB Protocol #:	0805002956
Study Title:	Sensorimotor Integration During Online Movement Corrections
Expiration Date:	04/12/2012

The above-referenced protocol was given renewed approval following Expedited Review by the Institutional Review Board.

It is the Principal Investigator's responsibility to obtain review and continued approval of ongoing research before the expiration noted above. Please allow sufficient time for reapproval. Research activity of any sort may not continue beyond the expiration date without committee approval. Failure to receive approval for continuation before the expiration date will result in the automatic suspension of the approval of this protocol on the expiration date. Information collected following suspension is unapproved research and cannot be reported or published as research data. If you do not wish continued approval, please notify the Committee of the study termination.

This approval by the Biosci IRB does not replace or supersede any departmental or oversight committee review that may be required by institutional policy.

Adverse Reactions: If any untoward incidents or severe reactions should develop as a result of this study, you are required to notify the Biosci IRB immediately. If necessary a member of the IRB will be assigned to look into the matter. If the problem is serious, approval may be withdrawn pending IRB review.

Amendments: If you wish to change any aspect of this study, such as the procedures, the consent forms, or the investigators, please communicate your requested changes to the Biosci IRB. The new procedure is not to be initiated until the IRB approval has been given.

197

CONSENT FORM
Sensorimotor Integration During Online Movement Corrections
Visuomotor Learning Laboratory, ECB and ISTB1
Harrington Department of Bioengineering, Arizona State University

You are being asked to read the following material to ensure that you are informed of the nature of this research study and how you will participate in it, if you consent to do so. Signing this form will indicate that you have been so informed and that you have given your consent. Federal regulations require written informed consent prior to participation in this research study so that you can know the nature and risks of your participation and can decide to participate or not to participate in a free and informed manner.

INTRODUCTION
The purposes of this form are to provide you (as a prospective research study participant) information that may affect your decision as to whether or not to participate in this research and to record the consent of those who agree to be involved in the study.

RESEARCHERS
Christopher Buneo, Assistant Professor in the Harrington Department of Bioengineering, along with his research students Gregory Apker and Timothy Darling have invited you to participate in a research study.

STUDY PURPOSE
Several studies have been conducted exploring how movement plans are updated online when the goal location of an arm movement is suddenly changed. However, none of these studies have explored the role of sensory feedback on the timing of these movement corrections. You are being invited to participate in a study to examine the role of vision in rapidly updating arm movement plans. The information gained in this experiment will allow us to better understand how the brain integrates sensory information to correct ongoing movements.

DESCRIPTION OF RESEARCH STUDY
If you decide to participate, you will join a study designed to determine how movement plans are rapidly updated by the brain. During a trial you will be comfortably seated in a chair facing a mirror which reflects the image of a computer monitor. Light emitting diodes (LEDs) will be attached to the index finger of your dominant arm and will be used to track the motion of your fingertip, which will be viewed on the computer monitor as a small sphere. During the experiment, an additional 'target' sphere will appear on the computer monitor and you will be required to move your fingertip so that it appears to touch the target sphere. On some trials the target sphere will suddenly change location, requiring you to alter your movement accordingly, and on some of these trials the sphere that corresponds to your fingertip will disappear while you are moving. On all trials the idea will be to place your fingertip on the target sphere as quickly and as accurately as possible. You will be allowed up to 15 minutes to get accustomed to the task. Following these practice trials the experiment will commence and will last no longer than 2 hours.

If you say YES, then your participation will last for no longer than 2 hours per experimental session up to three experimental sessions in room 160 of the B wing of the Engineering Center on Arizona State University's Tempe Campus Location.

By signing below you certify that you are between 18 and 65 years of age and are generally healthy. You also certify that you have NO history of neurological disease.

RISKS
There is some negligible risk of eye damage from direct and prolonged viewing of LEDS at close range. Thus, you will be asked not to view the LEDS directly but to keep them behind the viewing mirror at all times. This should be easy to do, as the arm movements in this experiment can only be tracked (and viewed by you) when the arm is in this position.

As with any research, there is some possibility that you may be subject to risks that have not yet been identified, though the researchers have significant experience using these techniques and the chances they have not seen these risks are extremely small.

BENEFITS
This study will be of no direct benefit to me. There are possible future benefits to the understanding of the brain and how it integrates sensory information to enable rapid changes in movement plans. These include better rehabilitation protocols and prosthetic systems for individuals with nervous system damage.

NEW INFORMATION
If the researchers find new information during the study that would reasonably change your decision about participating, then they will provide this information to you.

CONFIDENTIALITY
All information obtained in this study is strictly confidential unless disclosure is required by law. The results of this research study may be used in reports, presentations, and publications, but the researchers will not identify you. In order to maintain confidentiality of your records, Christopher Buneo, Gregory Apker and Timothy Darling will be assigning a subject code and my identity will be known only by the principal investigator (Buneo) and those individuals who work in his laboratory. Christopher Buneo alone will control access to the results when they are published and afterwards.

WITHDRAWAL PRIVILEGE
It is ok for you to say no. Even if you say yes now, you are free to say no later, and withdraw from this study at any time. Your decision will not affect your relationship with Arizona State University or otherwise cause a loss of benefits to which you might otherwise be entitled. Participation in this study is completely voluntary; as such the investigators collecting data understand that you may decide to withdraw from this study, at any time, for any reason and such a withdrawal will have **NO** consequences to your grades, treatment, employment status, or other relationship with the investigators or Arizona State University.

COSTS AND PAYMENTS
There is no payment for your participation in the study.

COMPENSATION FOR ILLNESS AND INJURY
If you agree to participate in the study, then your consent does not waive any of your legal rights. However, no funds have been set aside to compensate you in the event of injury.

VOLUNTARY CONSENT
Any questions you have concerning the research study or your participation in the study, before or after your consent, will be answered by Gregory Apker in person or can be answered by him via email correspondence at gapker@asu.edu, by appointment in his office located in ISTB1 181 at Arizona State University's Tempe Campus, or via phone at (480) 229-2544. The principle investigator, Christopher Buneo, can similarly be reached for inquiries via email at cbuneo@asu.edu, by appointment in his office, located in ISTB1 181B at Arizona State University's Tempe Campus, or via phone at (480) 727-0841. Written correspondence can be mailed to either of the investigators at the following address:

Gregory Apker/Christopher Buneo
Visuomotor Learning Lab
ECG 334
Box 879709
Harrington Department of Bioengineering
Arizona State University
Tempe, AZ USA 85287-9709

If you have questions about your rights as a subject/participant in this research, or if you feel that you have been placed at risk, you can contact the Chair of the Human Subjects Institutional Review Board, through the ASU Research Compliance Office, at 480-965-6788.

This form explains the nature, demands, benefits and any risk of the project. By signing this form you agree knowingly to assume any risks involved. Remember, your participation is voluntary. You may choose not to participate or to withdraw your consent and discontinue participation at any time without penalty or loss of benefit. In signing this consent form, you are not waiving any legal claims, rights, or remedies. A copy of this consent form will be given (offered) to you.

Your signature below indicates that you consent to participate in the above study.

_____   _____   _____
Subject's Signature   Printed Name   Date

INVESTIGATOR'S STATEMENT
"I certify that I have explained to the above individual the nature and purpose, the potential benefits and possible risks associated with participation in this research study, have answered any questions that have been raised, and have witnessed the above signature. These elements of Informed Consent conform to the Assurance given by Arizona State University to the Office for

Human Research Protections to protect the rights of human subjects. I have provided (offered) the subject/participant a copy of this signed consent document."

Signature of Investigator_____ Date_____

CONSENT FORM
Sensorimotor Integration During Online Movement Corrections
Visuomotor Learning Laboratory, SCOB 360
School of Biological and Health Systems Engineering, Arizona State University

You are being asked to read the following material to ensure that you are informed of the nature of this research study and how you will participate in it, if you consent to do so. Signing this form will indicate that you have been so informed and that you have given your consent. Federal regulations require written informed consent prior to participation in this research study so that you can know the nature and risks of your participation and can decide to participate or not to participate in a free and informed manner.

INTRODUCTION
The purposes of this form are to provide you (as a prospective research study participant) information that may affect your decision as to whether or not to participate in this research and to record the consent of those who agree to be involved in the study.

RESEARCHERS
Christopher Buneo, Assistant Professor in the School of Biological and Health Systems Engineering, along with his research students Gregory Apker and Jacqueline Fitton have invited you to participate in a research study.

STUDY PURPOSE
Several studies have been conducted exploring how movement plans are updated online when the goal location of an arm movement is suddenly changed. However, none of these studies have explored the role of sensory feedback on the timing of these movement corrections. You are being invited to participate in a study to examine the role of vision in rapidly updating arm movement plans. The information gained in this experiment will allow us to better understand how the brain integrates sensory information to correct ongoing movements.

DESCRIPTION OF RESEARCH STUDY
If you decide to participate, you will join a study designed to determine how movement plans are rapidly updated by the brain. During a trial you will be comfortably seated in a chair facing a mirror which reflects the image of a computer monitor. Light emitting diodes (LEDs) will be attached to the index finger of your dominant arm and will be used to track the motion of your fingertip, which will be viewed on the computer monitor as a small sphere. During the experiment, an additional 'target' sphere will appear on the computer monitor and you will be required to move your fingertip so that it appears to touch the target sphere. On some trials the target sphere will suddenly change location, requiring you to alter your movement accordingly, and on some of these trials the sphere that corresponds to your fingertip will disappear while you are moving. On all trials the idea will be to place your fingertip on the target sphere as quickly and as accurately as possible. You will be allowed up to 15 minutes to get accustomed to the task. Following these practice trials the experiment will commence and will last no longer than 2 hours.

ASU IRB
Approved
Sign_____
Date_ 4/11/11 - 9/12/12

COSTS AND PAYMENTS
There is no payment for your participation in the study.

COMPENSATION FOR ILLNESS AND INJURY
If you agree to participate in the study, then your consent does not waive any of your legal rights. However, no funds have been set aside to compensate you in the event of injury.

VOLUNTARY CONSENT
Any questions you have concerning the research study or your participation in the study, before or after your consent, will be answered by Gregory Apker in person or can be answered by him via email correspondence at gapker@asu.edu, by appointment in his office located in ISTB1 181 at Arizona State University's Tempe Campus, or via phone at (480) 229-2544. The principle investigator, Christopher Buneo, can similarly be reached for inquiries via email at cbuneo@asu.edu, by appointment in his office, located in ISTB1 181B at Arizona State University's Tempe Campus, or via phone at (480) 727-0841. Written correspondence can be mailed to either of the investigators at the following address:

Gregory Apker/Christopher Buneo
Visuomotor Learning Lab
ECG 334
Box 879709
Harrington Department of Bioengineering
Arizona State University
Tempe, AZ USA 85287-9709

If you have questions about your rights as a subject/participant in this research, or if you feel that you have been placed at risk, you can contact the Chair of the Human Subjects Institutional Review Board, through the ASU Office of Research Integrity and Assurance, at 480-965-6788.

This form explains the nature, demands, benefits and any risk of the project. By signing this form you agree knowingly to assume any risks involved. Remember, your participation is voluntary. You may choose not to participate or to withdraw your consent and discontinue participation at any time without penalty or loss of benefit. In signing this consent form, you are not waiving any legal claims, rights, or remedies. A copy of this consent form will be given (offered) to you.

Your signature below indicates that you consent to participate in the above study.

_____   _____   _____
Subject's Signature   Printed Name   Date

INVESTIGATOR'S STATEMENT
"I certify that I have explained to the above individual the nature and purpose, the potential benefits and possible risks associated with participation in this research study, have answered any questions that have been raised, and have witnessed the above signature. These elements of Informed Consent conform to the Assurance given by Arizona State University to the Office for